

ANALYSIS OF THE PHYSICAL PROPERTIES OF DIFFERENT TYPES OF
NEUTRON STARS

A THESIS SUBMITTED TO
THE GRADUATE SCHOOL OF NATURAL AND APPLIED SCIENCES
OF
MIDDLE EAST TECHNICAL UNIVERSITY

BY

MUSTAFA ÖZGÜR TAŞKIN

IN PARTIAL FULFILLMENT OF THE REQUIREMENTS

FOR

THE DEGREE OF DOCTOR OF PHILOSOPHY

IN

PHYSICS

SEPTEMBER 2005

Approval of the Graduate School of Natural and Applied Sciences.

Prof. Dr. Canan Özgen
Director

I certify that this thesis satisfies all the requirements as a thesis for the degree of Doctor of Philosophy.

Prof. Dr. Sinan Bilikmen
Head of Department

This is to certify that we have read this thesis and that in our opinion it is fully adequate, in scope and quality, as a thesis for the degree of Doctor of Philosophy.

Prof. Dr. Oktay Hüseyin
Co-Supervisor

Prof. Dr. Nilgün Kızıloğlu
Supervisor

Examining Committee Members

Assist. Prof. Ünal Ertan (SABANCI UNV.) _____

Prof. Dr. Nilgün Kızıloğlu (METU, PHYS) _____

Prof. Dr. Altan Baykal (METU, PHYS) _____

Prof. Dr. Oktay Hüseyin (AKDENİZ UNV.) _____

Prof. Dr. Halil Kırbıyık (METU, PHYS) _____

I hereby declare that all information in this document has been obtained and presented in accordance with academic rules and ethical conduct. I also declare that, as required by these rules and conduct, I have fully cited and referenced all material and results that are not original to this work.

Mustafa Özgür Taşkın

ABSTRACT

ANALYSIS OF THE PHYSICAL PROPERTIES OF DIFFERENT TYPES OF NEUTRON STARS

Taşkın, Mustafa Özgür

PhD, Department of Physics

Supervisor: Prof. Dr. Nilgün Kızıloğlu

Co-Supervisor: Prof. Dr. Oktay Hüseyin

September 2005, 124 pages.

This thesis is composed of three published articles. Each chapter is devoted to an article. In the first part the origin of some of the single radio pulsars with relatively low magnetic fields ($B < 10^{12}$ G) and with characteristic ages (τ) less than 10^7 years is questioned. We proposed that such pulsars might occur as a result of the disruption of high-mass X-ray binary systems after a second supernova explosion. In these binaries, mass accretion on to the surface of X-ray pulsars may lead to the decrease in the magnetic field from its value at birth ($B \simeq 10^{12} - 10^{13}$ G) down to $B < 10^{12}$ G similar to the processes in low mass X-ray binaries.

In the second part we put together many observational data of SGRs and AXPs and analyzed them with the main purpose of the removal of contradiction between the real age (t) of these objects and their characteristic times of period change (τ). SGRs and AXPs are neutron stars that undergo star-quakes. Magnetic activity increases from time to time. We suggest that as a result of these processes plasma is ejected from the NS and propeller mechanism starts to work. Due to the propeller effect \dot{P} increases, τ decreases. Indeed, high \dot{P} values are

observed in SGRs and in half of the AXPs. Then, for a long time NS loses its activity, its \dot{P} decreases, τ increases and rapid cooling begins. It seems that there is a possible transition between each NS stage (AXP,SGR, dim). This transient cycle may be repeated once or several times until the spin period of the neutron star becomes $P > 10 - 12$ s. Observational data and mainly the data of AXP 1E 1048-5937 and DRQNS RX J1308.8+2127 support this idea.

In the third part dependence of the X-ray luminosity (L_x) of young single pulsars, due to ejection of relativistic particles, on electric field intensity, rate of rotational energy loss (\dot{E}), magnetic field, period, and some other parameters of neutron stars are discussed. Influence of the magnetic field and effects of some other parameters of neutron stars on the $L_x - \dot{E}$ and the $L_x - \tau$ (characteristic time) relations are considered. Evolutionary factors also play an important role in our considerations. Only the pulsars whose X-ray luminosity in the 2-10 keV energy band is greater than 10^{33} erg/s have pulsar wind nebula around them. The pulsars from which γ -ray radiation has been observed have low X-ray luminosity in general.

Keywords: Pulsars: Evolution, Origin, X-ray; SNR; Magnetars: AXP, SGR, DRQNS

ÖZ

FARKLI TİPLERDEKİ NÖTRON YILDIZLARININ FİZİKSEL ÖZELLİKLERİNİN ANALİZİ

Taşkın, Mustafa Özgür

Doktora, Fizik Bölümü

Tez Yöneticisi: Prof. Dr. Nilgün Kızıloğlu

Ortak Tez Yöneticisi: Prof. Dr. Oktay Hüseyin

Eylül 2005, 124 sayfa.

Bu tez yayınlanmış üç makaleden oluşmuştur. Her kısım bir makaleye ayrılmıştır. İlk bölümde kısmen düşük manyetik alanlı ($B < 10^{12}$ G) ve karakteristik yaşları (τ) 10^7 yıldan küçük bazı tek radyo yıldızlarının kökeni sorgulanmıştır. Bu pulsarların, ikinci supernova patlamasından sonra büyük kütleli X-ışını ikili sistemlerinin dağılmasıyla oluşabilece-

ğini önerdik. Bu ikili sistemlerde X-ışını pulsarının yüzeyine aktarılan madde düşük kütleli X-ışını ikili sistemlerinde olduğu gibi, pulsarın manyetik alanının doğuştan gelen değerinin ($B \simeq 10^{12} - 10^{13}$ G) altına inmesine yol açar ($< 10^{12}$ G).

İkinci bölümde, SGR ve AXP lerin gerçek yaşlarıyla (t) ile periyodlarındaki değişimin karakteristik zamanı (τ) arasındaki çelişkiyi gidermek amacıyla birçok veriyi bir araya getirdik ve analiz ettik. SGR ve AXP ler yıldız sarsıntısı geçiren nötron yıldızlarıdır. Zaman zaman manyetik etkinlik artar. Bu süreçlerin sonucunda nötron yıldızından plazma fırlatılacağını ve pervane mekanizmasının çalışmaya başlayaca-

ğını önerdik. Pervane etkisiyle \dot{P} artar, τ azalır. Gerçekten de SGR larda ve AXP lerin yarısında yüksek \dot{P} değerleri gözlenmiştir. Daha sonra yıldız uzun bir süre

etkinliğini kaybeder, \dot{P} azalır, τ artar ve hızlı bir soğuma başlar. Değişik nötron yıldızı safhaları arasında bir geçiş var gibi gözükmektedir (AXP, SGR, sönük). Bu geçici döngü nötron yıldızının periyodu 10 - 12 saniyenin üzerine çıkana kadar bir veya birkaç kez tekrarlanabilir. Gözlemsel veriler ve özellikle AXP 1E 1048-5937 ve DRQNS RX J1308.8+2127'nin verileri bu fikri desteklemektedir.

Üçüncü bölümde, relativistik parçacıkların püskürtülmesi nedeniyle, genç tekil pulsarların X-ışını parlaklığının nötron yıldızının elektrik alan şiddetine, birim zamanda dönme enerjisini kaybetme hızına (\dot{E}) ve periyoduna olan bağımlılığı tartışılmıştır. Manyetik alanın ve diğer bazı parametrelerin nötron yıldızının L_x - \dot{E} ve L_x - τ (karakteristik zaman) ilişkilerine etkisi dikkate alınmıştır. Evrimsel etkenler dikkat edilecek noktalar arasında önemli rol oynuyorlar. Pulsar rüzgarı nebulası sadece X-ışını parlaklığı 2 - 10 keV enerji aralığında 10^{33} erg/s nin üstünde olan pulsarların etrafında vardır. Γ ışınması olan pulsarların genelde X-ışını parlaklıkları düşüktür.

Anahtar Sözcükler: Pulsarlar: Evrim, Köken, X-ışını; SNR; Magnetarlar: AXP, SGR, DRQNS

TO
OBEN SEZER

*Your true friendship was the greatest of all
blessings. I feel sorry not to take the greatest
care to acquire all*

ACKNOWLEDGMENTS

It gives the author great pleasure to acknowledge the fruitful discussions with Prof. Dr. Nilgün Kızılođlu. I found how a question, that most of the time seem simple, could be the strongest one. I hope the chocolates I ate during astrophysics seminars can lessen the bitter taste of life.

I would like to express my deepest gratitude to Prof. Dr. Oktay Huseyin but for whose guidance this thesis would have never seen the light of the day. Working with him was not only a pleasure but it was also a lifetime experience. Those who saw Amadeus, the movie by Milos Forman, will remember the composer Antonio Saliari. I feel like watching the masterpiece, but unlike Saliari, I can not stop myself trembling by the desire to learn more.

I sincerely appreciate Sinan Kaan Yerli for the patience he showed when he faced my heart-killing questions in L^AT_EX. If one day I will finally be able to use it professionally it is because of him.

I would like to send my special thanks to Abdullah Göksu, the one man from whom I have learned a lot about human nature as well as the nature itself. His friendship is invaluable.

There are moments when even a simple greeting or a smile make you fell fresh. Those are the times that I am grateful to Ercan Aydın, Mete Kurşun, Rıfat Öcal, Bora Yıldız, Esin Akbaba, Tuğba Bolat and Döndü Şahin.

I would like to mention Sevim Aygar, Sultan Köksal, Zeynep Eke, Gülşen Özdemir Parlak and Adil Yüksek for all their help during my education. Thank you all!

TABLE OF CONTENTS

PLAGIARISM	iii
ABSTRACT	iv
ÖZ	vi
DEDICATON	viii
ACKNOWLEDGMENTS	ix
TABLE OF CONTENTS	x
CHAPTER		
1	INTRODUCTION	1
2	ORIGIN OF PULSARS WITH PERIODS BETWEEN 0.1 - 0.3 SECONDS AND AGES BETWEEN 5×10^5 - 10^7 YEARS	5
2.1	Introduction	5
2.1.1	The P - \dot{P} Diagram	8
2.1.2	A Cornerstone in the History : PSR 1913+16	14
2.2	Further Quest	16
2.2.1	Testing the Origin of Pulsars with $0.1 < P$ < 0.3 s and with $5 \times 10^5 < \tau < 10^7$ yrs . .	17
2.2.2	Testing the Selection Effects	22
2.3	Conclusions	27
3	REMOVING THE DIFFERENCE BETWEEN CHARACTERIS- TIC AND REAL AGE OF MAGNETARS USING THEIR SPEC- TRAL DATA	29
3.1	Peculiar Properties of Magnetars	29
3.2	Phenomenological Impressions	34

	3.2.1	Age	35
	3.2.2	Magnetic Field	36
	3.2.3	Problems to Overcome	39
3.3		Running after Theory	41
	3.3.1	Early Models	41
	3.3.2	Models Based on Accretion	42
		3.3.2.1 First Generation Models	42
		3.3.2.2 Second Generation Models	46
	3.3.3	Magnetar Models	48
3.4		Notices on Spectra of Magnetars	49
	3.4.1	X-Ray Luminosities and Distances	53
	3.4.2	Black-body Temperatures	60
	3.4.3	Photon Index	63
3.5		Pulse Profiles and Some Spectral Properties of SGRs	65
3.6		Pulse Profiles and Some Spectral Properties of AXPs	68
3.7		Relations between Different Parameters of AXPs and SGRs	70
3.8		Discussion and Conclusion	72
	3.8.1	Removal of the Difference between τ and t	72
	3.8.2	Why Temperature and X-ray Luminosity of AXPs and SGRs do not Depend on the Degree of Activity?	78
	3.8.3	P- \dot{P} Diagram for Different Types of Neu- tron Stars	80
4		DEPENDENCE OF THE X-RAY LUMINOSITY AND PULSAR WIND NEBULA ON DIFFERENT PARAMETERS OF PUL- SARS AND ON THE EVOLUTIONARY EFFECTS	84
	4.1	Introduction	84
	4.2	Dependence of X-ray radiation of pulsars and their wind nebula on different parameters of pulsars	85
	4.3	The evolutionary factors	95
	4.4	Discussion and Conclusions	104

5	GENERAL CONCLUSIONS	108
	REFERENCES	114

LIST OF TABLES

2.1	Names, proper motions μ , distance (d), distance from the galactic plane $ z $ and $\log \tau$ values of 5 PSRs from the first sample and subsequent 12 PSRs from the second sample	22
3.1	Reliable observational and derived parameters of AXPs and SGRs. Period history and \dot{P} for SGR 0526-66 are not well known. Their values for this object may change up to two times. The data in the columns whose column number is marked with * is from Guseinov et al. (2003a).	51
3.2	Data of SNRs that are associated with AXPs and DRQNSs.	55
3.3	Data for DRQNSs. The + sign means that for DRQNS RXJ0002+62 46 the SNR age is used. The * sign is put to stress that \dot{P} value is calculated using the age of the SNR and other parameters such as B, \dot{E} are found from P and \dot{P} of this source. Data are taken from Guseinov et al. (2003a).	59
4.1	All 33 radio and X-ray pulsars with detected X-ray radiation in 0.1 - 2.4 keV and/or in 2 - 10 keV bands and with $\tau < 10^6$ yr. All 15 pulsars which have $\log \dot{E} > 35.6$ and $\tau < 10^5$ yr. All pulsars which are connected to SNRs (PWNe). Two of these pulsars are in Magellanic clouds and the others are Galactic pulsars with $d \leq 7$ kpc. In the first column G denotes strong glitch. In column 12 $\beta = 2\delta\theta/\theta$ (θ : SNR diameter, $\delta\theta$: angular distance of pulsar from the geometric center of SNR.)	87

LIST OF FIGURES

2.1	A general P - \dot{P} diagram that shows different types of pulsars all together. Only HMXBs are absent in this plot.	10
2.2	A portion of the P - \dot{P} diagram is displayed so that the groups of pulsars under study are clearly seen. Pulsars in the first group are shown with + whereas the ones in the second group are shown with o. The rest can be seen as small triangles	18
2.3	Distance from the galactic plane versus logarithm of the characteristic age is plotted. As the value of logarithm increases the age increases. (a) These pulsars are in the first group;(b) this time pulsars belong to the second group.	20
2.4	(a) The distribution of distances from the Sun for pulsars at different galactic longitudes in the first group;(b) the same distribution for pulsars in the second group.	24
2.5	Radio Luminosities at 400 MHz with respect to galactic longitudes are shown in (a) for pulsars in the first group; in (b) for pulsars in the second group.	25
2.6	Radio Luminosities at 1400 MHz with respect to galactic longitudes are shown in (a) for pulsars in the first group; in (b) for pulsars in the second group.	26
3.1	Scattering of X-ray luminosities with age in magnetars. The energy band of the luminosities is 1 - 10 keV. The SNR age is used if the object is connected to a SNR. For SGRs luminosities in their quiescent state are considered.	54
3.2	Black-body temperatures versus age of magnetars are seen. For SGRs quiescent data are used. AXP 1E1841-045, 1E2259+586 and DRQNS 1E0820-4247 and Cas A are connected to SNRs; for these objects SNR ages are used. Data for black-body temperatures are available in two energy bands 0.1 - 2.4 keV and 1 - 10 keV.	61
3.3	In this figure power law index (α) of magnetars and related objects DRQNSs are plotted with respect to their characteristic age. If the object is connected to SNR, SNR age is used. For SGRs data in their quiescent states are presented.	63

3.4	The time rate of change of period in magnetars is plotted against their X-ray luminosities. The luminosities are as usual cover the energy range 1 - 10 keV. SGRs are shown with their quiescent state data.	65
3.5	The distribution of black-body temperatures with respect to X-ray luminosities of magnetars can be seen in this figure. For SGRs data in their quiescent states are used.	70
3.6	Power law index (α) versus X-ray luminosities for magnetars are presented. For SGRs data in their quiescent state are used.	71
3.7	Pulsed fractions of magnetars are shown against their X-ray luminosities. Quiescent-state data are used for SGRs.	72
3.8	A slight dependence of power law index (α) on the black-body temperature of magnetars can be read from the figure. SGRs are indicated by their data in quiescent state.	73
3.9	P- \dot{P} Diagram for PSRs, AXPs, SGRs, XBs and DRQNSs. + symbol represents PSR, * represents AXP, box represent SGR, filled box represent DRQNS and x represent XB. For DRQNS RXJ0002+6246 \dot{P} is calculated using its period and age of the associated SNR. This source is indicated by the number 1 in the figure. It is necessary to take into account that \dot{P} values for magnetars with large \dot{P} may change up to two times.	80
4.1	Log L_x (2-10 keV) versus log \dot{E} diagram of all 30 pulsars with $\tau < 10^6$ yr which have observed X-ray radiation. 28 of these pulsars are located up to 7 kpc from the Sun and 2 of them are in Magellanic Clouds. '+' signs denote the 2 pulsars in Magellanic Clouds. 'x' signs show the positions of pulsars with $10^5 < \tau < 10^6$ yr and '*' signs show the positions of pulsars with $\tau < 10^5$ yr. '□' signs denote single X-ray pulsars. Seven of these pulsars have log B > 12.7 (denoted with 'B') and from 8 of them γ -rays have been observed (denoted with 'G').	90
4.2	Log L_x (2-10 keV) versus log τ diagram of all 30 pulsars with $\tau < 10^6$ yr which have observed X-ray radiation. 28 of these pulsars are located up to 7 kpc from the Sun and 2 of them are in Magellanic clouds. '+' signs denote the 2 pulsars in Magellanic Clouds. 'x' signs show the positions of pulsars with $10^5 < \tau < 10^6$ yr and '*' signs show the positions of pulsars with $\tau < 10^5$ yr. '□' signs denote single X-ray pulsars. Seven of these pulsars have experienced strong ($\Delta P/P > 10^{-6}$) glitches (denoted with 'G').	91

4.3	Log L_x (2-10 keV) versus $\log \dot{E}$ diagram for 15 of the 30 pulsars shown in figures 4.1 and 4.2; these 15 pulsars have $12.2 \leq \log B \leq 12.7$. '+' sign denotes the pulsar in Magellanic Cloud. 'x' signs show the positions of pulsars with $10^5 < \tau < 10^6$ yr and '*' signs show the positions of pulsars with $\tau < 10^5$ yr. '□' sign denotes the single X-ray pulsar.	98
4.4	Log L_x (2-10 keV) versus $\log \tau$ diagram for 15 of the 30 pulsars shown in Figures 4.1 and 4.2; these 15 pulsars have $12.2 \leq \log B \leq 12.7$. '+' sign denotes the pulsar in Magellanic Cloud. 'x' signs show the positions of pulsars with $10^5 < \tau < 10^6$ yr and '*' signs show the positions of pulsars with $\tau < 10^5$ yr. '□' sign denotes the single X-ray pulsar. ■ shows the positions of the pulsars which are present in Figure 4.2 but not included in the fit of this figure. . .	99
4.5	P versus \dot{P} diagram for all 48 pulsars represented in Table 4.1 with $\tau < 10^6$ yr and distance ≤ 7 kpc including the 2 pulsars in Magellanic Clouds. 'o' represents the 33 pulsars from which X-ray radiation have been detected in 2-10 keV and/or 0.1-2.4 keV bands. '+' signs denote the 15 pulsars with $\log \dot{E} > 35.55$ from which no X-ray radiation has been observed.	101
4.6	Log \dot{E} versus distance diagram for all 48 pulsars represented in Table 4.1 with $\tau < 10^6$ yr and distance ≤ 7 kpc including the 2 pulsars in Magellanic Clouds. 'o' represents the 33 pulsars from which X-ray radiation have been detected in 2-10 keV and/or 0.1-2.4 keV bands. '+' signs denote the 15 pulsars with $\log \dot{E} > 35.55$ from which no X-ray radiation has been observed. 'x' signs represent the 8 pulsars with $10^5 < \tau < 10^6$ yr.	102
4.7	Galactic latitude (b) versus Galactic longitude (l) diagram for all 48 pulsars represented in Table 4.1 with $\tau < 10^6$ yr and distance ≤ 7 kpc including the 2 pulsars in Magellanic Clouds. 'o' represents the 33 pulsars from which X-ray radiation have been detected in 2-10 keV and/or 0.1-2.4 keV bands. '+' signs denote the 15 pulsars with $\log \dot{E} > 35.55$ from which no X-ray radiation has been observed. 'x' signs represent the 8 pulsars with $10^5 < \tau < 10^6$ yr.	103

CHAPTER 1

INTRODUCTION

Publish and perish

Giordano Bruno

In the history of science critical improvements are principally achieved by phenomenological studies and deep physical intuition. In the early years of quantum mechanics, it is after Bohr's suggestion to Schrodinger that the energy levels in hydrogen atom are explained. Schrodinger analyzed the data on the emission lines and noticed that each line is separated from the other by a distinct amount which follows a rule as for the terms in a mathematical series. Later, in the development of particle physics, the Swiss theorist E. Stückelberg introduced the concept of baryon number (Veltman (2003)). Heavy phenomenological efforts differentiating the kind of reaction which is allowed and the one which is forbidden under the conservation of such a number helped to systematize our knowledge on particles.

The author believes that the same can be done in astrophysics where all the information we acquire heavily relies on observations. That is why special care

has been taken to gather reliable data since they are the starting point of the works presented in this thesis. The thesis is organized as follows:

In chapter 2 the $P - \dot{P}$ diagram is used to find the origin of some pulsars that have specific properties (Guseinov et al. (2004d)). In the first two parts we made an introduction to the subject by describing the $P - \dot{P}$ diagram and we talked about the historical concepts that our reasoning has the roots. The other sections describe how we proceeded step by step in building up our ideas. We discussed our results in the conclusions.

Nowadays, magnetars offer a wide field of research where many newly introduced ideas as well as previously developed theories compete. These diverse studies on magnetars will enlarge our knowledge about the fate of massive stars. The important effect of magnetic field in the evolution of stars will be interpreted more appropriately.

For this reason, in Chapter 3 almost all the data available in the literature are collected and presented in tables. These data are analysed in the light of the well-known facts in accretion theories and of the recently developed ideas in the magnetar model. While performing these analyses our primary motive was to remove difficulties in different models. Guseinov et al. (2003) collected and analyzed all the existing data on P and \dot{P} , noise and γ -ray bursts. As a continuation of this paper, we turn our attention to different physical parameters of anomalous X-ray pulsars (AXPs), soft gamma repeaters (SGRs) and dim radio quiet neutron stars (DRQNSs). The majority of their spectral characteristics is our concern (Guseinov et al. (2003c)).

In this chapter first few sections are prepared to introduce the general frame of the topic. Properties of the magnetars as well as the models are described. Following sections are devoted to the discussion of X-ray luminosities, black body temperatures and photon indices. In this section, we also give the reliable data for distances. We discuss the pulse profiles, the ratio of pulsed radiation to the total radiation and compare the spectral properties of anomalous X-ray pulsars and soft gamma repeaters in active and quiescent states. In the last section we discuss the implications of the new idea developed throughout the chapter. Combining the observational facts on the DRQNSs we search clues to establish a connection between these objects and magnetars. We propose an alternative evolutionary scenario to understand the nature of these objects. By this way we claim to overcome some severe problems of magnetar models such as the discrepancy between the characteristic ages of magnetars and the ages of their associated supernova remnants (SNRs).

Young pulsars are the subject of Chapter 4. That they can emit radiation in different energy bands make them a vulnerable research field. Moreover, supernova remnants are most likely seen around them. The connection itself is another topic that deserves deeper investigation. The nebula around the young pulsars are morphologically categorized and the fact that some remnants are powered by the central source has been known since from their discovery. Therefore, there may be possible ways to gain insight on both the remnants and the pulsars through observations. For this reason, we collected data about the parameters of ~ 50 young pulsars such as their periods, period derivatives, X-ray luminosities in two

energy bands, distances, types of the associated supernova remnant and its coordinates (Guseinov et al. (2004e)). We then derived some other parameters such as their rotational energy loss, magnetic field and their characteristic age. We looked for some correlations between all these parameters and we tried to analyse the effects of evolutionary factors on pulsar wind nebula.

The last chapter is devoted to the conclusions and discussion. We summarized our results and commented on them. Part of the ideas, if possible, are developed further.

*The reasonable man adapts himself to the world,
the unreasonable one persists in trying to adapt the world to himself.
Therefore, all progress depends on the unreasonable man.*

George Bernard Shaw

CHAPTER 2

ORIGIN OF PULSARS WITH PERIODS BETWEEN 0.1 - 0.3

SECONDS AND AGES BETWEEN 5×10^5 - 10^7 YEARS

L'histoire des Sciences montre que les progrès de la Science ont constamment été entravés par l'influence tyrannique de certains conceptions que l'on avait fini par considérer des dogmes. Pour cette reason, il convient de soumettre périodiquement à un examen très approfondi les principes que l'on a fini par admettre sans plus les discuter.

Louis de Broglie¹

2.1 Introduction

The spectacular growth of radio astronomy during the 20 years following the second world war was marked by the introduction of a series of new observational techniques, each of which opened new fields of research. Each advance in technology was applied initially to a specific problem, but guided the scientists into different directions. The discovery of the first pulsar is one of such unexpected events, although almost all of its general characteristics had already been worked out in the mean time between this surprising contact witnessed by English radio astronomers (Hewish et al 1968) and the pioneering work by Landau (1932) in

¹ "The history of science shows that the progress of science was hindered by the tyrannical influence of certain concepts that was considered as dogma. For this reason, it is suitable to put periodically the principles that we accept without discussing under dip examination"... Nouvelles Perspectives en Microphysique (New Perspectives in Microphysics).

which he mentioned the possibility of stars being composed of neutrons right after the discovery of neutron by Chadwick.

It is not possible to list all of the works but besides many unnoticed valuable studies it is worth referring to the remarkable ones. In 1934 two astronomers, Walter Baade and Fritz Zwicky, also proposed the existence of a new form of star, the neutron star which would be the end point of stellar evolution. In this way a possible connection between a supernova remnant and the formation of a neutron star was established. Later this possibility was renewed by Colgate and White (1966). The reason behind the emission mechanism of the Crab, the well known supernova remnant from the ancient Chinese time, was successfully explained by Shklovskii (1953) on the basis of synchrotron emission. The amount of energy that will be needed to feed the nebula was predicted to be $\sim 10^{38}$ erg/s by Pikel'ner in 1956. It was found that this energy should be continuously pumped into the environment.

Oppenheimer and Volkoff in 1939 made an important contribution. They talked about the stability of a star and formulated the hydrostatic equilibrium for the first time. They used the equation of state to predict the total mass, the density and the diameter of a neutron star. It turned out to be that the structure is strongly affected by the equation of state of matter at nuclear densities. Migdal's suggestion about the super-fluidity of neutron star matter in 1959 was proved to be very useful. What came next is the argument for the first time by Ginzburg (1964) that the magnetic field strength should be enhanced during the collapse of a star. His idea is based on the law of conservation of magnetic flux

in a conducting medium. At the same time Hoyle et al. (1964) as well as Woltjer (1964) were working on the strong magnetic fields of neutron stars. The rapid rotation of super-dense stars attracted the attention of Hoyle et al. 1964 and Tsuruta and Cameron (1966).

In 1967, Pacini's work signaled out the incoming of a clearer model. He stated that a rotating neutron star should act like a magnetic dipole and we should expect the neutron star to slow down due to magnetic dipole radiation. Finally, as a continuation to Pacini's ideas Gold's theory was widely accepted as a promising model. From then, pulsars have been identified as rotating neutron stars. Although many features are still waiting to be enlightened this model later named as **lighthouse model** provided a basic understanding. It simply says that the emission of a pulsar can be explained by a magnetic dipole radiation. It presumes two axes one of which is the rotation axis. The other axis is reserved for the magnetic field. In this picture a rotating magnetic dipole will induce an electric field and this field being incomparably stronger than the gravitational field will pull out charged particles from the surface of the star. As expected these particles are accelerated to extremely high energies around magnetic poles by the magnetic field and emit electromagnetic radiation at the frequency of rotation.

The emission from ultra-relativistic charged particles moving in a magnetic field should be concentrated in a beam along the direction of motion. If the magnetic field axis is inclined with respect to the rotation axis, as the star rotates the beam like emission pattern crosses the line of sight of the observer and is recorded in the form of a pulse per each stellar revolution. In this manner the

most peculiar property of a pulsar, that the radiation has a well defined periodicity, finds its explanation as a natural consequence of the model. It should be remembered that the pulsation idea was indicated for the very first time by Annuel and Guseinov (1968).

Growing interest on the subject has boosted the investigations. Countless observations have not only increased the number of pulsars but also shown an increase in their periods which indeed meant that they have been slowing down. Vast data sets concerning the period (P) and the rate of change of period in time (\dot{P}) have been gathered in a very short time. Centered on these key parameters endless efforts have been put forward to strengthen our theoretical background and ended up with an interestingly helpful tool.

2.1.1 The $P - \dot{P}$ Diagram

Any researcher in the domain of pulsars is expected to meet with the so-called $P-\dot{P}$ diagram. By all means it can be considered as the analog of the H-R diagram. It is not wrong to say that our current knowledge can be figured out through its guidelines.

Such a diagram is constructed in Figure 2.1 to establish a preliminary background and to follow the evolution of pulsars. The data was taken from the Internet site of the ATNF Pulsar Catalog. This online database has been known to be updated regularly but it should be kept in mind that some data may still need revision. Due to lack of their \dot{P} values some of the short period pulsars have been removed from the plot.

Although the primary motive in this work is to deal with a certain part of the single radio pulsars, just to show the general picture other types of pulsars are also indicated. Different symbols are used in order to distinguish one kind from the other. Plus sign is used for isolated pulsars. Circles signify the pulsars with a binary nature. Triangles show a problematic group. Filled triangles are for anomalous X-ray pulsars whereas unfilled ones are for soft gamma repeaters. Pulsars that are associated with a supernova are symbolized by squares.

With the simple model in our disposal fundamental characteristics of pulsars can be linked to P and \dot{P} . Fast rotation provides enormous rotational kinetic energy that can be calculated as $\dot{E} = 4\pi^2 I \dot{P} / P^3$, where I is the moment of inertia of the neutron star. A combination of spin period and the spin down rate yields the surface magnetic field. This is given by $B \simeq 3.3 \times 10^{19} (P \dot{P})^{1/2}$ G where the coefficient is found using the conventional values for the neutron star radius $R \simeq 10^6$ cm, the moment of inertia $I \simeq 10^{45}$ g/cm² for a spherical geometry and the basic electro-dynamical constants. Lines are drawn to demonstrate each of these physical quantities. Two of the constant rotational kinetic energy lines (light-dotted lines) are marked as 10^{35} and 10^{38} erg/s respectively just for reference. They give an idea about the energy budget of the single pulsars. Two of the constant magnetic field lines are labeled in terms of 10^{12} G with 1 TG and 10 TG respectively. One more concept remains to be placed on the graph: it is the age. Under the assumption that a pulsar has slow down significantly and its magnetic field has stayed constant during the evolution, the characteristic age $\tau_c = P/2\dot{P}$ can be accepted as a good approximation for the true age $t = \tau_c [1 - (P_0/P)^2]$ where P_0

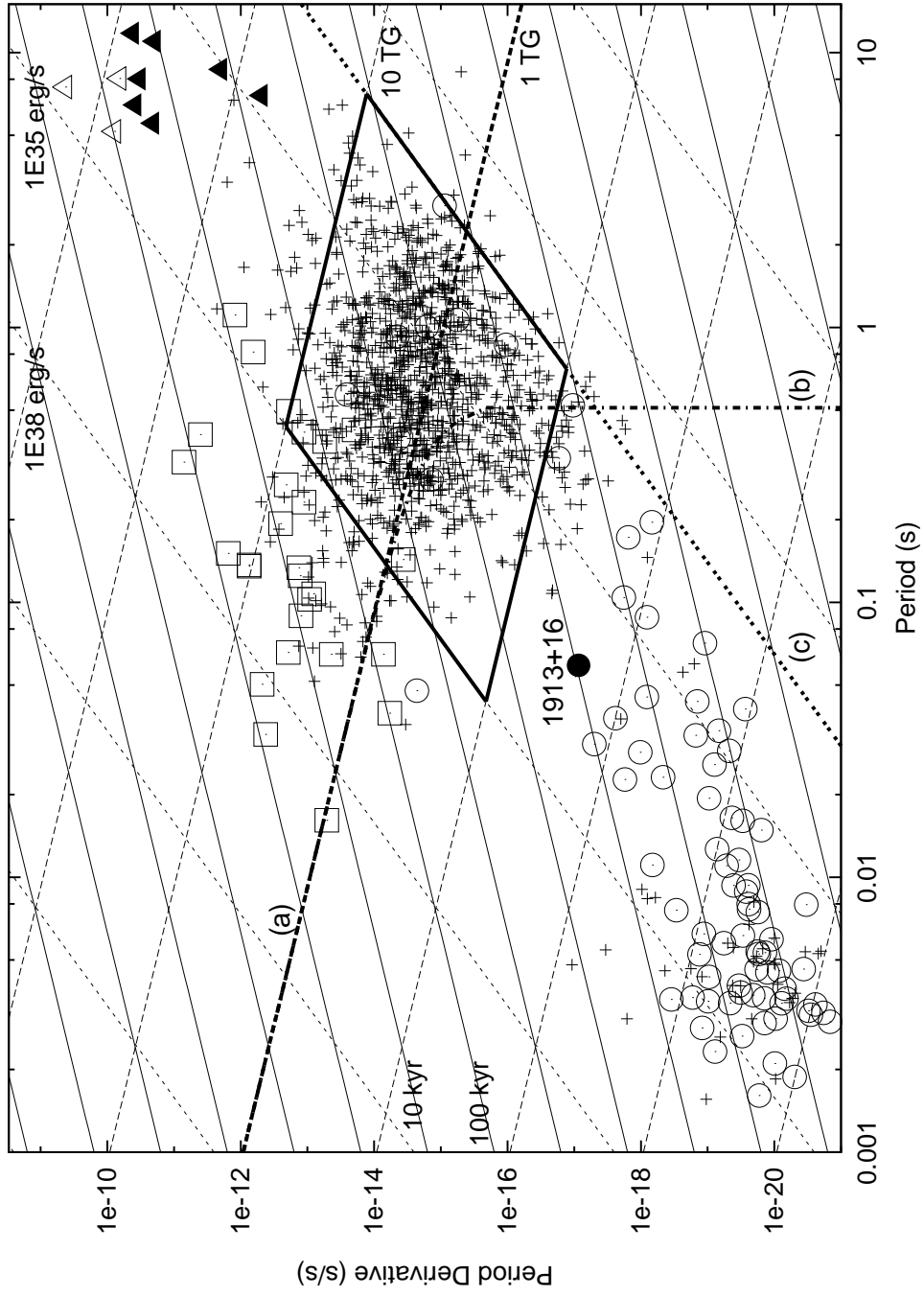


Figure 2.1: A general $P - \dot{P}$ diagram that shows different types of pulsars all together.

stands for the period of the pulsar at birth. Slightly tilted solid lines that extend from lower left corner to upper right corner represent the constant characteristic ages. This is the reason behind the complex diamond like appearance of any P- \dot{P} diagram. This pattern enables one to make good estimations and to test the predictions of any reasonable model.

At first sight it is easy to notice that pulsar population is largely confined to a certain area, which is highlighted by bold solid lines (see Figure 2.1). Within that region the magnetic field varies between 10^{11} G and 10^{13} G. The average period is close to ~ 1 s. Ages range from 10^5 yr to 10^9 yr. Averages values of 10^{12} G and 10^7 yr are apparent from the plot. The border on the right side falls on a line that has a specific meaning (line (c)). It is called the **death line**. With few exceptions that must be treated carefully no pulsars are seen below this line. Sturrock (1971) and Ruderman and Sutherland (1975) have suggested the pair creation due to the voltage generated by the pulsar as the cause of the emission. They have found a critical voltage value after which pulsar activity seems to cease. The value is approximately given by $B/P^2 \sim 0.2$ where B is the surface magnetic field in terms of 10^{12} G.

Another important point must also be stressed. Having in mind the nature of the event that gives birth to a pulsar, one might expect the new members to have short periods and high spin-down rates. This combination makes their appearance on the P- \dot{P} diagram towards the upper left corner of the pulsar population. Indeed, the existent pulsar supernova associations (data with square symbols) fall hopefully in this same region. Regarding the distribution within the validity

of data we can conclude that supernova remnants live up to a few 10^4 yr or at most 10^5 yr.

These observations and rough estimates fit well into the general picture: Pulsars are the evolutionary end products of a massive star which explodes at the end of its life as a supernova. They have high magnetic fields and manage to convert very effectively their rotational kinetic energy into electromagnetic energy by means of magnetic dipole radiation. Pulsars are born spinning fast, but as they age they slow down with a decreasing spin-down rate as long as the magnetic field remains constant during the evolution. The time spent between the birth and the crossing of the death line is taken as the lifetime of a pulsar. High magnetic field pulsars face their fate earlier than the low field pulsars. In that sense the importance of the magnetic field to a pulsar is much like the meaning of mass to a star. As a result if one were to follow the evolution of a pulsar on the $P-\dot{P}$ a typical path would be along the constant magnetic field line. An example which actually corresponds to $B=10^{12}$ G is shown with bold dashed line in Figure 2.1 (line (a)). In this framework the piling up of pulsars towards longer periods is easily understood.

► *How long are we going to be satisfied with this view? How effective is our understanding?*

In their attempt to answer these questions Gunn and Ostriker (1970) analysed mainly the distances of pulsars from the galactic plane ($|z|$). They recognized that locations of pulsars in the z direction was larger compared to massive stars and

supernova remnants and this height above the galactic plane was dependent on the period of the pulsar, thus on its age. At that time a class of objects, O-B stars, that have enormously large velocities were associated with supernova explosions in close binaries after Zwicky (1957) and Blaauw (1961); a proper motion for Crab was determined (Trimble 1968). Gunn and Ostriker linked these information and immediately concluded that pulsars may acquire high velocities at birth and migrate from the galactic plane with young pulsars being closer to the plane where they were born whereas older ones being traveled further away. Stimulated with these observational facts they also explained the long period cut-off in the period distribution of pulsars by magnetic field decay with a decay time $\sim 10^6 - 10^7$ yr.

According to this new idea pulsars are no longer allowed to travel along the constant magnetic field lines all the way down to the death line. As the magnetic fields decays, after a certain characteristic time there will be a deviation from the original trajectory. The track will begin to drop and eventually become vertical when the field decay starts to dominate the evolution. Since \dot{P} is proportional to B^2 , as the field strength diminishes the period will not change abruptly and converge to a limiting value. One of these possible ways is shown in Figure 2.1 (line (c)). For this line the decay time is 10^7 yr.

Later Lyne et al. (1982) found a way to estimate the ages of pulsars using their $|z|$ distances and transverse velocities. The results for the kinematic ages were systematically lower than the characteristic ages and provided strong evidence in favor of the field decay hypothesis. Alternative models in which the rotation axis

tends to align with the magnetic axis were sentenced by Michel and Golwire (1970) and by Davis and Goldstein (1970). Even though a simple exponential decay law could account for this behavior there was not efficient physical mechanism that would unite all the studies.

2.1.2 A Cornerstone in the History : PSR 1913+16

Following the line of reasoning of Zel'dovich and Guseynov (1964), Hayakawa and Matsuoka (1964), Novikov and Zel'dovich (1966) and Shklovskii (1967) Scorpion X-1 (Sco X-1), which was discovered by Giancoli et al. (1963), was identified as the first high mass x-ray binary (HMXB). Until the launch of the first x-ray satellite UHURU in 1971 a many HMXBs were determined in rocket flights. This is understandable since massive stars can easily be observed in the optic band. Besides, the main aim in rocket observations was rather to locate the possible sources than to resolve them with high sensitivity. Researchers became aware of a growing number of low flux x-ray sources throughout the operation of UHURU. Their origin was first considered to be extra-galactic. A new wave of information spread. Data of many LMXBs presented in Giacconi et al. (1973) were analysed and most of the properties of this population were understood. Even using the poor data of Nova Cen X-2 (Harriees 1967, Rao et al. 1969) and Cen X-4 (Evans et al. 1970) their nova type explosions and their light curves were predicted by Amnuel et al. (1973,1974). However, the absence of radio pulsars in binaries was struggling.

During the course of discussions the detection of the binary radio pulsar PSR

1913+16 by Hulse and Taylor (1975) had a double fold impact. The companion star was also a neutron star. This matter by itself was fascinating. Accurate timing measurements were done to test the statements of general relativity. The second striking property of this system was the combination of short rotation period (59 ms) and low magnetic field ($B \sim 3 \times 10^{10}$ G). The shortness of the spin period pointed out the youthfulness of the pulsar. On the other hand magnetic field was almost two order of magnitude lower than that of a typical pulsar. One might put aside this case as an exception, but the binary nature of the source still leaves the case suspicious. Two exceptions at one time would be too much. Moreover, if the low magnetic field is to be understood in terms of decay we would expect a long period, not a short one.

The puzzle seemed to be solved with the help from Bisnovatyi-Kogan and Komberg (1974,1976). In their papers they discussed the relationship between radio pulsars and close binaries in which they might have been formed. They also mentioned that the pulsar can accrete matter from its companion. In the accretion phase the pulsar can be seen in x-rays and its rotation should be accelerated while its surface magnetic field should weaken importantly. After accretion has ceased it possess a remarkably weak field. When the x-ray phase ends and the companion star explodes as a supernova the pulsar is released as a radio pulsar. The binary can remain bound or be disrupted depending on the dynamics of the explosion. Consequently, the existence of millisecond pulsars with $B < 3 \times 10^{10}$ G was predicted in these articles.

We can therefore conclude that the investigations of LMXBs led to very important results not only for x-ray astronomy but also for radio astronomy.

2.2 Further Quest

During the last ~ 40 years the evolution of single pulsars has been studied on the P- \dot{P} diagram. Today, we may roughly explain the locations of pulsars on different parts of this diagram. However, it is still difficult to understand why a large number of them have periods in the interval 0.1-0.3 s and magnetic fields between 10^{11} and 10^{12} G.

In pursuit of likely explanations we concentrated on two groups of pulsars. One group is the subject of our interest whereas the other one can be thought as a control group by which we check the validity of our arguments. In order to do reliable comparisons we put some restrictions on the data. These criteria are necessary to deal only with a sample of single pulsars and to see clearly the regions where the examined pulsars are located.

We had to limit the distances. There are several vigorous opinions behind this act. When the distances are projected onto the galactic plane the clustering around the Sun is noticeable. The number of pulsars significantly drops after almost 4-5 kpc beyond the Sun. While dispersion measure is the most common method of finding distances, the electron density distribution that this method heavily relies on is unfortunately not precisely established. As a result as we go deeper towards the galactic center we are more likely to face with unwanted deviations. Thus the farther the pulsars are the larger the error is in their distances.

On the top of that, many distant pulsars were discovered in recent surveys especially at narrow latitude intervals (for complete data see ATNF Pulsar Catalog (2005), Guseinov et al. (2003) and the references therein). None of the previous searches so far had such a sensitivity. This might have created a bias for our work. Therefore, we took 5 kpc from the Sun as the upper limit.

The members of both groups have similar characteristic ages. The number of the members in each group is almost the same so that their number versus age distributions are similar. We believe that the second group represents a sample of pulsars with typical properties. For this group the period ranges from 0.6 s to 1.3 s. Their characteristic ages are between 6×10^5 yr and 10^7 yr. Accordingly \dot{P} is greater than 3×10^{-15} s/s. On the other hand, the first group that we focus on has the following boundaries. Period values changes between 0.1 s and 0.3 s. Ages go from 5×10^5 yr to 10^7 yr. Under these circumstances we think that evolutionary tracks of both of the groups will be similar on the P- \dot{P} diagram so that it will be more logical to compare any apparent differences.

2.2.1 Testing the Origin of Pulsars with $0.1 < P < 0.3$ s and with $5 \times 10^5 < \tau < 10^7$ yrs

In accordance of our criteria a P- \dot{P} diagram showing the groups we are working on is plotted in Figure 2.2. Some arrangements are made on the figure. Pulsars in the first group are marked with +. The other group appears as circles. Two constant characteristic age lines (line (a) for $\tau_c = 5 \times 10^5$ yr and line (b) for $\tau_c = 10^7$ yr) are traced bold to realize the boundaries better. Arrows are placed on

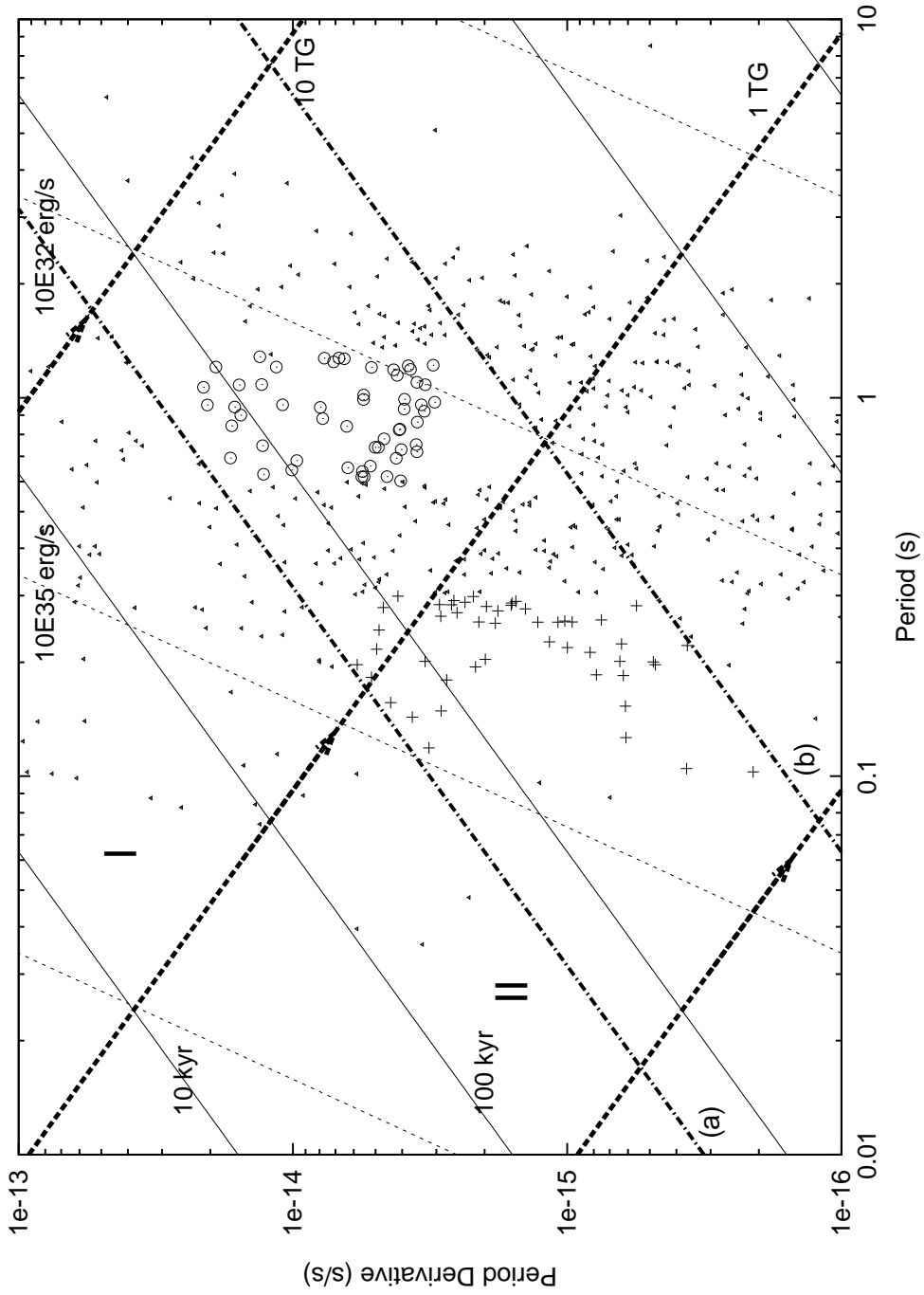


Figure 2.2: A portion of the $P - \dot{P}$ diagram is displayed so that the groups of pulsars under study are clearly seen. Pulsars in the first group are shown with + whereas the ones in the second group are shown with o. The rest can be seen as small triangles

the constant magnetic field lines to indicate the direction of usual evolutionary trend. The place in between the constant magnetic field lines corresponding to $B = 10^{12}$ G and $B = 10^{13}$ G is numbered as I. Similarly the region numbered as II lies between constant magnetic field lines having $B = 10^{11}$ G and $B = 10^{12}$ G. Some other useful data of the pulsars are listed in Table 2.1.

Looking carefully at the graph we see that all the pulsars that are aged up to 10^5 yr have magnetic fields higher than 10^{12} G. In addition to this all 23 pulsars which have genetic connection with a supernova remnant are found in this part of the P- \dot{P} diagram. Thus without any doubt pulsars are mostly born in this region and have almost always these magnetic field values. However, we can not completely exclude the possibility of possessing magnetic fields several times lower than the conventional value at birth, at least for some of them.

We can also read from the figure that up to line (a) region I is more populated than region II where the number is unequivocally small. The situation changes rapidly when we pass to the right of line (a). Region II becomes comparably populated. Many pulsars that belong to our first group suddenly pop up. In contrast such a discontinuity does not occur in region I.

We may justify these observations by following another approach. For this reason, we analysed $|z|$ distribution of pulsars in our samples. Distance from the galactic plane ($|z|$) versus characteristic age (τ) are represented for both of the groups in Figure 2.3 (see Table 2.1 and the references cited in the table for data).

As it is seen, for the pulsars from the first group there is not an apparent

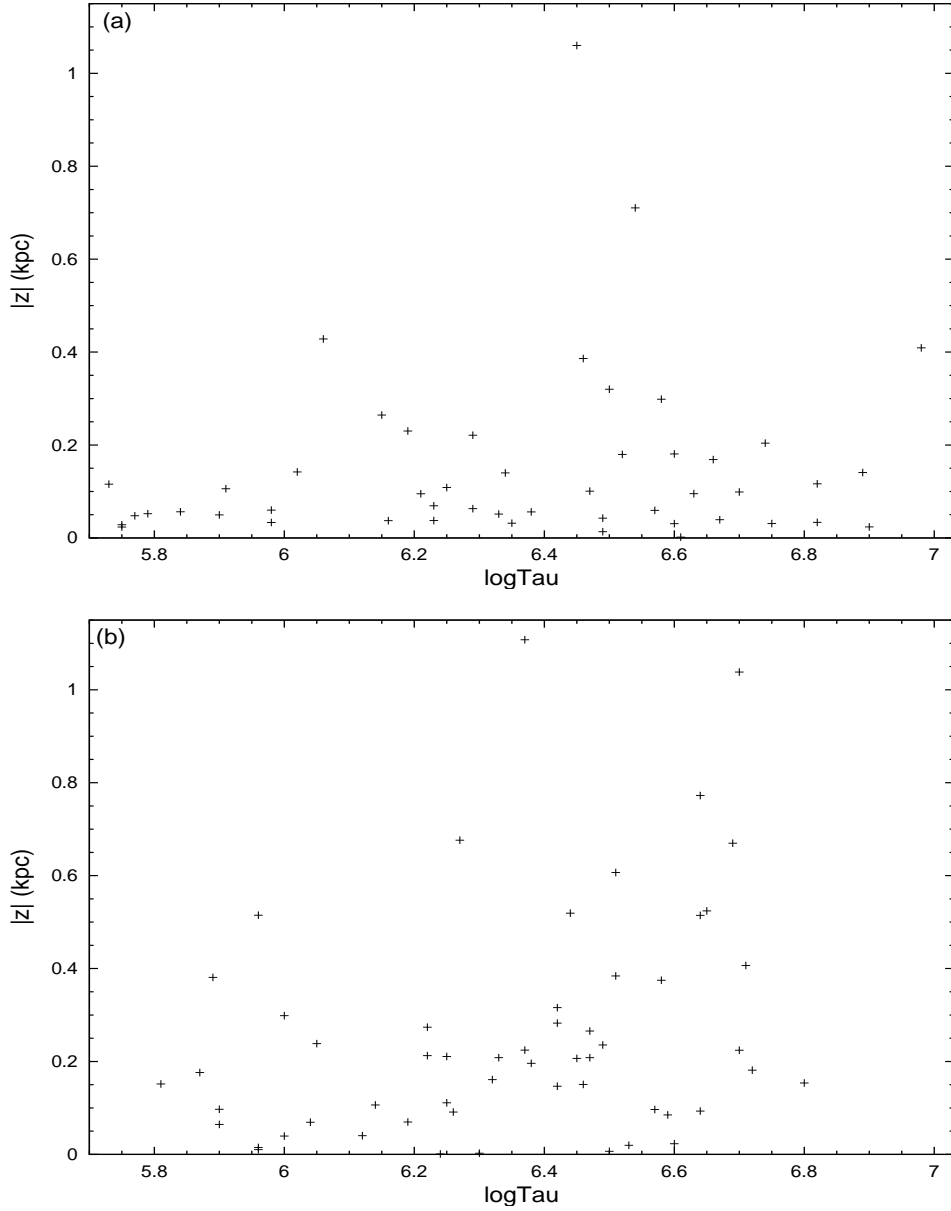


Figure 2.3: Distance from the galactic plane versus logarithm of the characteristic age is plotted. As the value of logarithm increases the age increases. (a) These pulsars are in the first group;(b) this time pulsars belong to the second group.

correlation between $|z|$ and τ . There is no considerable increase in $|z|$ with increasing τ . At every age there is a large number of pulsars at lower $|z|$ values. It can be argued that for younger pulsars in Figure 2.3(a) the height above the galactic plane seems to increase with age, but there is not a linear proportionality

whereas for the second group a linear dependence is obvious. The dependence in Figure 2.3(b) is acceptable since these single born pulsars can move away from the plane due to their high velocities. By the time they got old they should have traveled large distances. This is, indeed, in complete accordance with a wide spread in $|z|$ towards higher τ . We surely noticed that members of the first group have on the average smaller $|z|$ then those of the second group. For the sake of safety we carried the same analysis for an older sample ($10^7 \text{ yr} < \tau < 10^8 \text{ yr}$) and saw the same dependence that appeared in the control group. However, at such ages changes in the beaming factor and decrease in the pulsar voltage start to affect the population, hence start to create uncertainties. Naturally this may influence the average value of $|z|$.

Thinking simple, the path taken is related to the velocity along that path. The space velocity for each pulsar can be calculated knowing its proper motion (Lyne et al. 1982, Bailes et al. 1990, Harrison et al. 1993, Fomalont et al. 1997) and its distance (Guseinov et al. (2004)). The proper motion itself comes from interferometric and scintillation measurements. As Table 2.1 indicate pulsars from the first group have low space velocities.

As a final statement we found that kinematic characteristics of these two groups are actually different. As the magnetic field of single pulsars with ages $5 \times 10^5 - 10^7 \text{ yr}$ almost do not change, both of the groups will continue to live within regions I and II and their evolutionary behaviors will resemble each other. The smallness of average $|z|$ and the lack of young pulsars with short periods in region II all point out that some of the pulsars with $B \simeq 10^{11} - 10^{12} \text{ G}$ and $P \simeq$

Table 2.1: Names, proper motions μ , distance (d), distance from the galactic plane $|z|$ and $\log \tau$ values of 5 PSRs from the first sample and subsequent 12 PSRs from the second sample

PSR	μ (mas yr^{-1})	d ^e (kpc)	$ z $ ^f (kpc)	$\log \tau$ ^f
J0358+5413	13.9 ^a	2	0.028	5.75
J1453-6413	26.9 ^b	1.84	0.142	6.01
J1559-4438	14.0 ^a	1.63	0.181	6.60
J1932+1059	88.1 ^c	0.2	0.013	6.49
J2055+3630	4.2 ^d	4.2	0.409	6.98
J0502+4654	11.3 ^d	1.7	0.091	6.26
J0630-2834	38.1 ^a	1.8	0.519	6.44
J0653+8051	19.0 ^d	2.3	1.038	6.70
J0837+0610	51.0 ^c	0.6	0.266	6.47
J0946+0951	43.4 ^c	0.98	0.670	6.69
J1136+1551	371.3 ^c	0.24	0.224	6.70
J1509+5531	99.8 ^c	1.4	1.108	6.37
J1709-1640	3.0 ^a	0.9	0.212	6.21
J1913-0440	8.6 ^d	3.1	0.384	6.51
J1919+0021	2.2 ^d	2.95	0.316	6.42
J2225+6535	182.4 ^d	2.0	0.238	6.05
J2354+6155	22.8 ^d	3.1	0.010	5.96

^a Fomalont et al. (1997)

^b Bailes et al. (1990)

^c Lyne et al. (1982)

^d Harrison et al. (1993)

^e Guseinov et al. (2004)

^f ATNF Pulsar Catalog

0.1 - 0.3 s are born with these characteristics and are directly placed in the low-B large- τ part of the P- \dot{P} diagram.

2.2.2 Testing the Selection Effects

Sensitivity of radio telescopes, the interstellar medium, flux limitations as well as other technical difficulties and the radio spectrum of pulsars are some of

the factors that are categorized as selection effects. They affect the statistical distribution of pulsars and shape our knowledge.

- *Can it be true that different velocities and average $|z|$ values arise because other properties of pulsars under consideration are different? Do the important differences that we saw between Figure 2.3(a) and Figure 2.3(b) depend on the distance?*

Omitting all other variables and concentrating only on a specific latitude (b) and longitude (l) we wait for $|z|$ to increase with distance as we go away from the Sun. For both of the groups we plotted in Figure 2.4 the distance from the Sun (d) versus the galactic longitude (l) and searched for a sharp difference (see Guseinov et al. (2002) for distances from the Sun and ATNF Pulsar Catalog for galactic longitudes). On the contrary, from Figure 2.4(a) and Figure 2.4(b) we deduced that pulsars in the second group are on the average slightly more distant from the Sun than those in the first group.

- *Can radio luminosities matter?*

The irregular nature of the interstellar medium is responsible for several effects. One of them is the scattering of radiation from free electrons. The result is a broadening in the pulse shape. This smearing becomes most severe for distant pulsars. Another aspect of the event is the reduction of observed flux at a certain frequency due to a rough dependence as $1/\nu^4$. For a given luminosity the flux falls off as the inverse square of the distance and may vary with position on the sky.

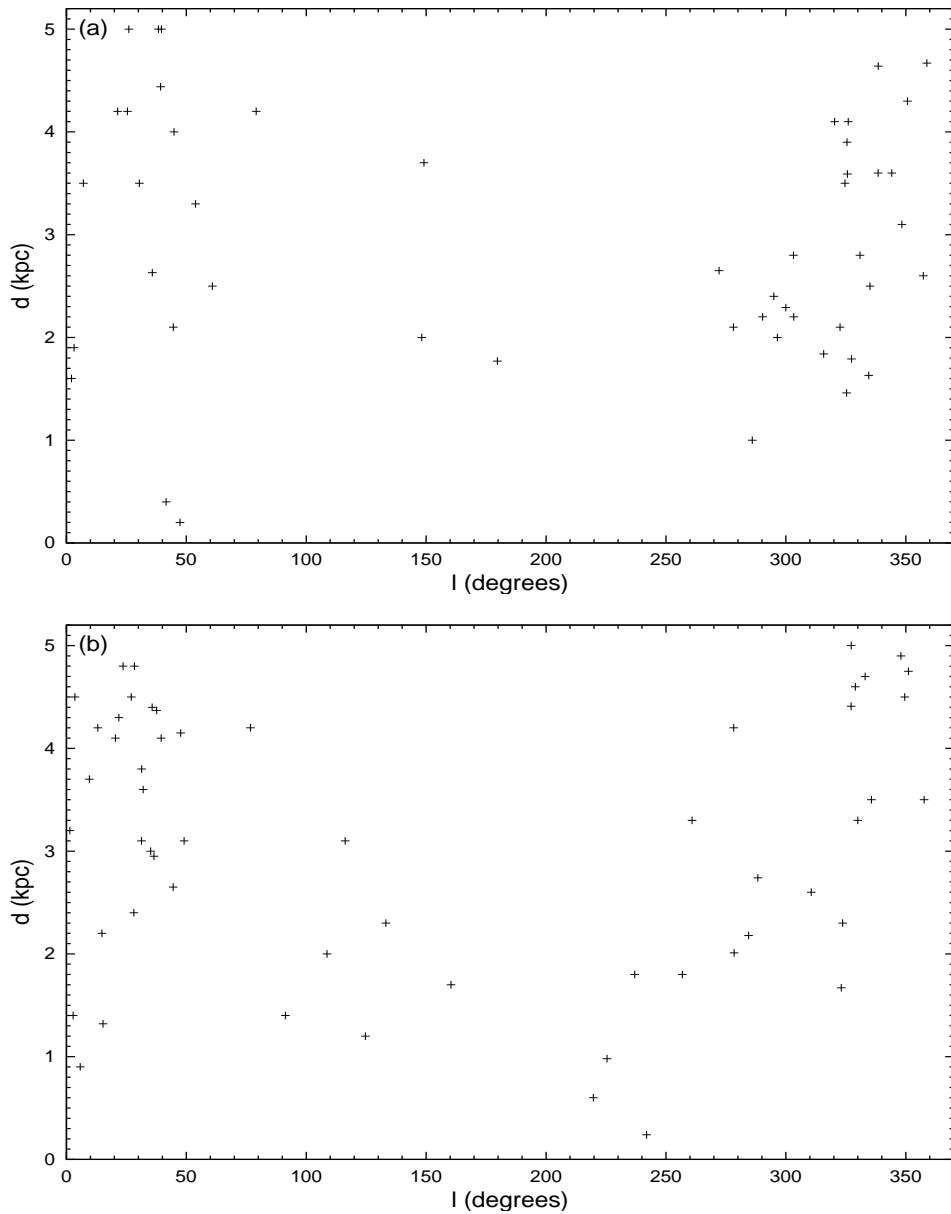


Figure 2.4: (a) The distribution of distances from the Sun for pulsars at different galactic longitudes in the first group;(b) the same distribution for pulsars in the second group.

To get rid off the irregularities, different searches with various sensitivities were performed at different frequencies. Most preferred ones are 400 MHz and 1400 MHz. We collected luminosities at these frequencies and plotted the logarithm of them with respect to galactic longitude (l) (see ATNF Pulsar Catalog for the

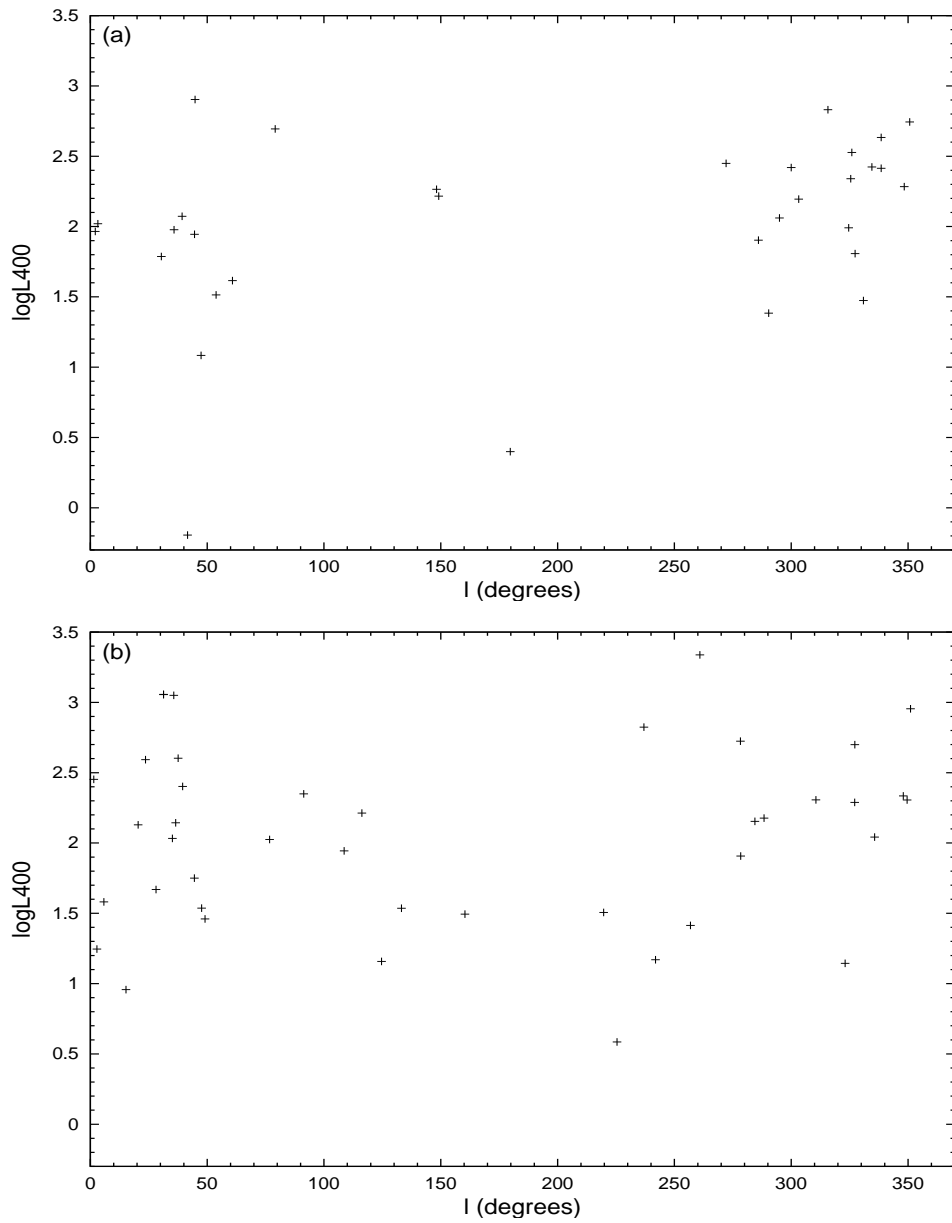


Figure 2.5: Radio Luminosities at 400 MHz with respect to galactic longitudes are shown in (a) for pulsars in the first group; in (b) for pulsars in the second group.

data). Logarithm of the luminosities at 400 MHz versus (l) are shown in Figure 2.5 whereas logarithm of the luminosities at 1400 MHz versus (l) can be seen in Figure 2.6 for our samples.

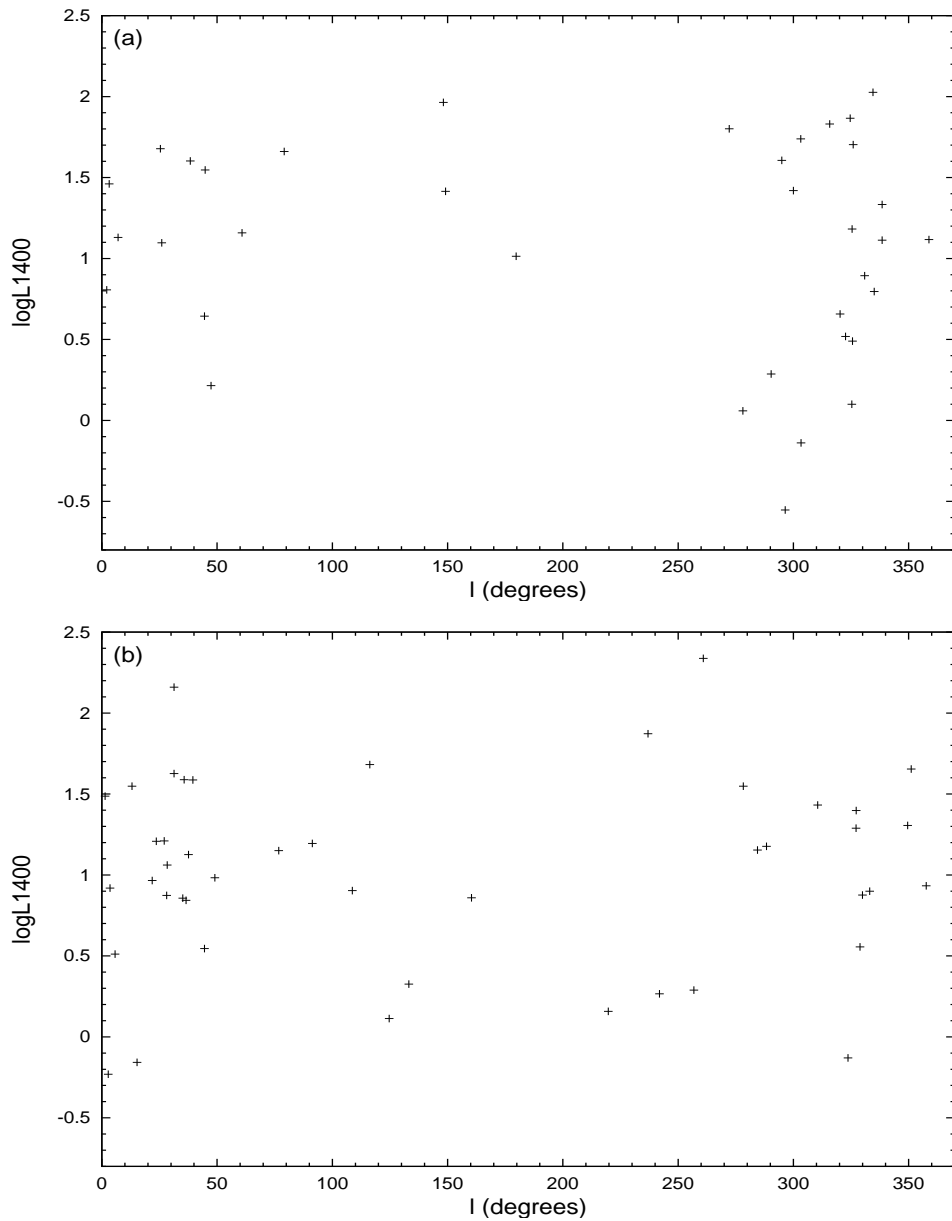


Figure 2.6: Radio Luminosities at 1400 MHz with respect to galactic longitudes are shown in (a) for pulsars in the first group; in (b) for pulsars in the second group.

In general it is known that radio luminosities of PSRs depend very weakly on their locations on the $P-\dot{P}$ diagram. Taking into account their locations all the pulsars in our groups should have similar luminosities. The distribution in the figures supply the evidence we need. We declare that neither the distances nor

the luminosities can alter our conclusions. They can not cause selection effects.

2.3 Conclusions

Motivated by our analysis we assert that part of the pulsars in the first group might have been appeared after a second supernova explosion in high mass x-ray binaries (HMXBs). In this way, after the explosion in the massive binary, X-ray pulsar must also be detected as a radio pulsar. If we compare a pulsar having such origin with a single born pulsar, the former must have several times smaller magnetic field compared to the single born pulsar even though both of them have the same initial magnetic field strengths, because there occurs magnetic field decay due to the accretion during the HMXB phase. This process is similar to the one that takes place during disk accretion in LMXBs (Bisnovatyi-Kogan and Komberg (1974,1976)).

These pulsars must conserve their orbital and center-of-mass velocities, the sum of which is on the average smaller than the space velocity of single born pulsars. As a supporting idea, distances of HMXBs from the plane of Galaxy are observed to be small. Therefore, real ages of the discussed pulsars may be smaller than their characteristic times. They must have small space velocities and their distances from Galactic plane must also be smaller than the single born pulsars with comparable ages. On the other hand, among two pulsars at the same age the one with a binary history must have significantly larger X-ray luminosity than the single born one because the time it has spent as a radio pulsar is smaller than the value of its characteristic time.

Examining the X-ray data in 0.1-2.4 keV and in 2-10 keV bands which were published by Becker and Trumper (1997), Becker and Aschenbach (2002) and Possenti et al., (2002) we remarked that radiation in x-rays was detected from PSRs J1057-5226, J0358+5413, J0538+2817 and J1932+1059. All of these PSRs belong to our first group and there is no other pulsar with τ in the interval $5 \times 10^5 - 10^7 yr$ from which X-ray radiation was observed. Two of the pulsars mentioned in these lists, namely J0826+2637 and J0953+0755, have several times larger characteristic times. Both of them are directly located in the belt along which pulsars from the first sample evolve. Another three pulsars observed in x-rays, namely J1952+3252, J0117+5914 and J1302-6350, are located on the P- \dot{P} diagram right in front of the first sample of pulsars, as they have $10^5 < \tau < 5 \times 10^5$ yr. Only Geminga pulsar which has a magnetic field about 1.7×10^{12} G is on the boundary of the second sample. All other pulsars in the lists are old millisecond pulsars.

We have given the impression that all our expectations are in agreement of what we have suggested about the origin of the pulsars having short periods in combination with gradually lower magnetic fields.

*Nel mezzo del cammin di
nostra vita
mi ritrovai per una selva
oscura
ché la diritta via era
smarrita
Dante²*

² "Midway upon the journey of our life, I found myself within a forest dark, for the straight-forward pathway had been lost"... Inferno-Canto I.

CHAPTER 3

REMOVING THE DIFFERENCE BETWEEN
CHARACTERISTIC AND REAL AGE OF MAGNETARS
USING THEIR SPECTRAL DATA

... for they are yet but ear-kissing arguments.

William Shakespeare¹

3.1 Peculiar Properties of Magnetars

A series of events at the end of 1970's revealed new mysteries to be solved by the astronomers. Following years became the era of competing new ideas.

One of these challenging events at that time was the discovery of an extraordinary new X-ray source. It was observed with the Einstein X-ray observatory on 17 December 1979, and was later called as 1E 2259+586. This source was reported to be located near the geometrical center of a supernova remnant (SNR) G109.1-1.0, which is also known as CTB 109 (Gregory & Fahlman (1980), Fahlman & Gregory (1981)). Estimations depending on different methods placed it at a distance between 3.6 and 5.6 kpc (Crampton et al. (1978), Tatematsu et al. (1987)

¹ King Lear

and Hughes et al. (1984)). This pulsar was said to be a young neutron star based on the estimated age of the associated SNR between 3-20 kyr (Rho & Petre (1997), Parmar et al. (1998), Hughes, Harten & van den Bergh (1981)) and its period was measured as 6.98s (Fahlman & Gregory (1981)). The spectrum of 1E 2259+586 consisted of a power law feature with an index $\alpha \sim 3.9$ and a black-body spectral component around ~ 0.4 keV (Corbet et al. (1995), Parmar et al. (1998)).

In astrophysics, in general, when a new object like the above X-ray pulsar enters into the field of research it is compared with a star or group of stars whose characteristics are well established and closest in nature. Any comparison with either high mass X-ray binaries (HMXBs), low mass X-ray binaries (LMXBs) or ordinary radio pulsars (PSRs) was therefore inevitable. As a result of long-run studies it was found that though its surprising behavior 1E 2259+586 was not on its own. Several other X-ray pulsars (XPs) were shown to have similar characteristics. After many trials the name anomalous X-ray pulsars (AXPs) which was thrown out in a conference by Thompson & Duncan in 1992 was attributed to this new family. The properties that were enough to make these objects classified as a distinguished group can be listed as follows (Mereghetti (2001a) and Mereghetti (2001b) for reviews and Tables 3.1 - 3.3 for detailed data):

- ▶ Contrary to most of the XPs they have softer spectra which can be decomposed into a power law with index $\sim 3 - 4.5$ and a black-body component

around ~ 0.44 keV.,

- ▶ They possess relatively low X-ray luminosity varying between 10^{34} - 10^{36} erg/s.,
- ▶ Measured spin periods fall in a band between 5 - 12 s.,
- ▶ They show stable spin period evolution with a long-term fast spin down trend.,
- ▶ Almost half of them are associated with SNRs.,
- ▶ In spite of intense searches no optical components were identified. Lack of orbital parameters put severe constraints on the mass of the possible companions.,
- ▶ No significant level of variability was observed in their X-ray flux on time scales from hours to years.

Similar developments were also seen in the γ -ray astronomy during these years. Since their discovery in late 1960's very little was known about γ -ray bursts. Due to very preliminary analysis on the first data sets, the only fact that was apparent was their distribution in the universe implying a cosmic origin. In this context, observation of a burst from a source which will later be known as SGR 1806-20 on January 7 1979 did not attract much attention except being gradually less energetic than the commonly known bursts. Later in the same year on March 5 1979 the situation became complicated with the discovery of

an unusually energetic γ -ray burst. The origin of the explosion is now known as SGR 0526-66, which is found in Large Magellanic Cloud (LMC). This burst was so powerful that it was noticed by all the satellites and gained fame as the March 5th event. Only after 19 days a third important source, currently named as SGR 1900+14, was detected on March 24 1979. None of these sources at the time of their discovery were analysed separately from the rest of the γ -ray bursts. As time went by, observers realized that these three objects have softer spectra. Moreover, several other bursts were recorded from these objects. This means that in opposition to the ones of cosmic origin that are single short-time events, these bursts exhibit interestingly a repeating behavior. Therefore, researchers put them aside and described them as soft gamma repeaters (SGRs). Statistical analyses revealed that (see for details Hurley (2000) and Tables 3.1 - 3.3)

► Two types of activity were reported.,

- Short bursts: There exist ~ 40 large outbursts during an active period. The peak luminosity of the bursts is in general few 10^{41} erg/s and is followed by a less energetic tail emission. Numerous (~ 100) mini bursts occur in the form of bunches between the large ones (Kouveliotou et al. (1996a), Kouveliotou et al. (1996b)). The spectrum can be considered soft with respect to normal γ -ray bursts with $kT \sim 20 - 65$ keV. They last approximately 0.1 s.
- Giant bursts: These violent events happen rarely and can emit energies of the order of 10^{44} erg or $kT \geq 1$ MeV. The duration is $\sim 0.2 - 1$ s.

A several minutes-long tail emission with ~ 30 keV spectrum is also seen.

- ▶ In quiescence (i.e., no burst activity) they have relatively faint and soft spectra which can be explained by a power law with index $\sim 2-3$. A black-body component of 0.4 - 0.5 keV can be added.,
- ▶ Spin periods change from 5 - 8 s.,
- ▶ Quiescent X-ray luminosities are given as \sim few 10^{34} - 10^{35} erg/s.,
- ▶ They are continuously slowing down with fast spin down rates.
- ▶ No convincing evidence was mentioned on possible SNR associations (Gaensler & Slane et al. (2001))

Until Thompson & Duncan (1995), (1996) drew attention to the similarities between the two sets of properties, AXPs and SGRs were considered as two distinct type of objects. They suggested that AXPs and SGRs should no longer be treated independently, but as if they belong to the same class. From then, they are unified under the name of magnetars, which is invented originally to explain SGRs in 1996 again by Duncan & Thompson. Moreover, most recent studies seemed to support the idea of unification. The strongest evidence was the detection of bursts, which are less energetic but otherwise qualitatively similar to those of SGRs, from two AXPs: 1E 2259+586 and 1E 1048.1-5937 (Gavriil et al. (2002), Kaspi & Gavriil (2002)). There appeared some other works that pointed out other aspects. An optical counterpart was suggested for 4U 0142+61

by Hulleman et al. (2000). New features like the pulsed flux up to 100 keV and hard tail emission came out in the timing and X-ray spectra of 1E 1841-045 (Kuiper et al. (2004)). Significant change in the X-ray flux of 1E 1048.1-5937 (Mereghetti et al. (2004)) was later justified by the presence of flares with > 100 days duration and an energy of 10^{41} erg (Gavriil & Kaspi (2004)). Almost 1.5 year after the first, Vela-like glitch (Kaspi et al. (2000)), a second, this time Crab-like glitch occurred in 1RXS J170849-400910 (Dall’Osso et al. (2003)). It looked like new questions were raised on the top of the previous ones. Any future predictions should consider carefully these informations in order not to be far from providing a satisfying solution.

3.2 Phenomenological Impressions

To know the field we are working on and to realize possible problems we can face, it might be a good idea to concentrate on the general features of magnetars. While doing this we will frequently refer to the properties of other astrophysical objects. We will try to develop gradually our understanding based on the observational facts and search for the answers of questions like:

- ▶ *What is their nature? What makes them so interesting? Which parts of our theories may need revision or extension?*

The most direct piece of information is the spin period (P) and its rate of change in time (\dot{P}). For this reason it is natural to look for some clues in the $P - \dot{P}$ diagram (see Figure 2.1). Looking at this diagram we immediately see that

members of this family are located in the upper right corner (data with filled triangles for AXPs and with unfilled triangles for SGRs). They form an isolated island.

3.2.1 Age

In the frame of our fundamental theories long spin periods, which is on the average ~ 8 s, means that these pulsars are very old. This value is almost an order of magnitude larger than the average value for PSRs. It is, of course, many times higher than the young PSRs and the ones in binaries in the diagram. We do not expect to see PSRs with spin periods this much high as they should have already passed the death line after which their level of radiation drops significantly. On the other hand, if we analyse \dot{P} values of magnetars we see that they are very high. This leads us into confusion about their ages. If we need to make a comparison we can only suggest the youngest PSRs although they can not match these spin-down rates. Thus, we may suggest that magnetars are young objects. It seems that we can justify this suggestion with some observations.

The $|z|$ values of AXPs and SGRs are very small (van Paradijs et al. (1995)). They are all located on the galactic plane (GP) at distances as far as $\sim 5 - 10$ kpc (see Table 3.1). It is extremely possible to find SNRs that have a probable connection with them. Indeed, three out of five AXPs are claimed to be genetically connected to SNRs. Though it needs some additional assumptions two SNRs can reasonably said to be linked with SGRs (Ankay et al. (2001), Tagieva & Ankay (2003)). Knowing that all young PSRs including the distant ones with

$\tau \lesssim 2 \times 10^4$ years are practically associated with SNRs (Guseinov et al. (2004), Kaspi & Helfand (2002)) we may limit the ages of magnetars to 10^4 or at most 10^5 years. As can be seen in Figure 2.1 direct calculations depending on their period and period derivatives give even smaller ages between 10^3 and 10^4 years. These connections are important in that we can define better distances for AXPs and SGRs. Using the SNR distances we can find more appropriate luminosities within certain limitations.

3.2.2 Magnetic Field

Glitches are rapid and unexpected changes in the spin period of the pulsars. Star-quakes and/or magnetospheric instabilities are thought to be the generating mechanisms (Ruderman (1969), Baym & Pines (1971)). Under the effect of these processes the crust of the neutron star spin-up rapidly since the response of the charged particles to this effect is fast whereas the response of the super-fluid matter is considerably slow. As a result, the spin period of the pulsar rises suddenly and returns gradually to its spin-down trend. These events are not observed in pulsars older than 10^5 years. They may be considered as one of the aspects in favor of the youthfulness of magnetars although no other magnetar apart from 1RXS J170849-400910 produced glitches. The parameters were very similar to those seen in young PSRs and there is a possibility for other magnetars to glitch. However, observations are far less to drive any conclusion.

From the point of energetic the role of magnetic field is obvious. During the formation of neutron stars the kinetic energy, that is required for the expansion of

the supernova envelope, can be supplied by a magnetic field twisted between the neutron star and the envelope (Amnuel et al. (1973)). Single PSRs slow down very effectively by losing their energy through magnetic dipole radiation. The magnetic field is involved as an important part in many theories to explain the radiation mechanisms of PSRs. It is known that the distribution of magnetic field strengths extends to $\sim 10^{13}$ G and there are also young PSRs in the high-field tail of this distribution. It may be normal to assume higher magnetic fields for young PSRs if we also take into account the magnetic field decay. Although we are not sure how strong the effect of field decay is considering long decay times $\sim 3 \times 10^6$ years but we can say that it is more realizable for older PSRs (Guseinov et al. 2004a).

Charged particles give rise to many phenomena through interactions by magnetic field. There are speculations about the existence of emission and/or absorption lines in 0.95 - 5.0 keV band in the high resolution CHANDRA spectrum of 4U 0142+61. If a cyclotron absorption line had been detected in this energy range, then it would have shown that there was a $(1.9 - 9.8) \times 10^{14}$ G magnetic field (Juett et al. (2002)). The feature at 5.0 keV during the outburst of SGR 1806-20 might be interpreted as a proton cyclotron line. If this is true, then it implies a surface magnetic field up to 10^{15} G (Ibrahim et al. (2002)). The observed values of P and \dot{P} when inserted into the conventional formula $B \sim 3.2 \times 10^{19} (P\dot{P})^{1/2}$ G lead also to values of $B \gtrsim 10^{14} - 10^{15}$ G.

A more stronger argument was mentioned in an important paper by Tagieva et al. (2003). Events of varying intensities, that are widely observed in astrophysics

from different objects, are stressed. These objects are in general grouped under the name of variable stars. UV-Ceti type and T-Tauri stars are among the most popular ones. They all experience unpredictable rises in brightness in the form of flares whose spectrum can extend from radio waves to X-rays. Flares are also known to occur in the Sun. In general, the characteristic time of flares is short (\sim few minutes for UV-Ceti stars). In an intense flare the intensity rises very quickly and falls off in time. During the relaxation time some small flares are also seen. Magnetic activity is the deriving factor behind these phenomena.

If we turn back to magnetars, SGRs undergo bursts that bear resemblance to flares. They are different in that the amount of energy released in a burst is much higher. According to the line of reasoning in Tagieva et al. (2003) we can roughly determine a time scale for the bursts in SGRs. Flare stars are usually dwarfs whereas SGRs are neutron stars. The difference in their sizes can help us if we accept a linear proportionality between the radius of the star and the duration of the flare. This will bring a factor of 10^{-4} between the two time scales. A flare of $\sim 2 - 3$ minutes will imply a burst of $\sim 10 - 20$ ms which can be taken as a lower limit since flares dure between few minutes to few hours ($(\Delta t)_{burst}/(\Delta t)_{flare} \propto R_{NS}/R_{FS}$ where FS is for flare star and NS is for neutron star). The compactness of neutron star in size and the similarities in the characteristics of flares and bursts point out that magnetic field might somehow be higher than the usual values and induce the bursts.

3.2.3 Problems to Overcome

Most of the time things are not as they are. There are some severe underlying difficulties in the observed properties of magnetars. We can start stating that there are still doubts about the SNRs around SGRs (Israel (2004)). The characteristic age of 1E 2259+586, which is calculated from its period and period derivative by assuming pure magnetic dipole radiation, is more than 30 times greater than the age of its associated SNR. To explain this large difference the magnetic field of the source should decay $\sim 5 - 10$ times. On the other hand, the opposite is true for the SNRs that are said to exist around SGRs. They can be ~ 10 times older than the characteristic ages of SGRs as in the case of SGR 1900+14 (see Tables 3.1 - 3.2 and Israel (2004)).

Another important difficulty is that the number of magnetars is too small to make any efficient population analysis. In the future the statistics will probably not get better. At present we have 5 SGRs and 8 AXPs. In this sample, two of the AXPs and two of the SGRs still preserve their candidate status. Moreover, the birthrate of magnetars within 7 - 8 kpc from the Sun is $\sim 50 - 60$ times smaller than the birthrate of SNRs (Guseinov et al. (2003a), Guseinov et al. (2005)) even if all the AXP-SNR associations are real.

The source of the persistent X-ray emission of the magnetars is subject to a long-lived debate. Observational restrictions brought the early suggestion that AXPs are powered by rotational energy loss of isolated neutron stars (Morini et al. 1988, Usov 1994). This argument is also valid for SGRs in their quiescent

states. However, a typical neutron star's moment of inertia of $I \sim 10^{45} \text{ g cm}^2$ and observed period P and period derivative \dot{P} values make rotational energy loss mechanism insufficient to power X-ray emission by several orders of magnitude ($|\dot{E}| \simeq 10^{33} \text{ erg s}^{-1}$). The energy that comes out is an order of magnitude smaller than the values observed even in the case of an extreme combination of the highest possible \dot{P} with the smallest P .

We may agree that magnetars are young neutron stars with a good chance of having high magnetic fields. However, we still do not have a complete description of the pulsar radiation in high magnetic fields and neither we understand the underlying physics. If the presence of high magnetic field is real we will have to find the way(s) it effectively powers the magnetars in a short time like 10^4 years. Besides, the discrepancy between their characteristic and real ages is waiting an explanation. There are other problems like the lack of magnetars with spin periods greater than 12 s and the unusual clustering of their spin periods in a narrow range. It is very strange not to observe any emission in radio bands from magnetars because it very difficult to relate this absence with likely presence of high magnetic fields. They should have higher radio fluxes than the single PSRs which have low radio luminosities from the birth (Allakhverdiev et al. (1997)). We are faced to think that there are various selection effects since a failure in the observation does not guaranty that the radiation does not exist. Otherwise, as Tagieva et al. (2003) highlighted there would be a discontinuity in the luminosity function of PSRs including the magnetars. Whether these sources are single or have somehow a binary history is a hot discussion topic in most of the theories

since our understanding will definitely be shaped by their nature.

3.3 Running after Theory

AXPs are currently subject to mounting field of research mostly because of the lack of a self-consistent and observationally verified explanation for their X-ray emission mechanisms. Many models have been developed. Some of them have tried to advance new approaches while many others have used the ideas that have solid historical background. From time to time interesting suggestions have been introduced. Having talked about the inability of the loss of rotational energy the rest of the historical studies focus on two major processes: (i) accretion of matter onto the neutron star, (ii) loss of magnetic energy by a decaying magnetic field. In the sections below we will go over advantages and problems of these models.

3.3.1 Early Models

The main subject of first models was AXPs. They were postulated to be massive white dwarfs formed as the end product of a merger of two $\sim 0.6 M_{\odot}$ white dwarfs with final magnetic field $B \sim 10^8$ Gauss (Paczynski 1990). This was not consistent with observations, in particular with the observed spin-down rates. Very strong objections arise for this model. The area on the surface from which the black-body component of the spectra is proposed to originate is comparable with that of a neutron star (Perna et al. (2001)). Assuming the same P and \dot{P} values with magnetars a white dwarf's spin-down luminosity is $\sim 3 \times 10^4$ times greater by the ratio of moments of inertia. It is not easy to explain the SNRs

around half of the AXPs energetically if the central source is a white dwarf.

3.3.2 Models Based on Accretion

The total luminosity of an accreting neutron star is proportional to the amount of matter falling onto its surface per unit time, i.e. \dot{M} . The rate at which the kinetic energy is transformed into radiation is determined by an efficiency factor. The efficiency for accretion is $\approx 10\%$ (Lipunov (1992)). This is almost 100 times more efficient than nuclear fusion reactions. It is no big surprise that accretion is an attractive tool.

The first proposal of this genre was accretion from interstellar medium (ISM). As said in Tagieva et al. (2003), the idea was remarkably used by Salpeter in 1964 to explain the earliest X-ray sources, but it was soon understood that ISM could not provide the observed luminosities. Either symmetrical or asymmetrical form of the accretion from ISM can only rise luminosities up to $10^{28} - 10^{29}$ erg/s. A further increase becomes impossible because as the neutron heats the accretion rate decreases by 8 orders of magnitude (Amuel & Guseinov (1972)). Therefore, it is obvious that accretion from ISM for magnetars is out of question.

3.3.2.1 First Generation Models

It is a well-established fact that members of a binary system loose matter during their evolutions. If the loss is through the inner Lagrangian point after the Roche-Lobe is filled then the matter has high angular momentum and settle in a disk around the other star. The disk is often called an accretion disk. In the case

where one of the stars in the system is a neutron star the interaction of matter in the disk with the magnetic field can produce radiations in different energy bands as a result of different physical processes. This made X-ray binaries the focus point of discussions.

Mereghetti & Stella (1995) first became aware of the potential of accretion and they concluded that AXPs might be interpreted as a subclass of LMXBs. In this picture, based on the idea of Lipunov & Postnov (1985) they are formed by the accretion-induced collapse of a magnetic white dwarf which has $B \sim 10^{11}$ Gauss and have spin periods between 6 - 12 seconds. Accordingly, they are rotating close to their equilibrium spin periods corresponding to their X-ray luminosity and magnetic fields. A correlation between the period noise and the X-ray luminosity of 1E 2259+586 similar to the normal X-ray binaries was thought as an evidence (Baykal & Swank (1996)).

It should be remembered that standard magnetized accretion disk model of Ghosh & Lamb (1979a), (1979b) assumes neutron stars as aligned rotators and there is steady accretion. There is a continuous matter supply. However, any disk formation around AXPs was not directly observed. In the equilibrium rotator regime due to gentle balance between magnetic pressure and accreting matter pressure transitions should occur between spin-up and spin-down (Lovelace, Romanova & Bisnovatyi-Kogan (1999)), which is contrary to constant spin-down seen in AXPs. Moreover, very special conditions such as critical accretion rates, a narrow range of white dwarf masses are needed for accretion induced collapse to occur (Van Paradijs et al. (1995)). The number of systems that can fit into

these requirements is very small.

Under these circumstances some modifications were foreseen by researchers. Undetermined optical counterparts and the absence of Doppler shifts in the pulse frequency forced Corbet et al. (1995) to think of AXPs as isolated neutron stars fed from a residual accretion disk. Van Paradijs et al. (1995) advanced this idea. They stated that AXPs are single neutron stars accreting from a circumstellar disk. They also argued that long-term spin-down trends, low galactic latitudes and possible associations with SNRs might justify accretion from a debris disk as a part of disrupted binary companion after the common envelope phase in a HMXB evolution.

According to Ghosh et al. (1997) depending on the angular momentum content, in-falling material can flow to the neutron star's surface in two ways. This approach has the advantage of explaining two-component spectra in AXPs. Matter carrying less angular momentum in a collapsing common envelope is not affected by the magnetic field and accretes in a quasi-spherical geometry so that whole surface of the star is heated generating the black-body emission while matter with high angular momentum content forms a disk and hence is channeled by the magnetic field lines to the magnetic poles in order to create a power law spectral component. Contrary to Ghosh et al. (1997), Li (1999) put his criticism against this model and stated that spin-up should prevail in accreting systems rather than spin-down. In addition, we do not have enough information on the evolution of HMXBs during the common-envelop phase. SNRs are replaced in a

manner with the remains of common-envelope, which is clearly a strong oversimplification.

Once again, general features of the disk changed and accretion from a debris disk became the central issue. It was proposed that in the evolution process after the supernova explosion some amount of matter can fall back on the neutron star through a disk (Chevalier (1989), Lin, Woosley & Bodenheimer (1991)). Alpar (1999),(2001) took into account the possibility of a unified scheme to explain all kinds of neutron stars formed in supernovae. On the basis of this statement he suggested that all neutron stars are born with 10^{12} Gauss magnetic fields and that different classes of young neutron stars result from different mass inflow rates and histories. As a continuation to this suggestion Alpar et al. (2001) tried to add propeller torques to standard dipole torque. The results showed that up to a critical period the dipole torque is dominant but later propeller torques gain importance. The net effect is the modification of the PSRs evolutionary tracks towards longer periods and higher magnetic fields. According to this model old pulsars were predicted to be clustered in the upper right of the $P - \dot{P}$ diagram. This serious handicap was demonstrated by Tagieva et al. (2003). Relying on their kinetic ages a careful distinction between young and old PSRs revealed that as time goes on PSRs tend to move under pure dipole radiation. So, the attempt to apply the idea of fall-back disk to all PSRs failed.

In a parallel independent work, against stable accretion Chatterjee et al. (2000) employed thin disk models with variable mass accretion rates to describe AXPs. In their formulation, as the accretion rate decreases, the rotating neutron

star evolves through different evolutionary phases starting from a short propeller phase to AXP phase and more. They presumed slightly higher magnetic fields ($\gtrsim 10^{13}$ G). One apparent fact is that in this scenario AXPs were characterized as systems which had just finished the propeller phase. To preserve this scheme a fine tuning is necessary for the parameters such as accretion rate, magnetic field, size and mass of the disk.

3.3.2.2 Second Generation Models

A unified description of AXPs and SGRs has been circulating in the literature. Distinct from heavy theoretical approaches maintained mainly by Thompson & Duncan (1995), an important obstacle was surmounted by Guseinov et al. (2003a). They analysed temporal data of AXPs and SGRs and their evolution on the $P - \dot{P}$ diagram. Two of the exciting conclusions help us to clarify our path. They have noticed considerable changes in the period history of SGRs. Consistently their \dot{P} increased short after the intervals of magnetic activity. Guseinov et al. (2003a) indicated similar changes in 1E 1048.1-5937 and 1E 2259+586 and signaled out the incoming bursts. Comparing the braking indices of young and old single PSRs they decided that like young PSRs another mechanism must be working on in magnetars to make their period noise larger to decrease their \dot{E} . They concluded that this is related with the magnetic decay and burst activity.

The necessity of another mechanism was hinted in an early version of the paper by Tagieva et al. (2003). The propeller effect was proposed in addition to accretion from a fall-back disk if it exists. These two processes must be working

simultaneously.

The deduction has a simple concept as a vital part. $L_x/|\dot{E}|$ values of HMXBs, LMXBs and magnetars were compared. This ratio is inversely proportional to the specific angular momentum carried by unit accreted matter. It is observed that orbital separations of LMXBs are smaller than those of HMXBs and therefore the orbital velocities of LMXBs are on the average greater than those of HMXBs. That the specific angular momentum carried by the matter in the disk is higher in LMXBs can be acceptable. Some HMXBs are located very near to magnetars. If the fall-back disk does not exist the value of the above ratio for magnetars can be guessed looking on the $P - \dot{P}$ diagram. They should be of the order of or greater than the ratios for HMXBs (see Figure 3.9). This is valid even if the disk exists since we can be safe in assuming a smaller mass due to observational restrictions compared to the disks in X-ray binaries. This, in return decreases the angular momentum content and hence increases $L_x/|\dot{E}|$ values for magnetars. As a conclusion, in any case magnetars should have higher ratios with respect to LMXBs. The observations tell just the opposite meaning as if the specific angular momentum is high. Combining continuous slow down of magnetars and the previous conclusion we can come up with a meaningful interpretation only if we accept an additive process that extract angular momentum from these systems. This can be propeller mechanism.

Later, in successive papers Rotschild, Lingenfelter and Marsden approved the effect of propeller driven spin-down (Rothschild et al. (2001)). According to them the nature of the magnetars can be interpreted by their relation with the

surrounding ISM and/or the way they interact with SNRs. They claimed that the environment of magnetars is denser than the environment of ordinary PSRs (Marsden et al. (2001), Rothschild et al. (2002)). Later these claims are proved to be suspicious by Gaensler & Slane et al. (2001), Tagieva & Ankay (2003). Rothschild et al. (2002) gave a couple of models to explain the SGR bursts within the limits of propeller effect. The latest developments such as the enhanced X-ray and radio emissions in the spectra of magnetars seemed to take their part in the accretion models. The implications of the observations were discussed in Ertan & Alpar (2003), Ertan & Cheng (2004). One intriguing factor is the situation of a possible disk and its response to bursts. It was argued that the disk would be swept by the giant bursts. At this point, its future entered into a new scheme by the studies that question the stability and the chance of surviving the radiation pressure by Erkut & Alpar (2004) and Eksi & Alpar (2005).

3.3.3 Magnetar Models

In this category of theories, AXPs and SGRs are described under the title of magnetars as young isolated neutron stars. They are hypothesized to be spinning down by the emission of magnetic dipole radiation. Heyl & Hernquist (1997a), (1997b) noted that the powering mechanism could be residual thermal energy, which is powerful enough to supply the observed luminosities for about 10^3 years. This explanation presumes an envelope of primarily light elements such as hydrogen and helium around the neutron star.

Duncan & Thompson (1992) claimed that the origin of X-ray luminosity might

be the decay of magnetic field or angular momentum loss from Alfvén wave emission following differential movements in the stellar crust as a kind of seismic activity (Thompson & Blaes (1998), Thompson et al. (2000)). Using the relationship derived in terms of spin period (P) and period derivative (\dot{P}) magnetic field strengths of the order of 10^{14} - 10^{15} Gauss can be inferred ($B^2 = 10^{39} P\dot{P}$). Higher magnetic fields are also possible if the decay mechanism is different from dipole radiation (Heyl & Hernquist (1998)).

Currently, there are a number of approaches to model the spectra of magnetars. New ideas that recently emerged concentrate on the atmospheric effects of neutron star and on the general relativistic contributions as a result of light deflection due to the neutron star's large surface gravity (Perna et al. (2001)). Some of these studies (Perna et al. (2001)) require two-component models with many difficulties whereas some others (Özel (2001), Özel et al. (2001)) propose that the surface emission alone may account for the entire observed spectra, including power law tails on account of the broadness of the spectrum from strongly-magnetized neutron star atmosphere.

3.4 Notices on Spectra of Magnetars

Until the very recent day, a lot of observational data have been accumulated. Observations were often taken from different satellites. Various data processing methods were used and yielded different final results with different errors. Therefore, some care must be taken before making any conclusion based on the data.

Although we decided that the current status of the observational results (theoretical bases as well) is not enough to resolve the difficulties mentioned in the previous sections we have examined the data.

We mainly focused on the spectral properties of magnetars such as black-body temperatures, power law indices and X-ray luminosities. There is a simple law that relates X-ray luminosities, fluxes and distances to each other: $L_x = 4 \pi d^2 F_x$. To use the result of this equation effectively we paid attention to some general aspects. We preferred to use large energy ranges. At low energies (up to ~ 1 keV interstellar absorption is strong especially for distant magnetars. Middle energy ranges do not cover the whole spectral behavior of these stars. At higher energies the analysis is very restricted with the low count rates. Besides, instrumental misinterpretations are likely to appear more frequently. Hence, we largely used the data in 1 - 10 keV range. For a given flux X-ray luminosity strongly depends on the distance of the source. Since for fluxes we are limited by the sensitivities of satellites the importance of distance values is evident. It is hard to find in a single reference all the values we needed. Therefore, we had to make comparisons between different references. While doing that we always tried to be tied to our previously mentioned range, i.e., tried to choose either the luminosity and/or the flux in 1 - 10 keV band. This in return reduced the number of references. In some cases other available data such as the distance to an associated SNR, the hydrogen column densities along the line of sight helped us to achieve our goal. After fixing distances we did simple scaling to find the luminosities. If the values vary in a large range we used their averages. When a source is connected to a

Table 3.1: Reliable observational and derived parameters of AXPs and SGRs. Period history and \dot{P} for SGR 0526-66 are not well known. Their values for this object may change up to two times. The data in the columns whose column number is marked with * is from Guseinov et al. (2003a).

Name	Period (s)	\dot{P} (10^{-11} s/s)	τ (kyr)	B (10^{14} G)	\dot{E} (10^{32} erg/s)	d (kpc)	L_x (1-10 keV) (10^{34} erg/s)	L_x/\dot{E}	k Γ (1-10 keV)	PI (α) (1-10 keV)	PF
1	2*	3*	4	5	6	7	8	9	10	11*	12*
AXP 1048	6.45	3	3.4	4.4	44	8	8.7	20	0.55	3.0	0.70
AXP 2259	6.98	0.054	200	0.64	0.6	4	13	2167	0.43	3.6	0.30
AXP 0142	8.69	0.21	66	1.41	1.26	4	25	1984	0.40	3.7	0.08
AXP 1708	11.0	2.25	7.8	5.9	8.83	5	27	305	0.45	2.9	0.33
AXP 1841	11.77	4.1	4.6	7.2	9.9	7	20	202	0.55	3.4	0.25
SGR 1806	7.47	6	1.97	6.9	56.8	13	16	28	—	2.2	0.15
SGR 1900	5.16	6.8	1.2	6.2	195	8	13	7	0.50	2.1	0.11
SGR 0526	8.04	6.6	2	7.6	50	55	60	120	0.21	3.0	0.15

SNR we selected the age of the SNR as the real age of the pulsar.

We believe we succeeded in choosing the reliable values. They are summarized in Table 3.1 for AXPs, SGRs and in Table 3.3 for DRQNSs (For more complete sets of data please refer to Guseinov et al. (2003a)). The general view of Table 3.1 is as follows: there are 12 columns. First column is for the names of AXPs and SGRs. The second column shows the periods (P). The third column contains the period derivative values (\dot{P}). The following three columns (columns 4,5 and 6) uses the first two columns as input. According to the general picture in which pulsars loose energy by mainly magnetic dipole radiation the age, the magnetic field and the rotational energy loss are given as $\tau = (P/2\dot{P})$, $B \simeq 3.3 \times 10^{19} (P\dot{P})^{1/2}$ and $\dot{E} = 4 \pi I (\dot{P}/P^3)$. Columns 7 and 8 represent the distances and the X-ray luminosities that we adapted. In column 9 we calculated the ratio of L_x to \dot{E} . We listed black-body temperatures in the column 10 in the energy interval 1 - 10 keV. Column 11 indicates the power law photon indices for magnetars in again the same energy interval preferentially. The meaning of this number is that it generally defines the hardness or the softness of a spectrum. Finally, we gave the pulsed fractions in the last column. The structure is the same for Table 3.3 except that we did not take into account the power law indices and the pulsed fractions for DRQNSs due to large uncertainties. Some of the data about the SNRs which contain DRQNSs and AXPs are given in Table 3.2. All the figures we plotted depend on the values in these tables. Our aim is not to make a fit but to look for a correlation whether it exists or not. That is why we did not use error bars in the construction of figures. In very rare occasions we indicated a

range with a segment of line without data point on it.

3.4.1 X-Ray Luminosities and Distances

It seems that the evolved AXPs and SGRs must have lower X-ray luminosities (L_x). We expect this because magnetic field and/or its decay rate must decrease as the object gets older and also this should happen in the inactive periods. L_x can decrease due to the following reason: SGRs might not have a different nature than AXPs some of which show periodic but less energetic burst activities. Also, if it is true that L_x depends on the activity, then as the SGRs evolve, L_x is expected to decrease rapidly because cooling times of NSs is short. Using the cooling curves of PSRs (Yakovlev & Haensel (2003)) we infer that the characteristic cooling times for neutron stars with temperatures similar to those of AXPs and SGRs are about 100 years. The transition from the SGR to the AXP stage and then to the inactive dim stage may not take a long time and consequently we can not detect NSs having ages $\sim 10^3$ - 10^5 years in the X-ray band. Also distant magnetars can not be detected in their inactive periods due to the same reason. If the γ and X-ray activity do not appear after 10^5 yr then the locations of AXPs and SGRs on the $P - \dot{P}$ diagram cannot be extended to the places where τ values are higher. Field decay and loss of activity may result in lower values of B and higher values of τ . If AXPs had lost their activity (not only γ -ray bursts) they should have small luminosity, softer spectrum and larger spectral index than that of SGRs and currently known AXPs.

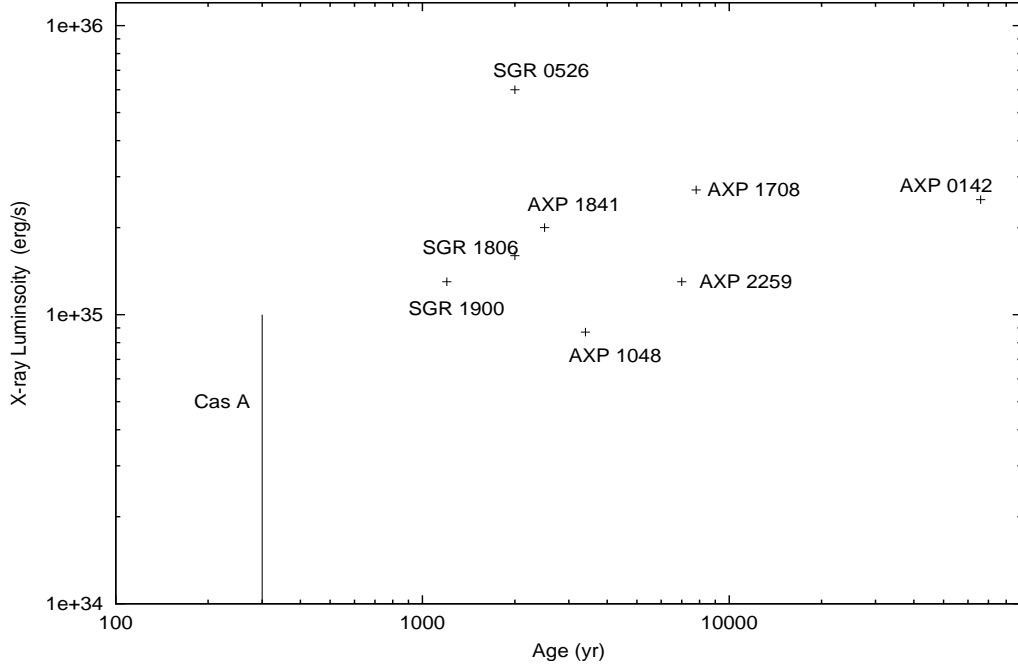


Figure 3.1: Scattering of X-ray luminosities with age in magnetars. The energy band of the luminosities is 1 - 10 keV. The SNR age is used if the object is connected to a SNR. For SGRs luminosities in their quiescent state are considered.

In Figure 3.1 luminosity versus characteristic ages (or SNR ages where appropriate) are displayed for AXPs, SGRs and Cas A which has $L_x \sim 10$ -1000 times higher than all the other DRQNSs. Below we discussed the values of L_x that are used in the construction of Figure 3.1.

AXP 1E1048.1-5937:

For this AXP L_x is 6.3×10^{33} erg/s in 2-10 keV band at a distance Corbet & Mihara (1997) of 3 kpc which is the minimum distance value given for this source. Seward et al. (1986) and Mereghetti & Stella (1995) give $d=10$ kpc. For this AXP, Mereghetti et al. (2002) give $d=5$ kpc and $L_x=3.4 \cdot 10^{34}$ erg/s in the 1-10 keV band. We have also taken into account the direction of this source in the Galaxy

Table 3.2: Data of SNRs that are associated with AXPs and DRQNSs.

Name	SNR	Type of SNR	SNR distance (kpc)	t (kyr)	\dot{P} $\times 10^{-11}$ (s/s)
AXP 1E1841-045 [1, 2, 3, 4]	G27.4+0.0 (Kes 73)	S	6.5	2.6	14
AXP 1E2259+586 [5, 6, 7, 8, 9]	G109.1-1.0 (CTB 109)	S	4	6.5	3.4
DRQNS RXJ0002+6246 [10, 11, 9]	G117.7+0.6	S	3	20	0.38
DRQNS 1E0820-4247 [10, 12, 13, 14, 9]	G260.4-3.4 (Puppis A)	S	2	3.7	0.064
DRQNS CXOJ0852+4617 [15, 16, 9]	G266.2-1.2	S	1	0.68	1.4
DRQNS 1E1207.4-5209 [10, 12, 17 – 20]	G296.5+10.0 (PKS 1209-51/52)	S	1.8	10	0.013

[1] Sanbonmatsu & Helfand (1992), [2] Helfand et al. (1994), [3] Vasisht & Gotthelf (1997), [4] Guseinov et al. (2003b), [5] Rho & Petre (1997), [6] Parmar et al. (1998), [7] Morini et al. (1988), [8] Green (1989), [9] Guseinov et al. (2004b) [10] Brazier & Jonston (1999), [11] Hailey & Craig (1995), [12] Kaspi et al. (1996), [13] Braun et al. (1989), [14] Dechristopher & Winkler (1994), [15] Aschenbach (1998), [16] Aschenbach et al. (1999), [17] Roger et al. (1988), [18] Vasisht et al. (1997), [19] Seward & Wang (1988), [20] Guseinov et al. (2004c)

and value of N_H and adopted $d=8$ kpc and $L_x=8.7 \cdot 10^{34}$ erg/s, and used this value. In spite of its small value of $\tau=3.4 \cdot 10^3$ yr, this AXP is not connected with an SNR. This is the reason why we can not improve its distance value.

As well known there are drastic \dot{P} changes of this source and this might be related with the reconnection of magnetic fields (and processes which accompany them). But note that even though this source bursts, its quiescent luminosity is small as seen in Table 3.1 and Figure 3.1.

AXP 1E2259+586:

Mereghetti et al. (2002) give $L_x=10^{35}$ erg/s in 1-10 keV at $d=4$ kpc for this AXP which has genetic connection with SNR G109.1 - 1.0. We have also used the age of $6.5 \cdot 10^3$ yr and $d=4$ kpc of its associated SNR (see Table 3.2). In Figure 3.1,

we have used an age of 7×10^3 yr and a luminosity of 1.3×10^{35} erg/s.

AXP 4U0142+615:

For this AXP, if we use F_x in 0.5-10 keV band which is 1.3×10^{-10} erg cm $^{-2}$ s $^{-1}$ (White et al. (1996)) and assume $d=2$ kpc (Gaensler & Slane et al. (2001)), we find that $L_x=6.2 \times 10^{34}$ erg/s. If a distance $d=5$ kpc (Hellier (1994)) is assumed, then luminosity becomes 3.9×10^{35} erg/s. The value of N_H for this object is a little more than that of AXP 1E2259+586 which lies approximately in the same direction Guseinov et al. (2003). If the N_H values of these objects have small uncertainty, then we would conclude that the distance of this object is not closer than that of AXP 1E2259+586, which is ~ 4 kpc. However, Mereghetti et al. (2002) give $d=1$ kpc and $L_x=3.3 \times 10^{34}$ erg/s in 1-10 keV band. The same flux in 1-10 keV band at $d=3$ kpc yields $L_x=3 \times 10^{35}$ erg/s. In For this source we used $L_x=2.5 \times 10^{35}$ erg/s.

AXP RXSJ170849-4009:

For this object X-ray flux is $F_x=2.3 \times 10^{-11}$ erg cm $^{-2}$ s $^{-1}$ in 0.8-10 keV band Israel et al. (1999a). If we use $d=10$ kpc (Israel et al. (1999a); Gaensler & Slane et al. (2001)) then $L_x=2.7 \times 10^{35}$ erg/s. However, Israel et al. (1999a) give $L_x=1.2 \times 10^{36}$ erg/s. The distance might be less than 10 kpc, if we take into account the direction of this source ($l=346^\circ$, $b=-0.2^\circ$) where N_H is high. Mereghetti et al. (2002) give $d=8$ kpc and $L_x=6.8 \times 10^{35}$ erg/s. We adopted for this source $d=5$ kpc and scaling the L_x value given in Mereghetti et al. (2002) we find $L_x=2.7 \times 10^{35}$ erg/s (see Table 3.1). Very close to the direction of this AXP ($l=346.3$, $b=-0.9$) there are HMXBs 1657-415 and 1700-377 and LMXBs 1702-429 and 1705-440.

These X-ray sources, in the error limit, have the same or very close values of N_H and distances $d=2 - 7$ kpc (Guseinov et al. (2000)). Therefore, the distance of this AXP must not be larger than 7 kpc. In Figure 3.1, we plot L_x value for this source $L_x=2.7 \cdot 10^{35}$ erg/s. The large value of L_x for this AXP must be connected with the burst activity. It is necessary to remember that this AXP has exhibited a glitch event Kaspi et al (2000).

AXP 1E1841-045:

We use $d \sim 7$ kpc for this source (Gaensler & Slane et al. (2001), Sanbonmatsu & Helfand (1992), Helfand et al. (1994)) and this leads to $L_x \sim 10^{35}$ erg/s in 2-10 keV band. The connection with the SNR G27.4+0.0 indicates that the distance might be $d=6.5$ kpc (see Table 3.2). We adopted $L_x=2 \cdot 10^{35}$ erg/s at $d=7$ kpc which is consistent with the value given in Mereghetti et al. (2002).

AXJ1845.0-0300:

In spite of the four years of observations of this source which has a pulse period (Torii et al. (1998)) of $P=6.97$ s the value of \dot{P} could not be determined yet. The connection with SNR G29.6+0.1 of age (Gaensler et al. (1999), Gotthelf et al. (2000)) $< 8 \cdot 10^3$ yr implies Guseinov et al. (2003) $\dot{P}=(0.13-0.2) \cdot 10^{-11}$ s/s. According to Mereghetti (2001) in 2-10 keV band $L_x=5 \cdot 10^{34}$ erg/s and in 1-10 keV band the X-ray luminosity is $7.4 \cdot 10^{34}$ erg/s at $d=8$ kpc (Mereghetti et al. (2002)). However, it is doubtful that this source is an AXP. We did not use this AXP in the construction of Figure 3.1 and did not include it in Table 3.1.

SGR 1806-20:

$F_x = 10^{-11}$ erg cm^{-2} s^{-1} in 0.5-10 keV band (Kouveliotou et al. (1998), Sonobe

et al. (1994), Mereghetti et al. (2000)), and distance $d=10$ kpc (Sonobe et al. (1994), Murakami et al. (1994)) yield $L_x=10^{35}$ erg/s, but if distance $d\sim 15$ kpc (Kouveliotou et al. (1998), Mereghetti et al. (2000), Kaplan et al. (2002), Corbel et al. (1997)) then $L_x=2.2\times 10^{35}$ erg/s. We adopt the distance 13 kpc and an average value of $L_x=1.6 \times 10^{35}$ erg/s.

SGR 1900+14:

For SGR1900+14, luminosity in 2-10 keV band at 5 kpc is at most 7×10^{34} erg/s in quiescence (Mereghetti et al. (2000)). But if $d = 10$ kpc in the same energy interval then $L_x=3\times 10^{35}$ erg/s (Murakami et al. (1999); Eikenberry et al. (2002)). We adopted $d=8$ kpc and as an upper limit we have used $L_x=1.8 \times 10^{35}$ erg/s. Mereghetti et al. (2000) give $L_x=2.5 \times 10^{34}$ erg/s as a lower limit at $d=5$ kpc. Using our adopted $d=8$ kpc, we find for the lower $L_x=6.4 \times 10^{34}$ erg/s. We use an average value of 1.3×10^{35} erg/s.

SGR 0526-66:

For SGR 0526-66 quiescent value of $L_x \simeq 4\times 10^{35}$ erg/s in 2-10 keV band (Marsden et al (1996), Danner et al. (1998)). In 0.5-10 keV band $L_x=10^{36}$ erg/s (Kulkarni et al. (2002)). We used $L_x=6 \times 10^{35}$ erg/s

DRQNSs:

L_x values are known for all DRQNSs except RX J0806.4-4123, 1RXS J214303.7+065419, RXJ 1605.03+3249, CXO J0852+4617 and RXJ 1836.2+5925. Geminga pulsar which has an age of 3.5×10^5 yr and has the lowest $L_x=10^{30}$ erg/s in 0.6-5 keV band (Halpern & Wang (1997), Brazier & Johnston (1999), Bertsch et al. (1992)). DRQNS in Cas A has the highest $L_x=(0.7-16)\times 10^{34}$ erg/s in 0.1-10 keV

Table 3.3: Data for DRQNSs. The + sign means that for DRQNS RXJ0002+6246 the SNR age is used. The * sign is put to stress that \dot{P} value is calculated using the age of the SNR and other parameters such as B, \dot{E} are found from P and \dot{P} of this source. Data are taken from Guseinov et al. (2003a).

Name	Period (s)	\dot{P} (10^{-11} s/s)	τ (kyr)	B (10^{12} G)	\dot{E}	d (kpc)	Lx (10^{32} erg/s)	L_x/\dot{E}	kT (keV)
1	2	3	4	5	6	7	8	9	10
1E1207.4-5209	0.42413	0.002	340	2.95	1.03×10^{34}	2	10 (0.5-6)	0.097	0.25
1E0820-4247	---	---	---	---	---	2	12 (0.1-2.4)	---	0.3
CXOJ0852+4617	---	---	---	---	---	1.5	5.2 (0.4-6)	---	0.4
RXJ0720.4-3125	8.39	0.0045	2956?	19.7	3.01×10^{30}	0.3	1.7 (0.1-2.4)	56	0.084
RXJ0420.0-5022	22.7	---	---	---	---	0.7	0.43 (0.1-2.4)	---	0.07
RX J0806.4-4123	11.37	---	---	---	---	0.4	---	---	0.085
RX J1308.8+2127	10.3	1.63	10	415	5.89×10^{32}	0.4	0.9 (0.1-2)	0.15	0.12
RXJ0002+6246	0.2418	0.019*	20 ⁺	6.9	5.31×10^{35}	3.5	2 (0.5-2)	3.8×10^{-4}	~ 0.1
Geminga	0.237	0.00114	350	1.66	3.38×10^{34}	0.16	0.01 (0.6-5)	2.9×10^{-5}	0.04

band (Chakrabarty et al. (2001)). As known the NS in Cas A is in a very dense medium. So the uncertainty in the L_x value given above results from the value of the un-absorbed flux. Among DRQNSs, we have plotted only the point source in Cas A since the others have much less luminosities. This point source has an age of ~ 300 yr and $L_x=10^{34}$ - 10^{35} erg/s in 0.1-10 keV band (see Figure 3.1).

On the average DRQNSs have L_x about 2-3 orders less than AXPs and SGRs. DRQNSs RXJ0720.4-3125, RXJ0420.0-5022 and RXJ1308.8+2127 with spin periods $P > 5$ s, have very low L_x of $\sim 10^{32}$ erg/s as can also be seen in Table 3.3.

3.4.2 Black-body Temperatures

In Figure 3.2 black-body temperatures (kT_{bb}) obtained mainly from ROSAT observations in 0.1-2.4 keV band and observations in 1-10 keV band (Mereghetti et al. (2002)) are displayed as a function of real ages (SNR ages) or characteristic times (τ) for AXPs, SGRs and for some DRQNSs. Among DRQNSs, 1E1613.48-5055 (which is in SNR 332.4-0.4) has the highest value of $kT_{bb} \sim 0.6$ keV in 0.1-2.4 keV band (Gotthelf et al. (1997)). This source is only a DRQNS candidate because it may be a member of a binary system (Pavlov et al. (2002)). On the other hand it is located in an S type SNR RCW103 and has a luminosity of $\sim 10^{33}$ erg/s. We take into consideration the uncertainties in data and do not use this source in Figure 3.1. For Cas A $kT_{bb}=0.5$ keV in the 0.1-10 keV band (Murray & Ransom (2001)). Geminga pulsar has the lowest $kT_{bb} \sim 0.05$ keV in 0.1-2.4 band (Halpern & Wang (1997)). All DRQNSs lie out of the range of Figure 3.2 with the exception of 1E 1207.4-5209, which is connected with SNR G296.5+10.0, and

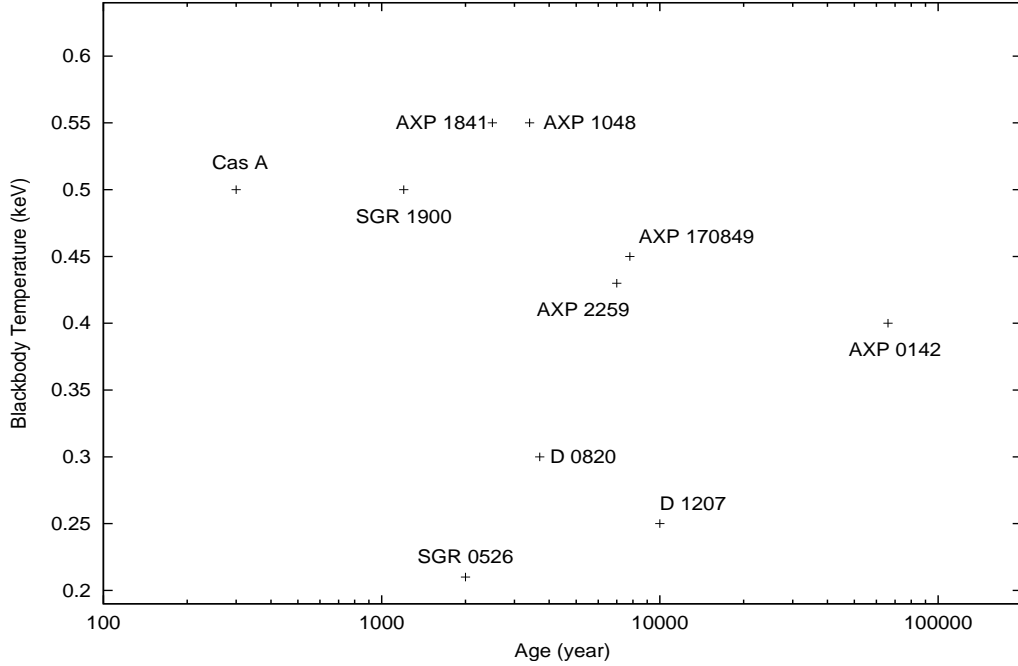


Figure 3.2: Black-body temperatures versus age of magnetars are seen. For SGRs quiescent data are used. AXPs 1E1841-045, 1E2259+586 and DRQNS 1E0820-4247 and Cas A are connected to SNRs; for these objects SNR ages are used. Data for black-body temperatures are available in two energy bands 0.1 - 2.4 keV and 1 - 10 keV.

1E0820-4247, which is connected with SNR Puppis A (see Tables 3.2 and 3.3).

The long period ($P > 5$ s) DRQNSs have kT_{bb} in the range 0.06-0.12 keV (Guseinov et al. (2003)).

Even though we cannot certainly know the ages of SGRs and AXPs, from Figure 3.2 we can say that kT_{bb} of AXPs and SGRs on the average feebly depends on age and therefore on \dot{P} also. \dot{P} values of these objects are given in Table 3.1. A correlation between kT_{bb} and \dot{P} could not be found (Marsden & White (2001)). However, if we take AXPs alone, then we may find a correlation between kT_{bb} and age and also correlation between kT_{bb} and \dot{P} since value of P of AXPs and

SGRs lie in a very narrow band. We expect that as the object gets older and the value of \dot{P} in AXP stage decreases kT_{bb} should decrease on the average and observational data, though not strongly, show such an effect. Evidently, during the long-lasting inactive periods temperature must be considerably small.

In general for pulsars L_x results from heating radiation (black-body radiation and bremsstrahlung) and power law (due to the injection of relativistic particles). L_x in 1-10 keV band vs τ (or age of SNR) and kT_{bb} in 0.1-2.4 keV band (mainly for AXPs and SGRs) vs τ given in Figures 3.1 and 3.2 show that L_x certainly do not depend, while kT_{bb} feebly depend on τ and ages. That is, they are independent of whether the NS is in AXP or in SGR state. Therefore, L_x values are not dependent and kT_{bb} is weakly dependent on magnetic decay rate. These results are strange in the frame of the magnetar model in which the magnetic decay is the radiation source. Evidently, this strangeness exists if we believe the data which are used and if the mass and the radius of all magnetars are equal.

The amount of black-body radiation for youngest PSRs is less than the amount of power law radiation whose source is the rotational energy. Therefore, total L_x of magnetars is not high enough to compare them with very young PSRs ($\tau < 10^5$ yr) with larger value of \dot{E} . But the amount of cooling radiation of PSRs and DRQNSs is very small when compared with that of magnetars. Indeed it is not hard to have longer cooling times in the magnetar model even without the magnetic decay. Such a situation may be realized if very high magnetic fields can decrease the neutrino flux considerably. However, we do not know whether this is true.

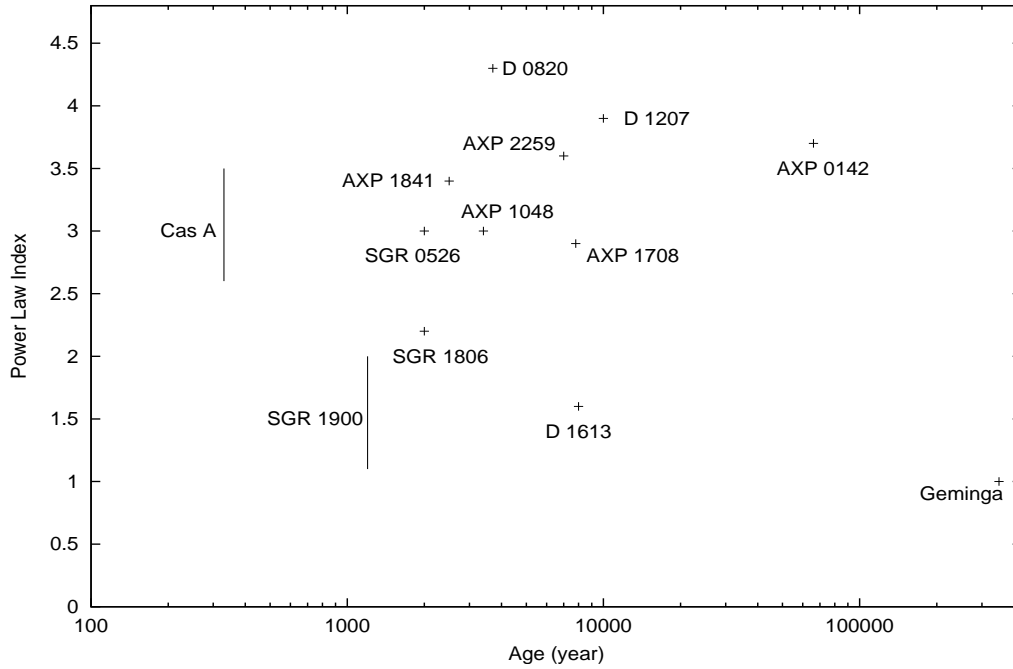


Figure 3.3: In this figure power law index (α) of magnetars and related objects DRQNSs are plotted with respect to their characteristic age. If the object is connected to SNR, SNR age is used. For SGRs data in their quiescent states are presented.

3.4.3 Photon Index

Figure 3.3 represents the photon index (PI) versus characteristic age in 0.1-2.4 keV or 1-10 keV bands for SGRs, AXPs and for some DRQNSs. The photon index value (White et al. (1996), Rho & Petre (1997), Israel et al. (1999), Mereghetti (2001)) for AXP 1E2259+586 is 3.9 in 0.1-2.4 keV band but it can be as low as 3 in 0.1-2.4 keV band (Parmar et al. (1998)). In Figure 3.3 we use PI=3.6. For AXP 4U0142+615 PI=4 in 0.5-10 keV band and it can be as low as 3.5 (2-10 keV) (Nagase (1998), Israel et al. (1999a), White et al. (1996), Mereghetti (2001)). It is necessary to note that this AXP has been an extremely stable rotator during

4.4 yr of RXTE monitoring (Gavriil & Kaspi (2002)). This stability must be the result of small burst activity and it follows also from its small value of luminosity, temperature, period derivative and large value of photon index. The next stable period is for AXP 1E2259+586.

SGRs, after bursts, have lower PI, and higher L_{bb}/L_{tot} which may be related to heating of the atmosphere and ejection of high energy particles. As seen from Figure 3.3, PI of SGRs in quiescence is, on the average, less than that of AXPs. This shows that PI depends on γ -ray bursts in result of magnetic decay. For SGR 0526-66 there is not enough information about spectral characteristics and about the pulse profiles in the transition period between the burst and quiescent phases.

If we take SGRs and AXPs separately from DRQNSs, Figure 3.3 shows that as τ of these objects increase, their PI increase. This is expected in the magnetar model. However, τ does not correctly reflect the real age. So, it is better to explain the situation as follows: PI should decrease as \dot{P} increases due to burst activity (Marsden & White (2001)). PI decreases because the burst adds high energy photons to the spectrum decreasing the slope of the power law spectrum. PI and kT_{bb} values of AXPs and SGRs depend on \dot{P} but with differing degrees. These considerations show that L_x should decrease as \dot{P} decreases. But observational data do not show any dependencies (see Figure 3.4).

As seen from Figure 3.2, AXP 1E1048-5937 has a high value of kT_{bb} when compared with AXPJ170849-4009 and a similar value of PI, but ~ 3 times lower L_x (Table 3.1). This shows that L_x of these objects are not related to kT_{bb} .

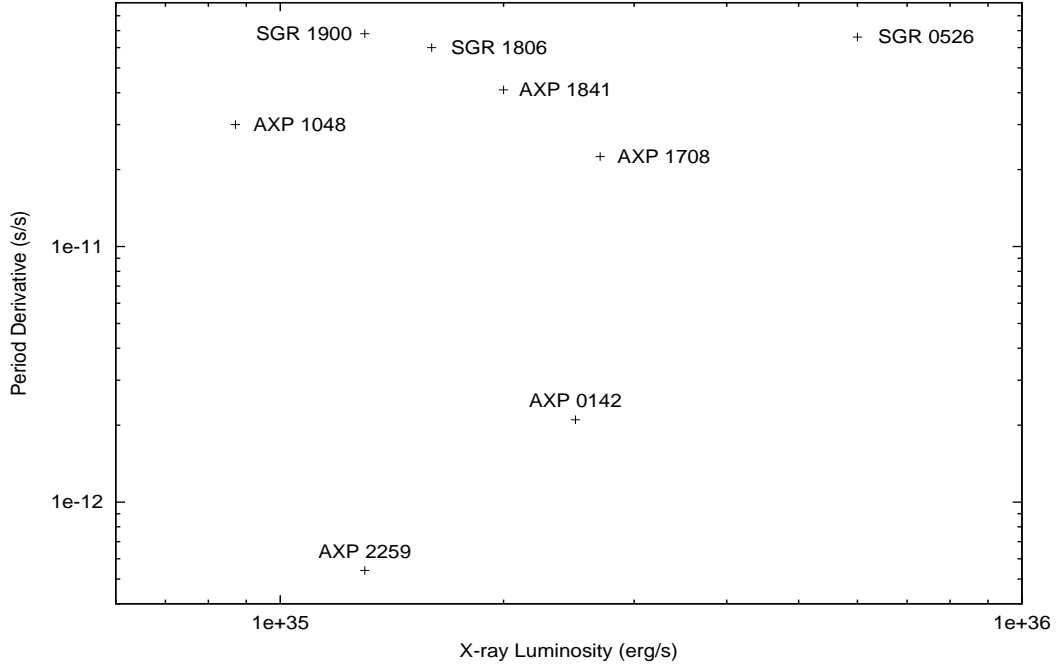


Figure 3.4: The time rate of change of period in magnetars is plotted against their X-ray luminosities. The luminosities are as usual cover the energy range 1 - 10 keV. SGRs are shown with their quiescent state data.

Therefore, the cooling times also do not have an important role when we compare the properties of AXPs and SGRs. Evidently, these may partially come from the errors in d , kT_{bb} and PI . However, here, these parameters may depend on the phase cycles of the pulses and also on the diameters of the objects. For AXPs, this is more important since their amount of pulsed radiation is more than SGRs.

3.5 Pulse Profiles and Some Spectral Properties of SGRs

Among 3 well-known SGRs, it is more suitable to investigate the changes between quiescent and active states for SGR 1900+14 compared to SGR 1806-20 because the changes in SGR 1900+14 are more apparent. The main problem

is that most of the observations analyze the burst but not the quiescent data. For SGR 0526-66 there is not enough information about the pulse profile in the transition period between the burst and quiescent states.

The shape of the pulse profiles of SGR 1900+14 for all of the quiescent data are almost the same (Hurley et al. (1999), Woods et al. (1999a), (1999b) Murakami et al. (1999)) These profiles have 3 peaks. A big peak is followed by two other peaks. The second one is broader than the third one. Last two peaks have similar intensities (Gögüs et al. (2002)).

During 1998 May 30 activity there is no significant change in the pulse profile of SGR 1900+14 compared to the quiescent state of 1996 September (Woods et al. (1999)) However, if the observations include the 1998 August 27 super-burst only a single peak appears with a large intensity (Woods et al (1999b), Kouveliotou et al. (1999)).It turns out to be that only the super-burst has a drastic effect on the nature of the pulse profile when compared to the other bursts. The pulse profiles in 2-5 keV and 5-10 keV bands are single-peaked with a phase coverage of $\sim 75\%$ in the quiescent state in 2000. Gögüs et al. (2002) shows that the bulk dipole magnetic field does not change due to the reconnection of the magnetic field. These authors determine the pulse shape and the pulsed radiation. They note that additional magnetic field components which may arise and disappear in active periods, have considerable contribution in pulsed X-ray radiation only in the super bursts.

During the bursts, the photon index rises sharply. Its value in the burst spectrum is almost twice its value in the pre-burst quiescent phase. But black-body

temperature does not change (Woods et al. (1999a), Kouveliotou et al. (2001)) and it is in agreement with the absence of difference in black-body temperatures of AXPs and SGRs. But then a difficult question arises. Why γ and X-ray burst activities do not heat the atmospheres of NSs (of course NS itself also)? This is also true for the latest activity (1998 August 27 and 2001 April 18 (Kouveliotou et al. (2001))).

During the burst, X-ray flux coming from the SGR 1900+14 is nearly equal to three times of its quiescent value (Woods et al. (1999a)) and it is a result of the increased power law component of radiation.

Unfortunately, for SGR 1806-20 there are only two pulse profiles available. They belong to the last burst (Kaplan et al. (2002)) (2000-08-07) It is interesting that its shape is very much like the one for SGR 1900+14 in its super-burst of 1998-08-27. Moreover, Mereghetti et al. (2000) study the pulse profile (1-10 keV) of a burst activity in two energy bands (1-4 keV) and (4-10 keV). There is no energy dependence but some small features between these two energy bands. Between 1996-2001 the shape of the pulse profile of SGR 1806-20 had not changed significantly and it had been single peaked. During this period the pulse profiles cover $\sim 80\%$ of the phase cycle, but in the 1999 observations they became narrower covering $\sim 50\%$ of the cycle. The count rate of the pulse profiles do not change noticeable with burst activity (Gögüs et al. (2002)). This also shows that bursts do not have important effect on the region where the pulses originate and in general on the surface temperature. SGR 1900+14 has drastic pulse profile changes on a time-scale of minutes in burst activity, in particular during and

after the giant flares. Different from SGR 1900+14 changes in the SGR 1806-20 pulse profiles are not dramatic, but measurable. The pulse shapes of both sources become very smooth after the burst activity (Gögüs et al. (2002)).

As we see above, the ratio of pulse width to the pulse cycle for SGRs 1900+14 and 1806-20 are practically equal. On the other hand pulsed fractions in quiescent states for both sources are about 10-20%.

3.6 Pulse Profiles and Some Spectral Properties of AXPs

It is seen that the pulse profiles of AXPs do not show big changes in time. AXPs 4U0142+61, 1E2259+586 and RXSJ170849.0-400910 do not show variations >20-30% in the pulsed flux around the average (Gavriil & Kaspi (2002), Gavriil et al. (2003)). Instead, in all of them, there is strong energy dependence especially for AXP 4U0142+61 (Paul et al. (2000)). For this reason, pulse profiles are examined in three energy bands. The main property of the profiles is that their shapes are sinusoidal.

The average pulse profiles of 4U0142+61, RXSJ1708-4009 and 1E2259+586 in the energy bands 2-4 keV and 6-8 keV are significantly different (Gavriil & Kaspi (2002)). The 2-4 keV band has a significant black-body component ($\sim 40-60\%$) of the total flux, depending on the source and on the model used. The 6-8 keV band is greatly dominated by the power-law component ($>95\%$) of the total flux (Özel et al. (2001)).

If we consider 1-10 keV band we see that the radiation of AXP RXSJ1708-4009 is 75% in power law component and it must be the result of burst activity.

Pulsed fraction is ~ 0.38 and ratio of the pulse width to the pulse cycle is $\sim 60\%$. Israel et al. (1999b) For AXP 1E1048.1-5937 the pulsed fraction is $\sim 70 - 75\%$ in 1-10 keV band (Paul et al. (2000), Mereghetti et al (2002)). On the other hand, L_{bb}/L_{tot} in 1-10 keV band for AXP 1E1048-5937 is about 3 times more than AXP RXSJ170849-4009 (Mereghetti et al. (2002)). As seen from Figures 3.1 and 3.2, AXP 1E1048-5937 which has lower value of total luminosity than AXP RXS J170849-4009, has higher value of T_{bb} . For these sources if we also take into account the data which we have discussed in section 2.3, we may see that AXP 1RXSJ170849-4009 has a high L_{tot} value but low L_{bb} value. The total luminosity of this source is high but there are no large changes in its period trend like the changes seen in AXP 1E1048.1-5937 (Guseinov et al. (2003)).

According to the data in Gavriil et al. (2003) the pulse width of AXP 1E2259+586 is about 75% and AXP 1RXSJ170849-4009 is about 70%. AXP 4U0142+61 has a pulse width of $\sim 70\%$ (Gavriil & Kaspi (2002), (Gavriil et al. (2003)) whereas it is given as $\sim 80\%$ in Paul et al. (2000). The pulse width of AXP 1E1048.1-5937 is about 50% and 70% in 4-8 keV and 0.5-1.5 keV respectively (Paul et al. (2000)). For AXP 1E1841-045 the pulse width is $\sim 80\%$ (Gotthelf et al. (1999)). Obviously, the pulse width depends on the energy band, as we see in the case of AXP 1E1048.1-5937, the pulse width of which is several times narrower than other AXPs and SGRs in the hard energy band. According to Mereghetti et al. (2002) the pulse width of AXP 1E1048.1-5937 in the 1.5-4 keV, 4-8 keV and 0.5-8 keV are $\sim 60-65\%$, 50% and 65% correspondingly. In the same bands pulse widths of AXP 1E1841-045 are $\sim 55\%$, $\sim 85\%$ and 65%. In all of the

cases we define the pulse width at the $\sim 20\%$ level of the pulse maximum.

3.7 Relations between Different Parameters of AXPs and SGRs

Figure 3.4 represents \dot{P} versus L_x of AXPs and SGRs in quiescent state. As seen, luminosities of these objects do not depend on $\dot{P}(B)$ and period noises, in other words on reconnection of magnetic field (Guseinov et al. (2003)). In Figure 3.5, it is also seen that there is no correlation between T_{bb} and L_x . Absence of the dependence between PI and L_x is seen in Figure 3.6. In Figure 3.7 it is seen that there is no dependence between the pulsed fraction of radiation and L_x . There may be a possible correlation between PI and T_{bb} for AXPs (see Figure 3.8). When T_{bb} increases PI weakly decreases.

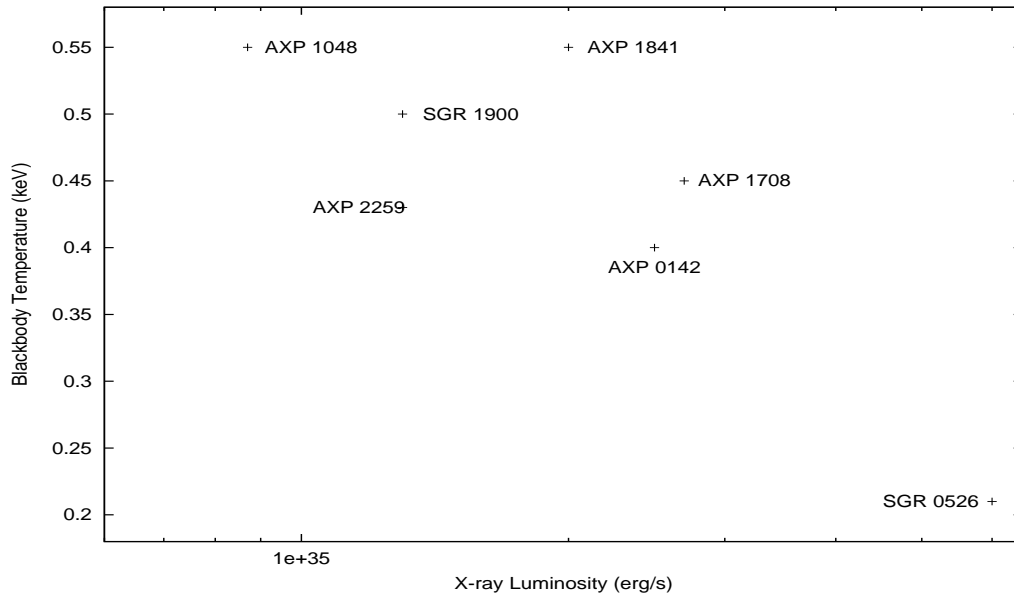


Figure 3.5: The distribution of black-body temperatures with respect to X-ray luminosities of magnetars can be seen in this figure. For SGRs data in their quiescent states are used.

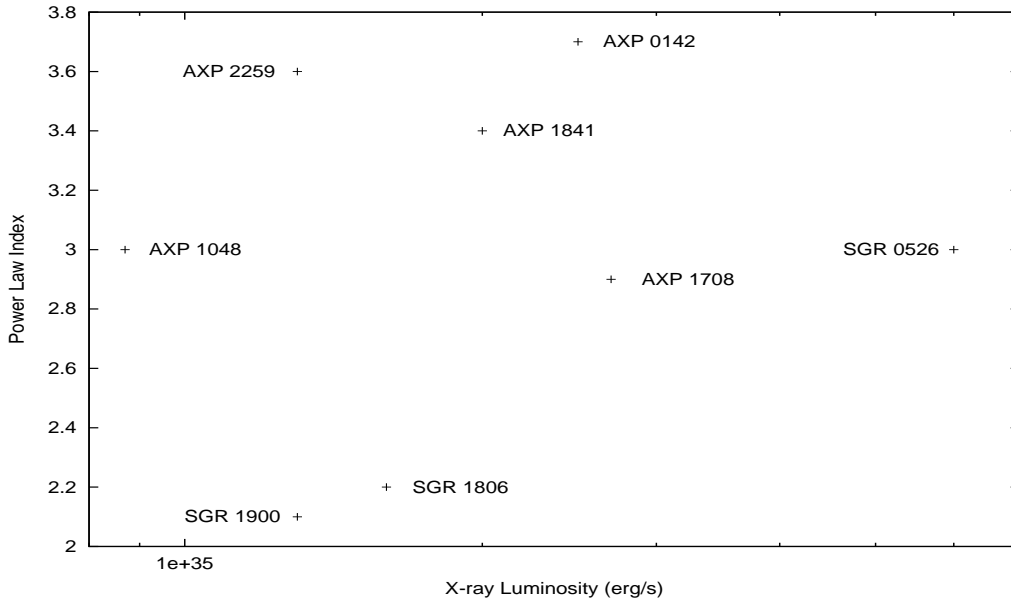


Figure 3.6: Power law index (α) versus X-ray luminosities for magnetars are presented. For SGRs data in their quiescent state are used.

AXP 1048-5937 has \dot{P} value close to SGRs and has large period noise (Kaspi et al. (2001a), Guseinov et al. (2003)). It has the smallest value of L_x (see Figure 3.1), small value of PI (see Figure 3.6), the highest value of T_{bb} (Figure 3.2) and the largest value of pulsed fraction (Figure 3.7) among AXP and SGRs. This source has the lowest value of L_x/\dot{E} ratio among the AXPs (Table 3.1). In addition, Kaspi et al. (2001) mention that the pulsed flux and the pulse profile can be stable even in the presence of significant torque variations in AXP 1E1048.1-5937.

Here we consider the braking as a result of mainly magneto-dipole radiation. Therefore to equate the value of $\tau=2\times 10^5$ yr for AXP 1E2259+586 to the age of SNR G109.1-1.0 (10^4 years⁷⁸ or $\sim(3-10)\times 10^3$ years (Rho & Petre (1997)), it is

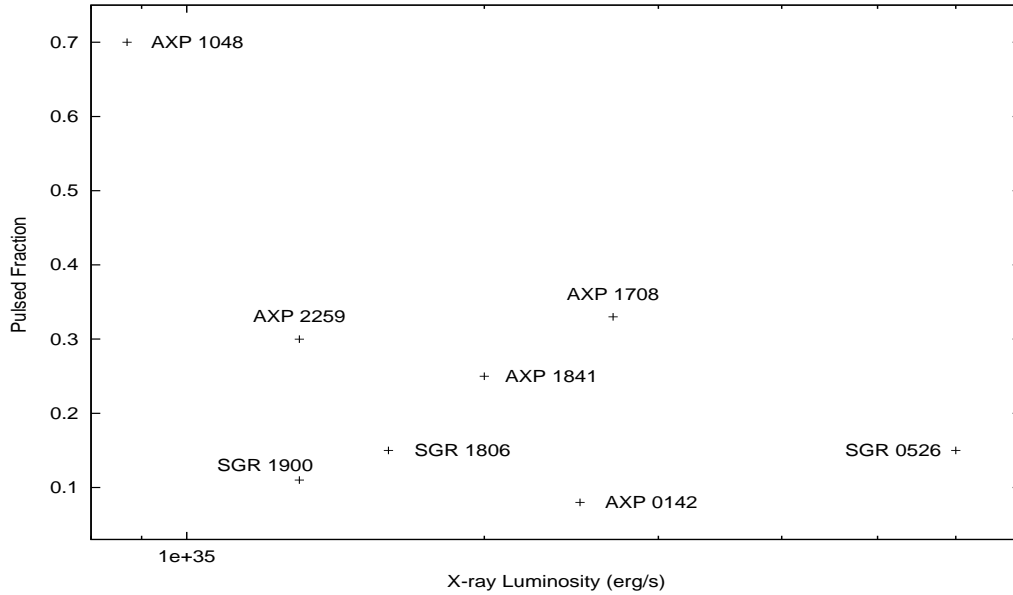


Figure 3.7: Pulsed fractions of magnetars are shown against their X-ray luminosities. Quiescent-state data are used for SGRs.

necessary to adopt an initial magnetic field value of $\sim 3 \times 10^{14}$ G in the existing magnetar model. Indeed, such a sharp decrease in magnetic field is possible. In this case we may adopt that all SGRs and AXPs have, ages $< 3 \times 10^4$ years, in other words ages close to AXP 1E2259+586 which has the largest value of τ and the smallest value of B. In this case the absence of SGRs and AXPs with $P > 12$ s are understandable.

3.8 Discussion and Conclusion

3.8.1 Removal of the Difference between τ and t

In the magnetar model processes of braking SGRs and AXPs considered as a result of magneto-dipole radiation. The value of magnetic fields are determined

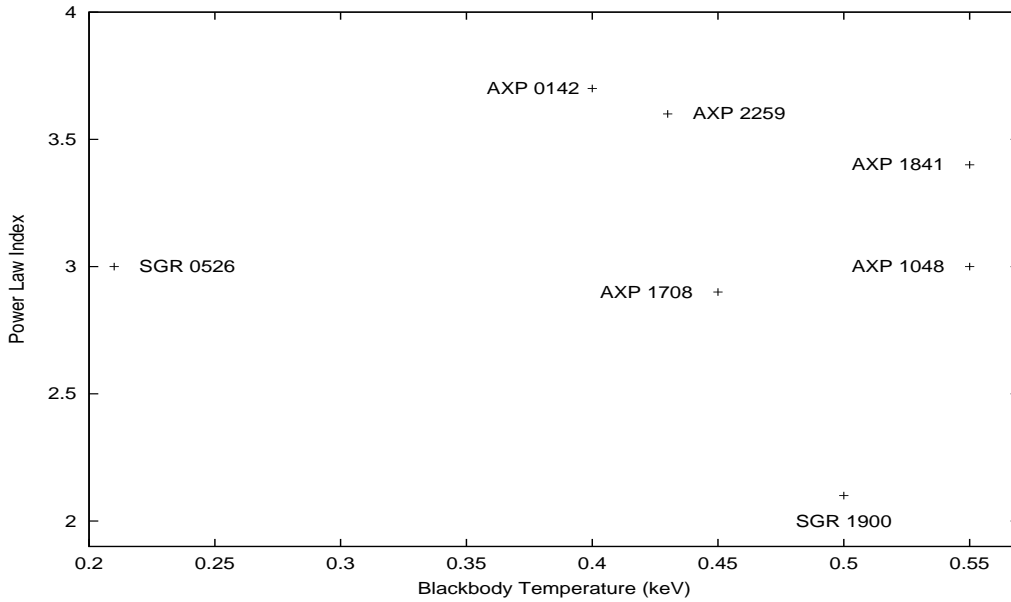


Figure 3.8: A slight dependence of power law index (α) on the black-body temperature of magnetars can be read from the figure. SGRs are indicated by their data in quiescent state.

from their value of P and \dot{P} . As in this model there is considerable magnetic decay, then the real ages of SGRs and AXPs can not be more than their characteristic ages τ . By contrast the values of τ of SGRs is not more than 2 kyr, therefore it is not easy to understand the absence of young SNRs which must not have small value of surface brightness and have connection with SGRs. The similar situation is seen in the case of AXPs 1048-5937, 1841-045 and 1708-4009 for which $\tau < 6$ kyr (see Table 3.1). On the other hand, practically all known PSRs with $\tau < 2 \cdot 10^4$ yr (Kaspi et al. (2002)) and two of the AXPs are certainly genetically connected with SNRs (Gaensler & Slane et al. (2001), Tagieva & Ankay (2003)). It is very important that AXP 1E2259+586, which has the smallest value of B and the largest value of τ among AXPs and SGRs, has connection with an SNR.

Therefore we must adopt that SGRs and AXPs are often born without normal SN explosions and without the formation of SNRs. But it is very difficult and do not have any basis.

As known SNRs which are genetically connected to AXPs 1E1841-045 and 1E2259+586 and the SNR possibly connected to SGR 0526-66 are S type. SNRs of PSRs are often C and F type. Around the other AXPs and SGRs pulsar wind nebula (PWN) also are absent. This shows that, AXPs and SGRs are sources with not strong enough ultra-relativistic winds and within several parsecs around these NSs, there is not enough amount of very hot plasma which might have been observed in the X-ray band. But it is not surprising because PWN or plerions are observed only around the PSRs and DRQNSs with the rate of rotational energy loss $\dot{E} > 3 \cdot 10^{34}$ erg/s. In other words, for these PSRs the value of \dot{E} is 300 times more than that of AXPs and SGRs. However, since PWN is not seen, it seems that the dominant mechanism which brake these NSs must be magneto-dipole radiation. Hence, τ must reflect the real age if it is possible to neglect the decay of magnetic field component perpendicular to the rotation axis. τ is higher than the real age if the decay of this component is considerable and if the increase of the activity of NS and transform to the SGR and AXP stages does not have a temporal character.

Like many other authors, we consider AXPs and SGRs as a group of objects with different degrees of γ -ray bursts activity. And we believe that these objects have magnetic fields more than PSRs and magnetic reconnection takes place. This is supported with the observations of two X-ray bursts (Gavriil et

al (2002)) from AXP1E1048-5937 and the bursts (Kaspi & Gavriil (2002)) from AXP 1E2259+586. Both AXP and SGR bursts are spectrally much harder than their quiescent pulsed emission (Gavriil et al (2002)). The shape of the light-curve of bursts support magnetic reconnection and the detection of pulsations in the optical flux of 4U 0142+624 which has large value of P support high value of B (Kern & Martin (2002)).

According to the astrophysical tradition and standard physical logic, SGRs as NSs with much more activities, must be younger than AXPs. This is also natural in the frame of the magnetar model. As seen, on the $P - \dot{P}$ diagram (Figure 3.9 and Table 3.1), in agreement with the above statements, the value of τ for SGRs are smaller than AXPs. On the other hand, among the two AXPs 1E2259+586 and 1E1841-045 which are connected with SNRs, AXP 1E2259+586 has the value of τ considerably larger than all other AXPs and without any doubt, SGRs. This fact and the absence of connections of SGR 1806-20 and SGR 1900+14 and AXPs 1048-5937 and 1708-4009 with SNRs quiet confidently shows that τ do not have correlation with real age of AXPs and SGRs.

When we explain the bursts of SGRs and persistent X-ray luminosities of SGRs and AXPs with magnetic field decay, then we must accept that $\tau > t$. But it contradicts with the observational data, therefore, magnetic dipole radiation certainly can not have a dominant role for large values of \dot{P} for these objects from birth. This brings great difficulties for the magnetar model.

In order to avoid these great difficulties, it is easy to adopt that SGRs and AXPs, at birth, have smaller values ($< 3 \cdot 10^{14}$ G) of surface magnetic fields when

compared with the proposal of the magnetar model ($< 10^{15}$ G). In this case to explain the large values of luminosities and small values of τ , the NS might make a transition to the active stage with AXP and SGR properties (i.e. become a magnetar). When the NS enters the active stage, its τ decreases rapidly depending on the degree of activity and \dot{P} increases. This is because in SGR and AXP activity periods plasma ejection occurs and propeller mechanism works. The magnetic field component perpendicular to the rotational axis may also rapidly increase ~ 2 -3 times. In those cases, their real ages t may considerably be larger than τ . Therefore, SGRs may be older than the same AXPs and may not have connection with SNRs (Gaensler & Slane (2001), Tagieva & Anay (2003)).

The other great difficulty of the magnetar model is often considered to be the absence of AXPs and SGRs with spin periods ($P > 12$ s) and with L_x several times smaller than the faintest AXP which has $L_x = 8.7 \cdot 10^{34}$ erg/s. This is wrong if the real age (t) is much more greater than the characteristic age (τ) as we see in the previous section. As we stated above the real ages of SGRs and AXPs with large value of \dot{P} are considerable higher than their values of τ . For the propeller mechanism to work, the NS should be in its active phase so that plasma should be ejected as a result of star-quakes, volcanic processes and reconnection of magnetic fields which results in heating of NS atmosphere. After not so long times (about several 1000 yrs which is similar to τ for all SGRs and the AXPs with large \dot{P} values) NS must return to the conditions close to previous conditions with small values of \dot{P} and effective values of magnetic field similar to that of AXP 1E2259+586 or several more.

Detection of pulsation in the optical flux of 4U0142+624 (Kern & Martin (2002)) and infrared counterpart of 4U0142+614 (Hulleman et al. (2000), Hulleman et al. (2001a)), 1E2259+586 (Hulleman et al. (2001b)) and 1E1048.1-5937 (Wang & Chakrabarty (2002), Israel et al. (2002)) which have spectra similar to the spectra of thin plasma support the out-flow of enough plasma. Gamma ray observation during the SGRs flare (Feroci et al. (2001)) and the discovery of the transient radio nebula following the flare (Frail et al. (1999)) provided an independent evidence for the existence of a particle out-flow (Woods (2002)). Consequently, the created plasma give possibility for successful work of propeller mechanism.

As known, there is almost no correlation between the period noise and the burst activity of SGRs and AXPs (Guseinov et al. (2003)). In general the direct effects of burst activity are insignificant to the overall torque noise in each of SGRs (Woods (2002)). The observed noise of SGRs and AXPs may mainly have connection with the propeller effect.

On the other hand, AXP 1E1048.1-5937 demonstrates that the pulsed flux and the pulse profile can be stable even in the presence of significant torque variations (Kaspi et al. (2001)) and this contradicts with the existent magnetar and fall-back matter theories. We think that AXP 1E1048.1-5937 in the stage when there is practically no magnetic activity (reconnection) but there are torque variations which shows that propeller mechanism is at work. On the other hand, this AXP has the smallest pulse width among the known SGRs and AXPs and has the highest black body temperature (T_{bb}). As it has such a high value of T_{bb}

with the stable pulse shape and pulsed fraction, its atmosphere must have high heating capacity and less heating conductivity. All of it is possible if this NS has low value of mass, large radius and massive and extended atmosphere. Small activity and its concentration in polar cap may lead to considerable difference in surface temperature, less total luminosity and narrower pulse than the other magnetars.

To lengthen the time between two active periods (AXP and SGR states) when braking of the NS depends only on the initial surface field intensity $B < 3 \cdot 10^{14}$ G, it is necessary to choose suitable inner parameters for NSs (Thompson & Duncan (1996)). On the other hand, it is known that reconnection of magnetic field and heating of NSs take place in result of changed conditions of electricity current and suddenly increased resistance. Such situation may be realized when there are star-quakes and when a current loop is thrown away to the atmosphere of the NS. We may adopt that release of energy partially takes place in the atmosphere of NS where electrical conductivity is smaller than the inner region. Of course reconnection energy does not have the dominant role in the total dissipated energy. The dominant dissipation comes from the star-quakes and processes similar to volcanic processes.

3.8.2 Why Temperature and X-ray Luminosity of AXPs and SGRs do not Depend on the Degree of Activity?

The cooling of PSRs has small characteristic time (Yakovlev & Haensel (2003), Kaminker et al. (2002)). Therefore if the processes of star-quake, out-flow of

plasma, outlet of the strong magnetic field on the surface and reconnection events do not repeat when the spin period $P > 12$ s then SGR and AXP properties come to an end. We must expect this because source of any activity is connected with rotational energy and the rotational energy rapidly decrease as P increase. It is necessary to take into account the fact that E always decreases continuously, but energy necessary for different types of activity accumulates in a longer time and dissipated in a considerably short time.

The small value of mass of the atmosphere and the large heating capacity of the NS, which is superconductive, lead rapidly to the cooling of the NS surface. Thus, it becomes understandable why the temperature of SGRs even after the strong bursts is similar to the temperature of the quiescent state. This also explains why SGRs have temperature close to AXPs.

The heat energy of NS which consists of degenerate neutron gas is

$$E = \frac{1}{2} \left(\frac{g\pi}{6} \right)^{2/3} \frac{m}{\hbar^2} N \left(\frac{V}{N} \right)^{2/3} T^2 \quad (3.1)$$

If we adopt that number of neutrons $N = 2 \cdot 10^{57}$, average matter density $\rho = 3 \cdot 10^{14}$ g/cm³ and temperature $T = 1$ keV then

$$E \approx 2 \times 10^{43} T^2 \text{ erg} \quad (3.2)$$

where T is given in keV. Therefore even super-bursts cannot have considerable influence on the surface temperature. Here NSs play a role similar to a thermostat, so why temperature and X-ray luminosity of AXPs and SGRs do not depend on the degree of the activity is understood.

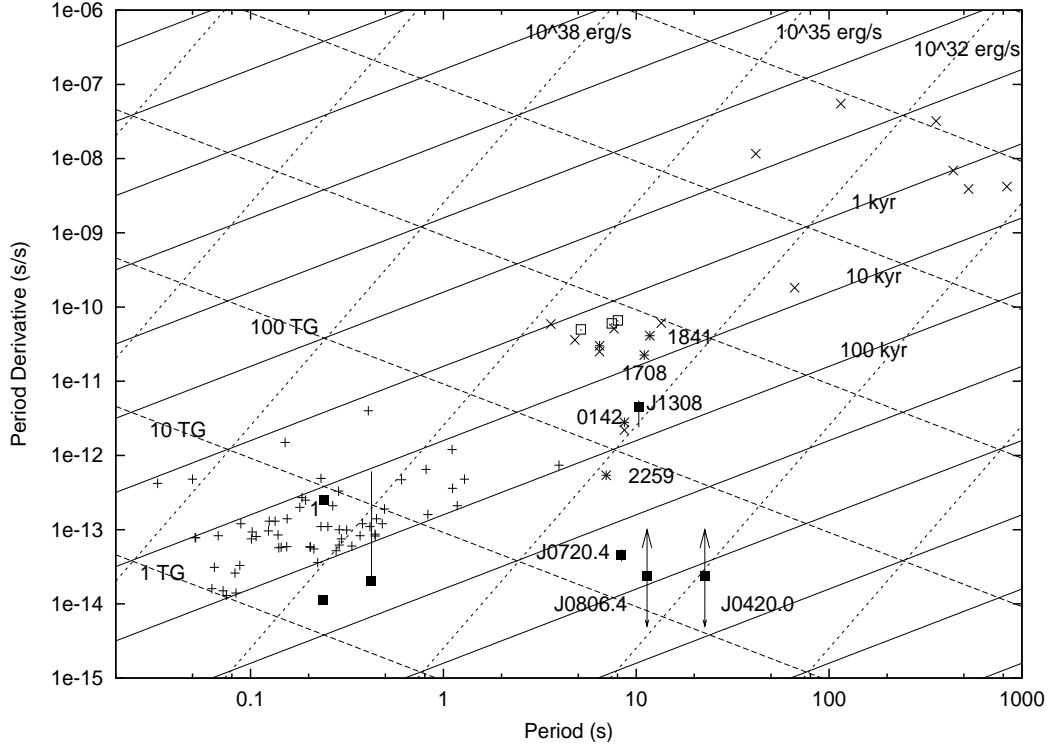


Figure 3.9: $P-\dot{P}$ Diagram for PSRs, AXPs, SGRs, XBs and DRQNSs. + symbol represents PSR, * represents AXP, box represent SGR, filled box represent DRQNS and x represent XB. For DRQNS RXJ0002+6246 \dot{P} is calculated using its period and age of the associated SNR. This source is indicated by the number 1 in the figure. It is necessary to take into account that \dot{P} values for magnetars with large \dot{P} may change up to two times.

3.8.3 $P-\dot{P}$ Diagram for Different Types of Neutron Stars

Now, we consider how well the positions of the sources on the $P-\dot{P}$ diagram support the proposed ideas in this paper. In Figure 3.9, $P-\dot{P}$ diagram for SGRs, AXPs, DRQNSs and young PSRs is displayed. As seen from the figure DRQNS J1308.8+2127, J0720.4-3125, J0420.0-5022 and J0806.4-4123 have values of spin periods P in 5.16-22.7 intervals (see Table 3.3). These NSs have values of $T_{bb}=0.06-0.12$ keV in 0.1-2.4 keV energy band (Table 3.3). According to Yakovlev

and Haensel (2003) NS may become cold up to such surface temperature in about 10^4 - $5 \cdot 10^5$ yr. But characteristic times for the last two DRQNSs are believed to be $>10^6$ yr. Therefore we may consider these objects as the late stage evolution of SGRs and AXPs but not ordinary PSRs whose radio emission came to end after crossing the death belt (Lyne & Graham-Smith (1998)).

DRQNSs with large spin periods have very important role on the P- \dot{P} diagram (see Figure 3.9) As seen RX J1308.8+2127, if we believe the data of Hambaryan et al. (2002), has very large value of \dot{P} similar to AXPs but has small temperature about 0.12 keV (see Table 3.3). Of course this contradicts with the fall-back disk model and also with the existing magnetar model. If the value of \dot{P} for this DRQNS is correct or the error is not more than 10 times then it should be in a stage where there is not enough activity to increase X-ray luminosity but there exists enough plasma around the NS for propeller mechanism to work effectively. DRQNS RXJ1308.8+2127 does not have connection with SNR. It is necessary to note that \dot{P} values of DRQNSs J0806.4-4123 and J0420.0-5022 may also be large. It seems that these 3 DRQNSs have $B \sim 10^{13}$ - 10^{14} G and now in a stage when NS losses its SGR or AXP activity. If only the temperatures of these DRQNS in Table 3.3 were two times greater, and especially if they had \dot{P} values ~ 5 times higher than given in Figure 3.9, this would be an exact evidence for the ideas in this work.

For NSs, it is known that the characteristic times of period change in a general form may be represented as

$$\tau = \frac{P}{(n-1)\dot{P}} \quad (3.3)$$

where "n" is the braking index. The braking index may change considerably if the effects that determine the value of \dot{P} depend on time. Only if the magnetic field B is vectorially constant and any other mechanisms which brake (or accelerate) NS are absent then the characteristic time is given as

$$\tau = \frac{P}{2\dot{P}} \sim \frac{P^2}{B^2} \quad (3.4)$$

All lines in Figure 3.9 (constant values of B, τ and \dot{E}) correspond to the last case.

We do not have to use the approach adopted for AXPs and SGRs to understand the locations of other types of NSs on the P- \dot{P} diagram and to explain the possible difference between their τ and t values in Figure 3.9. In some conditions that do not depend on the magnetic activity the role of the environment around the NS may be much more important. For example, in PSRs with very small X-ray luminosities due to cooling (Yusifov et al. (1995)) and in DRQNS with small periods. For instance, for 1E 1207.4-5209, which is inside the SNR G296.5+10.0, τ lies in a range 200-1600 kyr Sanwal & Pavlov et al. (2002) and it was given as 340 kyr in De Luca et al. (2002). The age of SNR G296.5+10.0 is 7 kyr (Kaspi & Manchester et al. (1996), Roger & Milne et al. (1988), Brazier & Johnston (1999)) and 10 kyr in Vasisht et al. (1997). It is clear that there may be large errors in τ , but we may still believe the cases where $\tau > 10t$. To

overcome this difficulty, strong magnetic field decay may also be necessary. But first it is necessary to improve the value of \dot{P} . For this reason, we believe that any improvements in the latest fall-back models (Rotschild et al. (2002), Menou et al. (2001), Rotschild et al. (2001)) are very important to explain the positions and evolutions of NSs on the P- \dot{P} diagram.

Distances to DRQNSs with spin periods $p=5-23$ s may not be larger than 0.7 kpc. Therefore they can be studied in X and optic bands more carefully. The results of these investigations may help to understand the nature of SGRs and AXPs.

Use soft words and hard arguments

English Proverb

CHAPTER 4

DEPENDENCE OF THE X-RAY LUMINOSITY AND PULSAR WIND NEBULA ON DIFFERENT PARAMETERS OF PULSARS AND ON THE EVOLUTIONARY EFFECTS

*I do not feel obliged to believe that the same God
who has endowed us with sense, reason and intellect
has intended us to forgo their use*

Galileo Galilei

4.1 Introduction

X-ray luminosity (L_x) of single neutron stars strongly depends on the rate of rotational energy loss (\dot{E}) (Becker & Trumper (1997), Possenti et al. (2002), Becker & Aschenbach (2002)). \dot{E} depends on the spin period (P) and time derivative of the spin period (\dot{P}) of neutron stars. As there exist many other parameters of pulsars determined from P and \dot{P} values, L_x must also depend on these parameters. This problem has already been analysed using values of L_x in 2-10 keV band for different groups of pulsars including also the old millisecond pulsars (Possenti et al. (2002)). We also prefer to use the L_x values in 2-10 keV band, because the absorption is strong in the softer X-ray band and also there must be a contribution of the cooling radiation to the soft X-ray part of the radiation of pulsar

which may complicate the problem. Below, using reliable distance values we have analysed in detail the dependence of $L_{2-10\text{keV}}$ on different pulsar parameters for young single pulsars for which the radiation is related to ejection of relativistic particles. In this investigation we have also used the values of pulsar radiation in 0.1-2.4 keV band and the radiation of pulsar wind nebula (PWNe) in both bands. Special attention has been paid to the evolutionary factors. There exist many pulsars with large values of \dot{E} and small values of age from which no X-ray radiation has been observed. Below, we have also discussed possible reasons of this.

4.2 Dependence of X-ray radiation of pulsars and their wind nebula on different parameters of pulsars

For the pulsed radio emission to occur and in order to produce radiation (excluding cooling radiation) in X-rays and also to form PWN, there must be ejection of high-energy particles. The production of these kinds of radiation and PWN must depend on different parameters of neutron star. Note that the magnetic field may not be pure magneto-dipole field and the angle between the magnetic field and the spin axis is uncertain. These facts also make the solution of the problems more difficult. We want to figure out whether X-ray radiation of pulsars and the formation of PWN depend on \dot{E} or the electric field intensity (E_{el}) more strongly for the case of pure magneto-dipole radiation. In order to clarify these problems, we have constructed X-ray luminosity (2-10 keV) versus \dot{E} diagram for all radio and single X-ray pulsars with characteristic time (τ) $< 10^6$

yr located up to 7 kpc from the Sun including also 2 pulsars in Magellanic Clouds (Figure 4.1). The data of these pulsars are represented in Table 4.1.

Depending on values of the magnetic field and the speed of rotation on the surface of neutron star, there arises induced electric field of which the intensity is represented as Lipunov (1992):

$$E_{el} = \frac{4\pi R B_r}{c} \frac{\dot{P}}{P} \sim \left(\frac{\dot{P}}{P}\right)^{\frac{1}{2}} \quad (4.1)$$

where R is the radius of neutron star, B_r the value of the real magnetic field strength and c the speed of light. In actuality, pulsars are located in plasma and expression (4.1) does not give the exact value of E_{el} . As the P- \dot{P} diagram which we use is always represented in logarithmic scale, the lines of constant E_{el} pass parallel to the lines of constant characteristic time

$$\tau = \frac{P}{2\dot{P}} \quad (4.2)$$

so that, we do not show the lines of $E_{el}=\text{constant}$ on the P- \dot{P} diagram. Calculated values of E_{el} may also contain some mistakes, because different pulsars may have different radius, moment of inertia (I) and braking index.

Often, there is PWN around the youngest pulsars which we include in Table 4.1. For such cases the X-ray luminosity value include both the X-ray radiation of the pulsar and of the PWN in most of the cases, as it is difficult to distinguish the $L_x(\text{PWN})$ part of the luminosity. On the other hand, since the contribution of the PWN to the X-ray luminosity can be at most comparable with the X-ray luminosity of the pulsar in general Becker & Aschenbach (2002), the change in the positions of the pulsars in the figures will be small in such cases that the

Table 4.1: All 33 radio and X-ray pulsars with detected X-ray radiation in 0.1 - 2.4 keV and/or in 2 - 10 keV bands and with $\tau < 10^6$ yr. All 15 pulsars which have $\text{Log } \dot{E} > 35.6$ and $\tau < 10^5$ yr. All pulsars which are connected to SNRs (PWNe). Two of these pulsars are in Magellanic clouds and the others are Galactic pulsars with $d \leq 7$ kpc. In the first column G denotes strong glitch. In column 12 $\beta = 2\delta\theta/\theta$ (θ : SNR diameter, $\delta\theta$: angular distance of pulsar from the geometric center of SNR.)

JName	Type	d (kpc)	P s	P s/s	Log τ	Log B	Log \dot{E}	SNR + l,b	SNR Type	β	Log L_x 0.1-2.4 keV	Log L_x 2-10 keV
J1846-0258	X	6.7	0.325	7.1E-12	2.859	13.70	36.9	G29.7-0.3	C	$\sim 0^{15}$	~ 35.18	35.32
J0534+2200	ROXG	2.0	0.034	4.21E-13	3.101	12.58	38.64	Crab	F	$\sim 0.19^{16}$	35.98	36.65
J1513-5908	RXG	4.2	0.151	1.54E-12	3.191	13.19	37.25	G320.4-1.2	C	0.24 ¹⁶	34.25	35.32
J1119-6127	RX	7.0	0.408	4.02E-12	3.205	13.61	36.37	G292.2-0.5	C	$\sim 0^{17}$	≤ 32.5	33.42
J0540-6919	ROX	50	0.051	4.79E-13	3.222	12.70	38.17	N158A	C	$\sim 0^{18}$	36.21	36.93
J1124-5916	RX	6.0	0.135	7.45E-13	3.458	13.01	37.07	G292.9+1.8	C		~ 32.7	34.67
J1930+1852	RX	7	0.137	7.51E-13	3.462	13.0	37.23	G54.1+0.3	F		~ 34.2	
J0537-6910	RX	50	0.016	5.1E-14	3.7	12.0	38.7	N157B	F		~ 36.0	36.11
J0205+6449	RX	3.2	0.066	1.9E-13	3.740	12.55	37.42	G130.7+3.1	F		32.28	34.26
G J1617-5055	RX	6.2	0.069	1.371E-13	3.903	12.49	37.21	332.5,-0.27	F		34.30	34.59
J2229+6114	RXG	5.5	0.052	7.8E-14	4.023	12.31	37.34	G106.6+2.9	C	0 ¹⁹	33.58	33.69
G J0835-4510	ROXG	0.40	0.089	1.25E-13	4.054	12.53	36.84	Vela	C	0.29, 0.30 ^{16,17}	32.46	33.18
J1420-6048	RXG	6.1	0.068	8.32E-14	4.113	12.38	37.01	G313.4+0.2?	F	0.2 ²⁰	34.26	34.30
G J1801-2451	RX	4.5	0.125	1.284E-13	4.189	12.61	36.41	G5.27-0.9	F	$\sim 0^{21}$	~ 33.0	33.18
G J1803-2137	RX	3.5	0.134	1.34E-13	4.197	12.63	36.35	G8.7-0.1	S?	0.7 ²²	33.06	32.29
J1702-4310	R	4.8	0.2405	2.24E-13	4.23	12.88	35.80	343.4,-0.85				
G J1709-4428	RXG	1.8	0.102	9.30E-14	4.241	12.49	36.53	G343.1-2.3?			33.15	32.58
J1856+0113	RX	2.8	0.267	2.08E-13	4.308	12.88	35.63	G34.7-0.4	C	0.51 ¹⁶ , 0.6 ¹⁷	≤ 33.0	33.03
J1048-5832	RXG	2.8	0.124	9.63E-14	4.308	12.54	36.30	287.4,+0.58			≤ 32.11	32.35
J1016-5857	RX	6.5	0.107	8.11E-14	4.321	12.48	36.41	G284.3-1.8	S	1 ²⁰ , 1.3 ²³	~ 33.5	
G J1826-1334	RX	3.4	0.101	7.55E-14	4.328	12.45	36.45	G18.0-0.7	F		~ 32.7	34.34
J1811-1925	X	5	0.065	4.22E-14	4.4	12.23	36.78	G11.2-0.3	F	$\sim 0^{24}$	32.8	34.54
J1747-2958	RX	2.0	0.099	6.14E-14	4.41	12.41	36.41	G359.2-0.8?	F		~ 34.0	

continued on next page

Table 4.1: (*Continued*)

JName	Type	d (kpc)	P s	\dot{P} s/s	Log τ	Log B	Log \dot{E}	SNR + 1,b	SNR Type	β	Log L_x 0.1-2.4 keV	Log L_x 2-10 keV
G J1730-3350	R	4.24	0.1394	8.51E-14	4.41	12.56	36.09	354.1,+0.09				
J1646-4346	R	6.9	0.232	1.13E-13	4.51	12.71	35.55	G341.2+0.9	C	0.7 ²²		
J1837-0604	R	6.2	0.0963	4.52E-14	4.53	12.34	36.30	26.0,+0.27				
J1015-5719	R	4.87	0.1399	5.74E-14	4.59	12.47	35.92	283.1,-0.58				
J2337+6151	RX	2.8	0.495	1.92E-13	4.611	12.99	34.79	G114.3+0.3	S	0.08 ^{16,25}	31.90	31.47
J1637-4642	R	5.5	0.1540	5.92E-14	4.62	12.50	35.81	337.8,+0.31				
J0940-5428	R	3.8	0.0875	3.29E-14	4.63	12.25	36.29	277.5,-1.29				
J0631+1036	RX	6.6	0.288	1.05E-13	4.639	12.74	35.24	201.2,+0.45				31.90
J1809-1917	R	3.3	0.0827	2.55E-14	4.71	12.18	36.25	11.1,+0.08				
J1105-6107	RX	7.0	0.063	1.58E-14	4.801	12.01	36.29	290.5,-0.85			~33.2	33.55
J1718-3825	R	3.3	0.0747	1.32E-14	4.95	12.02	36.10	348.9,-0.43				
J1531-5610	R	2.6	0.0842	1.37E-14	4.99	12.05	35.96	323.9,+0.03				
J1952+3252	RXG	2.0	0.040	5.84E-15	5.030	11.69	36.57	G69.0+2.7	?	0.14,0.15 ^{16,17}	33.64	33.07
J0659+1414	ROX	0.6	0.385	5.50E-14	5.044	12.67	34.58	G201.1+8.7			32.78	30.92
J0908-4913	R	4.5	0.1068	1.51E-14	5.05	12.12	35.69	270.3,1.02				
J0855-4644	R	6.4	0.0647	7.36E-15	5.15	11.85	36.03	267.0,-1.0				
G J1833-0827	R	5.67	0.0853	9.17E-15	5.17	11.97	35.77	23.4,+0.06				
J1509-5850	R	2.5	0.0889	9.17E-15	5.19	11.97	35.71	320.0,-0.62				
J1913+1011	R	4.1	0.0359	3.37E-15	5.23	11.56	36.46	44.5,-0.17				
J0117+5914	RX	2.4	0.101	5.85E-15	5.44	11.89	35.34	126.3,-3.46				30.44
Be J1302-6350	RX	1.3	0.048	2.28E-15	5.52	11.52	35.92	304.2,-1.00				32.57
Geminga	X	0.15	0.237	1.14E-14	5.53	12.22	34.53	195.13,+4.27				29.33
J1057-5226	RX	1.0	0.197	5.83E-15	5.73	12.04	34.48	286.0,+6.65			33.13	30.08
G J0358+5413	RX	2	0.156	4.4E-15	5.75	11.92	34.66	148.2,+0.81				31.75
J0538+2817	RX	1.5	0.143	3.67E-15	5.79	11.87	34.69	G180.0-1.7?	C		32.74	29.31

dependences found from the best fits do not change considerably. It must also be noted that the uncertainties in the distance values and in the measured 2-10 keV fluxes can not have significant influences on these dependences. The pulsars with $\tau < 10^6$ yr located up to 7 kpc for which the X-ray luminosity only in the 0.1-2.4 keV band is known are also displayed in Table 4.1. We have adopted reliable values of distance for the pulsars (Guseinov et al (2003c)) and X-ray luminosity data mainly have been taken from Possenti et al. (2002) and Becker & Aschenbach (2002).

The dependence between X-ray luminosity (2-10 keV) and \dot{E} is displayed in Figure 4.1. The equation of this dependence is:

$$L_{2-10keV} = 10^{-23.40 \pm 4.44} \dot{E}^{1.56 \pm 0.12}. \quad (4.3)$$

In Figure 4.2, X-ray luminosity (2-10 keV) versus τ diagram is represented for the same pulsar sample shown in Figure 4.1. The equation for the relation between X-ray luminosity (2-10 keV) and τ is:

$$L_{2-10keV} = 10^{41.79 \pm 1.04} \tau^{-1.98 \pm 0.23}. \quad (4.4)$$

As seen from Figures 4.1 and 4.2, the deviations of the data with respect to the best fits shown in the figures are larger in the L_x (2-10 keV) versus τ diagram compared to the L_x (2-10 keV) versus \dot{E} diagram, but there is no significant difference.

Some pulsars in Table 4.1 have γ -ray radiation. As seen from Figure 4.1, these pulsars are in general located below the best fit line. On the other hand, all the pulsars with large effective magnetic field (B) values ($\log B > 12.7$) are located

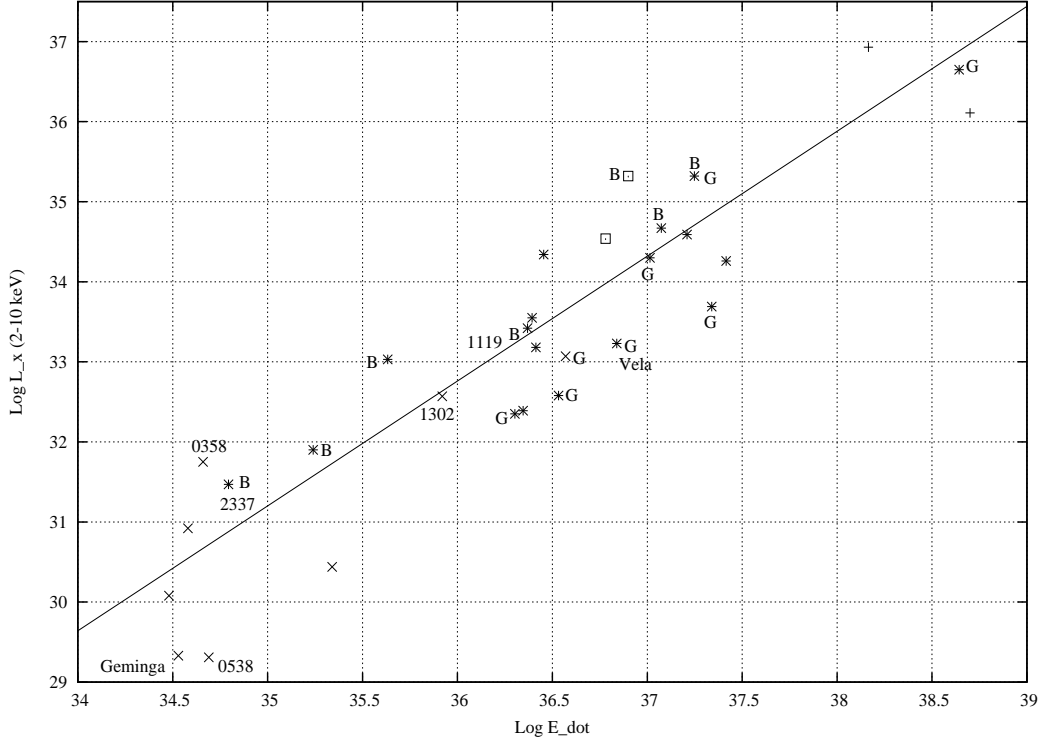


Figure 4.1: $\text{Log } L_x$ (2-10 keV) versus $\log \dot{E}$ diagram of all 30 pulsars with $\tau < 10^6$ yr which have observed X-ray radiation. 28 of these pulsars are located up to 7 kpc from the Sun and 2 of them are in Magellanic Clouds. '+' signs denote the 2 pulsars in Magellanic Clouds. 'x' signs show the positions of pulsars with $10^5 < \tau < 10^6$ yr and '*' signs show the positions of pulsars with $\tau < 10^5$ yr. '□' signs denote single X-ray pulsars. Seven of these pulsars have $\log B > 12.7$ (denoted with 'B') and from 8 of them γ -rays have been observed (denoted with 'G').

above the line (note that when there exist some additional mechanisms other than the magneto-dipole mechanism, $B > B_r$). We have not designated these pulsars in Figure 4.2 but notice that γ -ray pulsars in this figure are located in both parts with respect to the best fit line, whereas, all the pulsars with large values of B have positions below the line. This is also the result of different dependences of

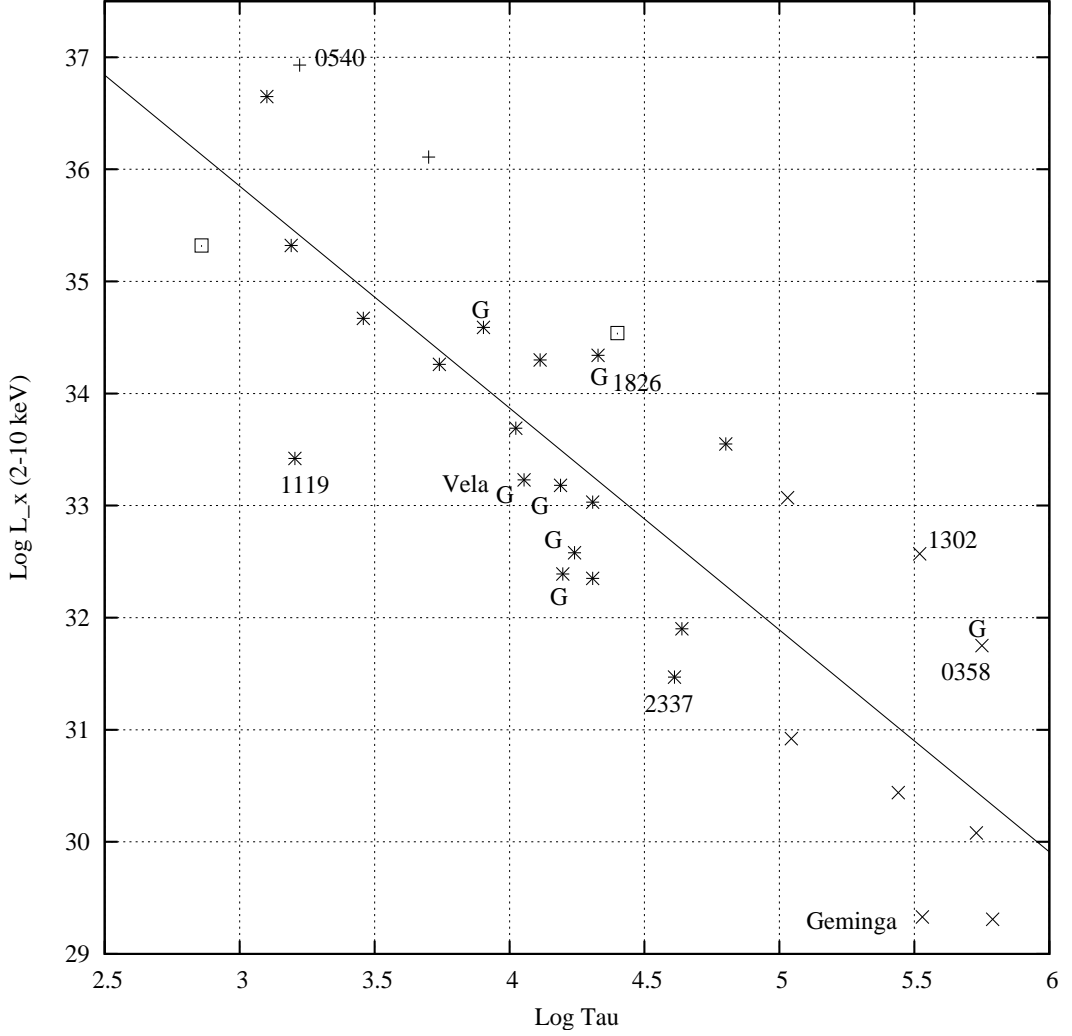


Figure 4.2: $\text{Log } L_x$ (2-10 keV) versus $\text{log } \tau$ diagram of all 30 pulsars with $\tau < 10^6$ yr which have observed X-ray radiation. 28 of these pulsars are located up to 7 kpc from the Sun and 2 of them are in Magellanic clouds. '+' signs denote the 2 pulsars in Magellanic Clouds. 'x' signs show the positions of pulsars with $10^5 < \tau < 10^6$ yr and '*' signs show the positions of pulsars with $\tau < 10^5$ yr. '□' signs denote single X-ray pulsars. Seven of these pulsars have experienced strong ($\Delta P/P > 10^{-6}$) glitches (denoted with 'G').

E_{el} (see expression (4.1)) and rate of rotational energy loss

$$\dot{E} = \frac{4\pi^2 I \dot{P}}{P^3}, \quad (4.5)$$

on the value of P (note that in this approximation we neglect the dependences

of the observational and the calculated parameters of pulsars on the radius and mass of neutron stars).

Which parameters of neutron stars do the deviations in Figures 4.1 and 4.2 mainly depend on? In order to understand this, we have examined pulsars in narrow \dot{E} intervals with large differences in their L_x values which lead to large deviations. The largest deviation is for the interval $\log \dot{E}=36.78-36.9$ where pulsars J1846-0258, J1811-1925, and Vela are present. These are not ordinary pulsars: pulsars J1846-0258 and J1811-1925 are strong X-ray pulsars which have not been detected in other bands, whereas, Vela pulsar, which has been known as a radio, optical and gamma-ray pulsar until recently, has been identified also in X-rays but with low luminosity (Lyne & Graham-Smith (1998)). The L_x (2-10 keV) value of Vela pulsar (Table 4.1) is more than one order of magnitude larger than the value given by Possenti et al. (2002). This is because we have also included the X-ray luminosity of the PWN around the Vela pulsar which is about 10 times greater than the X-ray luminosity of the pulsar (Pavlov et al. (2001)) and we have adopted a more reliable distance value (Guseinov et al. (2003c)) so that the luminosity value also increased about 3 times. Despite these facts, the position of Vela pulsar in Figure 4.1 is still well below the line and the difference between the luminosity values of Vela pulsar and pulsar J1846-0258 is still very large. Although, the period value of pulsar J1846-0258 is 4-5 times larger than the period values of Vela pulsar and pulsar 1811-1925, since the magnetic field

$$B = \sqrt{\frac{3c^3 I P \dot{P}}{8\pi^2 R^6}} \quad (4.6)$$

and \dot{E} values of pulsar J1846-0258 are larger than the values of the other two pulsars (even though the τ value is small), its luminosity (2-10 keV) value is larger (see Table 4.1).

The second largest deviation among large \dot{E} values in Figure 4.1 is in the $\log \dot{E}=37.21-37.42$ interval where pulsars J1513-5908, J0205+6449, J1617-5055, and J2229+6114 are located in. Pulsar J1513-5908, the youngest one among these pulsars, has the largest P, B and L_x values. Among the other pulsars in this group, the largest \dot{E} value belongs to pulsar J0205+6449 in this interval and this pulsar has a smaller value of τ , a larger value of B, and a period value in between the values of pulsars J1617-5055 and J2229+6114. In spite of this, the luminosity of this pulsar is less than the luminosity of pulsar J1617-5055. This is strange, because all four parameters (P, τ , B, \dot{E}) of pulsar J0205+6449 suggest a larger luminosity value. Furthermore, there is no supernova shell or PWN around pulsar J1617-5055. This contradiction is not because of the adopted distance values. Is this contradiction related to the uncertainties in the observational data? Although, the luminosity values of these 2 pulsars (J0205+6449 and J1617-5055) are comparable within error limits (Possenti et al. (2002)), one still can not explain why pulsar J0205+6449 does not have a larger L_x value. If the observational data are not significantly different than the actual values, then either there may be a considerable difference in the mass values of these 2 pulsars or the magnetic field may not be pure dipole.

Among the youngest pulsars, the largest deviations are in the $\log \tau=3.19-3.22$

interval. Among the pulsars in this interval, the smallest P and the largest \dot{E} values belong to pulsar J0540-6919 which has also the largest L_x value. In this interval, the smallest L_x value belongs to pulsar J1119-6127 which has the largest P and B values and the smallest \dot{E} value. According to Gonzalez & Safi-Harb (2003), J1119-6127 has unabsorbed L_x (0.5-10 keV) = $5.5_{-3.3}^{+10} \times 10^{32}$ erg/s at 6 kpc. There is no pulsed X-ray radiation observed from radio pulsar J1119-6127 and the position of the X-ray source is not coincident with the position of the radio pulsar; the observed point source may actually be a PWN (Pivovarov & Kaspi et al. (2001)).

Pulsar J0358+5413 has $\log \tau = 5.75$ and pulsar J0538+2817 has $\log \tau = 5.79$. The L_x value of pulsar J0358+5413 is about 300 times larger than the L_x value of pulsar J0538+2817, but the P , B and \dot{E} values of these 2 pulsars are roughly the same. Why is pulsar J0358+5413 much more luminous than pulsar J0538+2817? The absolute error of the L_x (2-10 keV) value of pulsar J0358+5413 is very large Possenti et al. (2002) and the L_x (2-10 keV) value is not a directly measured value but converted by Possenti et al. (2002) from the L_x value in softer band (Sun & Anderson et al. (1996)). So, the high L_x (2-10 keV) value of pulsar J0358+5413 can actually be much lower and the large difference in the L_x (2-10 keV) values of pulsars J0358+5413 and J0538+2817 can actually be much smaller.

If we consider the corrections to the positions of some of the pulsars discussed above taking also into account relations between L_x and \dot{E} , τ , B and P , and if we change the positions of the pulsars in the figures within error limits given

in Possenti et al. (2002) then, pulsar J1119-6127 will have a higher L_x value, whereas, pulsars J1826-1334, J1302-6350 and J0358+5413 will have lower values of L_x . In this case, the dependence between L_x and τ given in eqn. (4.4) will be improved with a more negative power of τ . If we apply the same approach for the positions of some of the pulsars in Figure 4.1, we see that the deviations do not decrease and the power of \dot{E} (eqn. (4.3)) increases negligibly.

Some of the pulsars shown in Figures 4.1,4.2 and in Table 4.1 have experienced strong glitches ($\frac{\Delta P}{P} > 10^{-6}$, denoted with 'G' in Figure 4.2). As seen from Figure 4.2, the deviations of the data do not seem to be due to the glitch activity.

4.3 The evolutionary factors

Since the values of P and \dot{P} and the other parameters change continuously during the pulsar evolution, the value of $L_{2-10keV}$ must also change in connection to this. We want to analyse how the $L_{2-10keV}$ luminosity of pulsars changes during the evolution of pulsars on the $P-\dot{P}$ diagram.

From eqn. (4.3) we see that

$$L_{2-10keV}^{(\dot{E})} \propto \left(\frac{\dot{P}}{P^3}\right)^{1.56} \quad (4.7)$$

and similarly from eqn. (4.4)

$$L_{2-10keV}^{(\tau)} \propto \left(\frac{\dot{P}}{P}\right)^{1.98} \quad (4.8)$$

using the expressions for \dot{E} eqn. (4.5) and τ eqn. (4.2). Now, using the expression for B eqn. (4.6), we can write eqn. (4.7) and eqn. (4.8) in the form:

$$L_{2-10keV}^{(\dot{E})} \propto \left(\frac{B^2}{P^4}\right)^{1.56} \quad (4.9)$$

and

$$L_{2-10keV}^{(\tau)} \propto \left(\frac{B^2}{P^2}\right)^{1.98}. \quad (4.10)$$

If both dependences eqn. (4.3) and eqn. (4.4) are applicable in finding the value of L_x , then the ratio of the luminosities for each pulsar found from equations (4.9) and (4.10) must roughly be the same throughout the evolution of a pulsar. From dependences eqn. (4.10) and eqn. (4.9) we get:

$$\frac{L_{2-10keV}^{(\tau)}}{L_{2-10keV}^{(\dot{E})}} \propto B^{0.84} P^{2.28}. \quad (4.11)$$

So, the ratio is strongly dependent on P which must be wrong because the ratio must not change significantly during the evolution if both dependences are reliable.

X-ray luminosity of the considered pulsars strongly depends on different parameters of pulsars and decreases with age down to $L_x \sim 10^{29}-10^{30}$ erg/s. During the evolution of these pulsars, the period value changes up to a factor of 10, \dot{P} up to 50 times, \dot{E} up to 10^4 times, and τ up to 500 times. During the evolution, value of B for each pulsar may decrease only up to a factor of 3, but magnitudes of the deviation of B values for different pulsars are larger.

As seen from Figure 4.5, an increase in the initial magnetic field value of a factor of 10 leads to a decrease in the age of X-ray pulsar of a factor of 10. As X-ray luminosity of young pulsars strongly depends on E_{el} and \dot{E} , as seen from the $L_x-\tau$ diagram (Figure 4.2) and Figure 4.5, the X-ray luminosity of the pulsars with largest initial B values drop very quickly below the threshold during the evolution, whereas, the X-ray luminosity of the pulsars with smaller initial values

of B last longer and drop below the threshold in about 10^5 yr. Therefore, it is necessary to consider a more homogeneous group of pulsars which have B values close to each other. Naturally, the best fit lines for the new sample must lead to a different equation for the L_x - τ dependence and practically the same equation for the L_x - \dot{E} dependence. In order to see this, we have constructed L_x vs. \dot{E} and L_x vs. τ diagrams (Figures 4.3 and 4.4) for the pulsars with B values in the interval $12.2 \leq \log B \leq 12.7$ (Figure 4.5). Again from the best fits, we get dependences between L_x and \dot{E} :

$$L_{2-10keV} = 10^{-27.46 \pm 6.48} \dot{E}^{1.66 \pm 0.18} \quad (4.12)$$

and L_x and τ :

$$L_{2-10keV} = 10^{45.98 \pm 1.51} \tau^{-2.99 \pm 0.36}. \quad (4.13)$$

From these two dependences it is seen that the dependence given by eqn. (4.3) is comparable to the dependence given by eqn. (4.12) within error limits, but the dependence given by eqn. (4.4) changed considerably (see eqn. (4.13)).

Dividing eqn. (4.13) by eqn. (4.12) and again using the expressions (4.5) and (4.2) we get:

$$\frac{L_{2-10keV}^{(\tau)}}{L_{2-10keV}^{(\dot{E})}} \propto B^{2.66} P^{0.66}. \quad (4.14)$$

As the effective B value decreases gradually during the evolution, the large increase in the P value compensates it and the ratio remains approximately the same. The dependences eqn. (4.12) and eqn. (4.13) are more reliable and reflect

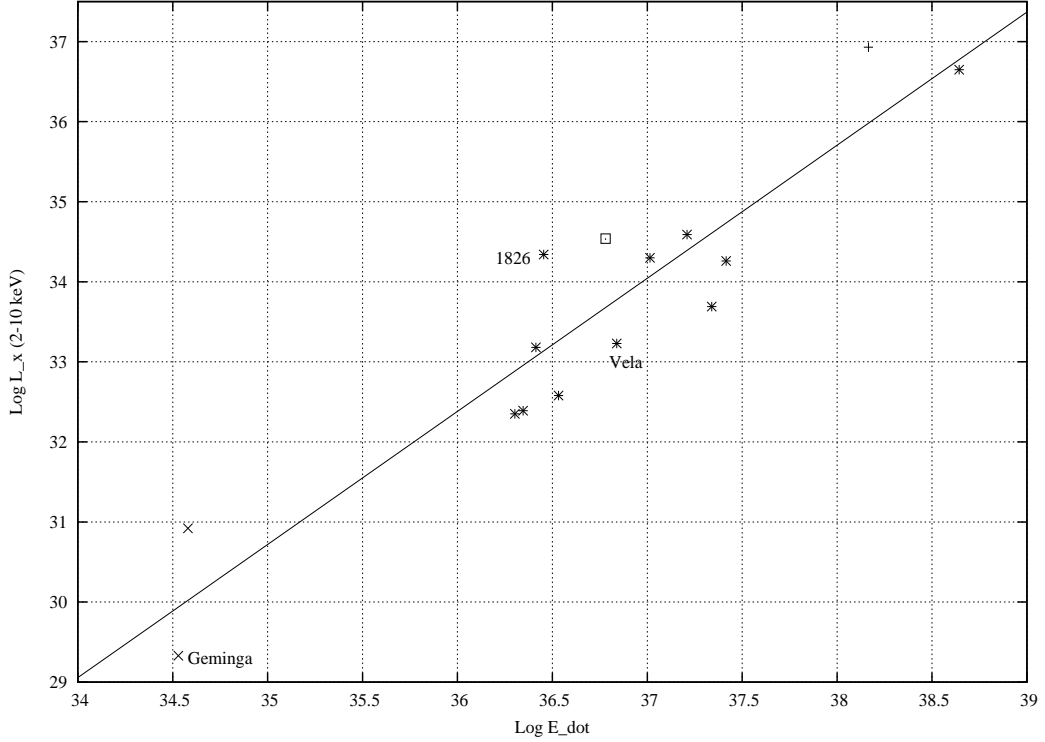


Figure 4.3: $\text{Log } L_x$ (2-10 keV) versus $\log \dot{E}$ diagram for 15 of the 30 pulsars shown in figures 4.1 and 4.2; these 15 pulsars have $12.2 \leq \log B \leq 12.7$. '+' sign denotes the pulsar in Magellanic Cloud. 'x' signs show the positions of pulsars with $10^5 < \tau < 10^6$ yr and '*' signs show the positions of pulsars with $\tau < 10^5$ yr. '□' sign denotes the single X-ray pulsar.

the evolutionary effects, because we have used a more homogeneous group of pulsars with similar evolutionary tracks in Figures 4.3 and 4.4. The ratio given by dependence eqn. (4.14) shows this fact.

The reason of the considerable difference between the dependences eqn. (4.4) and eqn. (4.13) can easily be seen in Figure 4.5. As seen from this figure, when the value of τ is small, first the constant τ line crosses the considered B interval (i.e. the interval of $12.2 \leq \log B \leq 12.7$) where the value of \dot{E} is large. Then, it crosses the region, which is not included in the B interval under consideration,

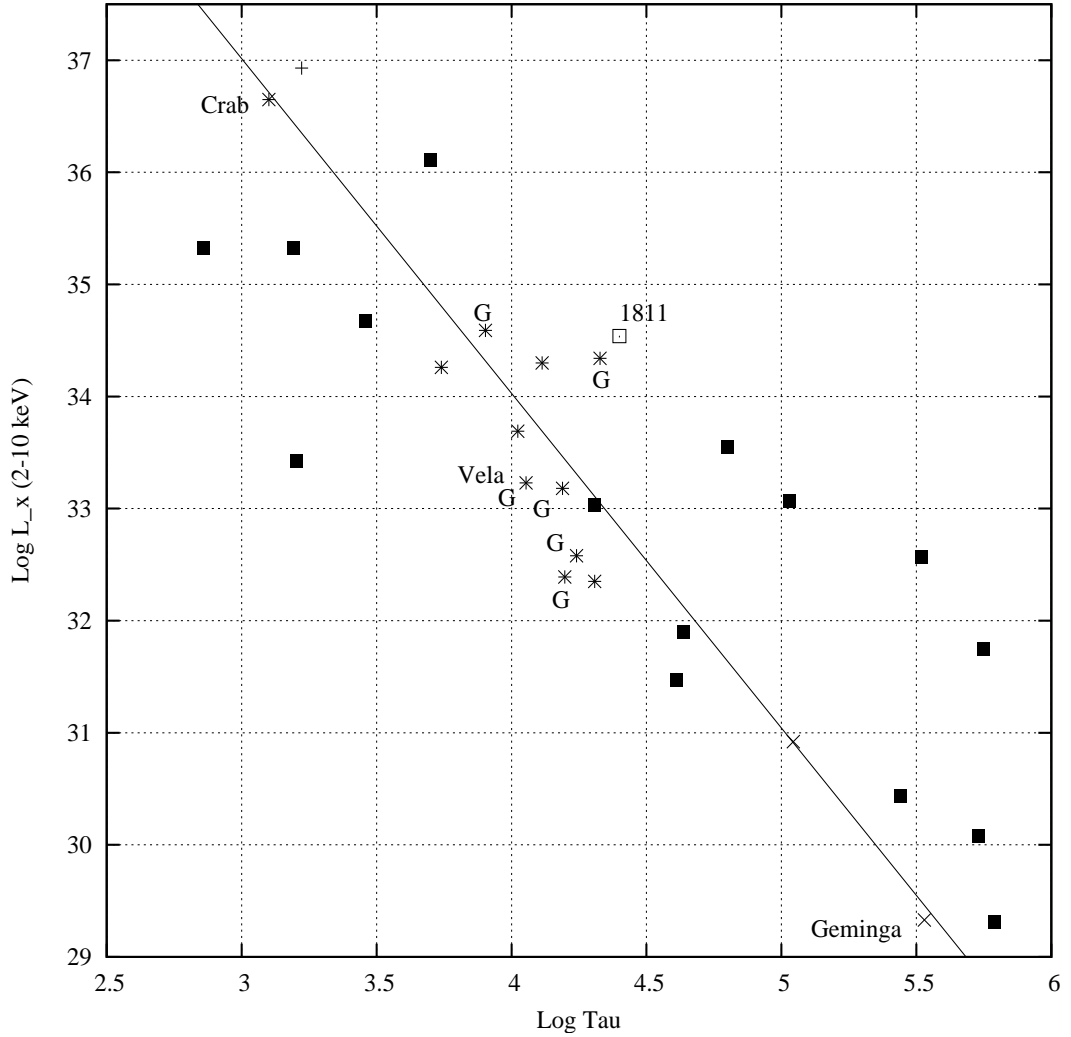


Figure 4.4: $\text{Log } L_x$ (2-10 keV) versus $\text{log } \tau$ diagram for 15 of the 30 pulsars shown in Figures 4.1 and 4.2; these 15 pulsars have $12.2 \leq \log B \leq 12.7$. '+' sign denotes the pulsar in Magellanic Cloud. 'x' signs show the positions of pulsars with $10^5 < \tau < 10^6$ yr and '*' signs show the positions of pulsars with $\tau < 10^5$ yr. '□' sign denotes the single X-ray pulsar. ■ shows the positions of the pulsars which are present in Figure 4.2 but not included in the fit of this figure.

where the value of \dot{E} is small. On the other hand, if the value of τ is large, then the constant τ line first crosses a region, outside the considered B interval, where pulsars with large values of \dot{E} are located, and then it crosses the B interval under

consideration where pulsars with small \dot{E} values are present. Therefore, for small values of τ , the pulsars which have smaller values of $L_{2-10keV}$ and which are not located in the considered interval have positions below the best fit line in Figure 4.4. On the other hand, for large values of τ , the pulsars which have larger values of $L_{2-10keV}$ and which are not located in the considered interval have positions above the best fit line in Figure 4.4. Excluding the pulsars with large deviations from the best fit line leads to the considerable difference between the dependences eqn. (4.4) and eqn. (4.13).

In Table 4.1, we have also included the 15 pulsars with $\tau < 10^5$ yr and/or $\log \dot{E} > 35.60$ from which no X-ray radiation has been detected. In Figure 4.5, all the 48 pulsars in Table 4.1 are displayed. Within and around this region of the P- \dot{P} diagram, there are pulsars with detected X-ray radiation. All of these pulsars without detected X-ray radiation are also located at $d \leq 7$ kpc from the Sun. One of these pulsars is connected to a supernova remnant (SNR). As seen from Figure 4.5 and Table 4.1, there are some pulsars without observed X-ray radiation which have smaller τ values and larger \dot{E} values compared to some pulsars with observed X-ray radiation. What is the reason for not detecting X-ray radiation from such pulsars? As mentioned in the previous section, the X-ray luminosity must depend not only on P and \dot{P} but also on some other parameters. The deviations of the data from the best fits in Figures 4.1-4.4 also show this fact. It is not easy to examine these "other parameters" which can not be calculated from values of P and \dot{P} and get reliable results. But it is possible to clarify why there exist those

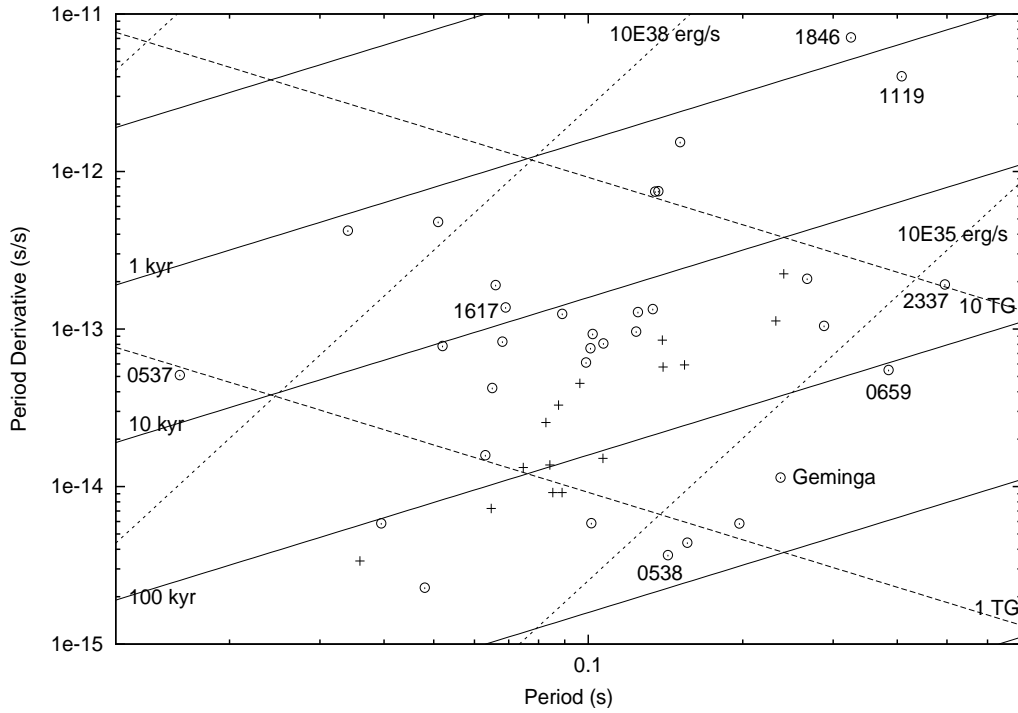


Figure 4.5: P versus \dot{P} diagram for all 48 pulsars represented in Table 4.1 with $\tau < 10^6$ yr and distance ≤ 7 kpc including the 2 pulsars in Magellanic Clouds. 'o' represents the 33 pulsars from which X-ray radiation have been detected in 2-10 keV and/or 0.1-2.4 keV bands. '+' signs denote the 15 pulsars with $\log \dot{E} > 35.55$ from which no X-ray radiation has been observed.

pulsars with smaller τ values and larger \dot{E} values from which no X-ray radiation has been detected by examining the selection effects.

It is clear that it is more difficult to observe the X-ray radiation of a pulsar if it is located at a large distance in the Galactic plane and in the Galactic center direction. All the 8 pulsars with $\tau > 10^5$ yr from which X-ray radiation has been observed as shown in Figure 4.5 are located at distances $d < 2.5$ kpc from the Sun (Figure 4.6). Directions of these and all the other pulsars in Table 4.1 are shown in b vs. l diagram (Figure 4.7).

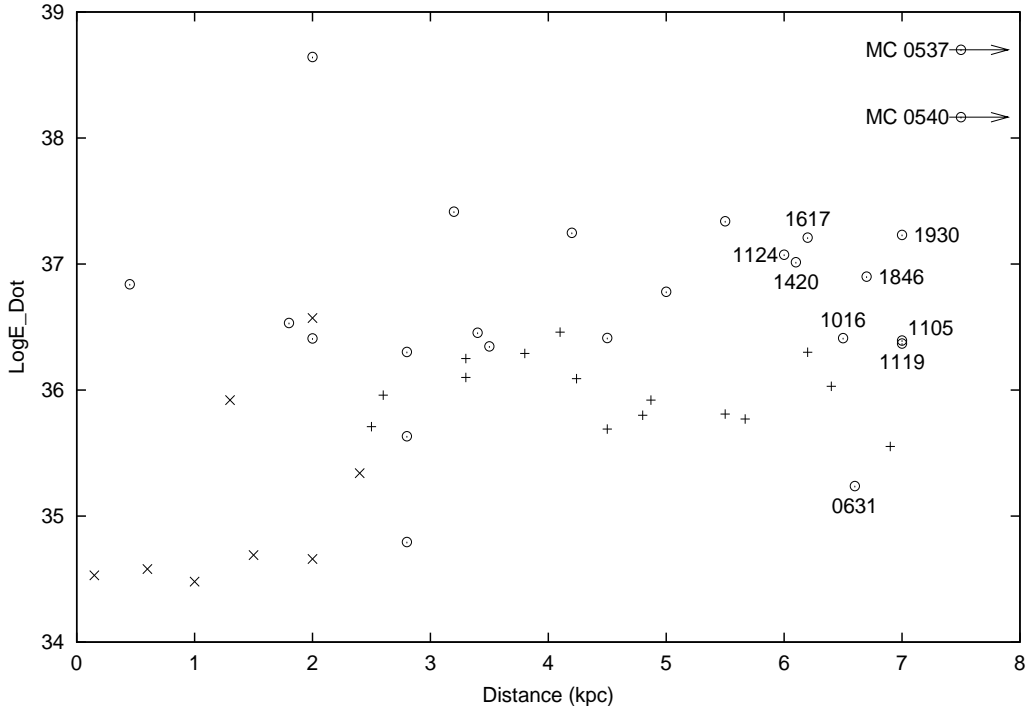


Figure 4.6: $\log \dot{E}$ versus distance diagram for all 48 pulsars represented in Table 4.1 with $\tau < 10^6$ yr and distance ≤ 7 kpc including the 2 pulsars in Magellanic Clouds. 'o' represents the 33 pulsars from which X-ray radiation have been detected in 2-10 keV and/or 0.1-2.4 keV bands. '+' signs denote the 15 pulsars with $\log \dot{E} > 35.55$ from which no X-ray radiation has been observed. 'x' signs represent the 8 pulsars with $10^5 < \tau < 10^6$ yr.

In Figure 4.6, \dot{E} -d diagram for all the 48 pulsars in Table 4.1 is represented. The pulsars without observed X-ray radiation are all located beyond 2 kpc from the Sun. It is normal to detect X-ray radiation from pulsars with large \dot{E} values even at large distances (see Figure 4.6), but there is a pulsar, namely J0631+1036, with detected X-ray radiation in the 2-10 keV band which is located at $d=6.6$ kpc and has a smaller \dot{E} value ($\log \dot{E}=35.24$). The reason for this is that this pulsar is located in the Galactic anti-center direction (see Figure 4.7). The other 8 pulsars

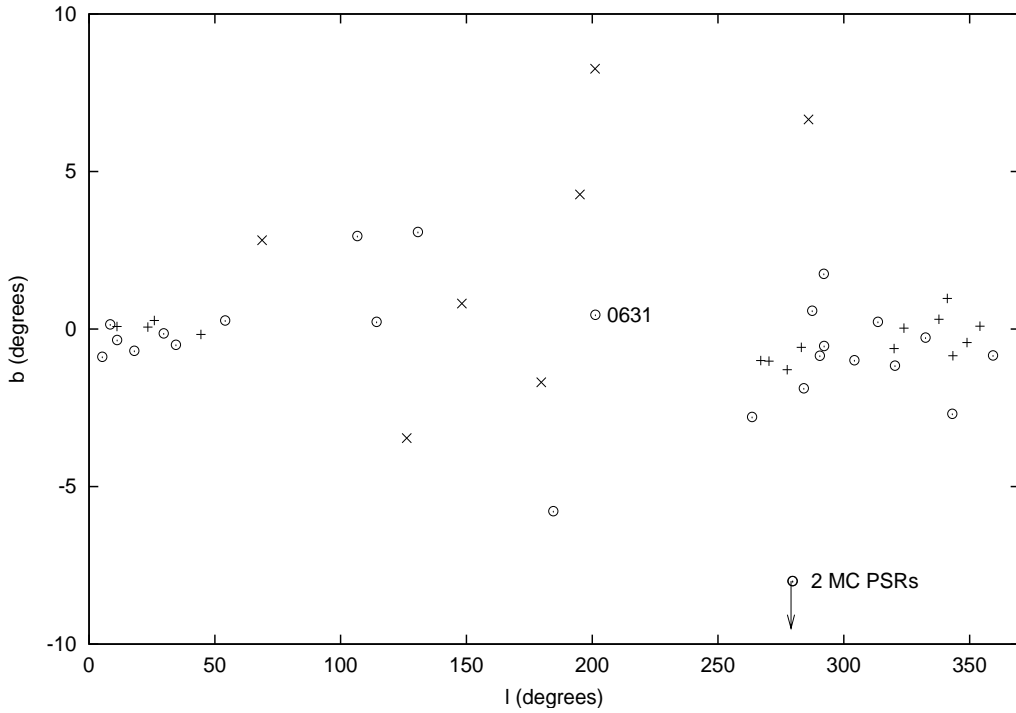


Figure 4.7: Galactic latitude (b) versus Galactic longitude (l) diagram for all 48 pulsars represented in Table 4.1 with $\tau < 10^6$ yr and distance ≤ 7 kpc including the 2 pulsars in Magellanic Clouds. 'o' represents the 33 pulsars from which X-ray radiation have been detected in 2-10 keV and/or 0.1-2.4 keV bands. '+' signs denote the 15 pulsars with $\log \dot{E} > 35.55$ from which no X-ray radiation has been observed. 'x' signs represent the 8 pulsars with $10^5 < \tau < 10^6$ yr.

with detected X-ray radiation and with distances between 6-7 kpc are located in the Galactic central directions. Six out of the 8 far away pulsars in the central directions are connected to SNRs that these are well examined pulsars. So, it must be considered normal to detect the X-ray radiation of these pulsars. On the other hand, the remaining 2 pulsars, namely J1105-6107 and J1617-5055, are not connected to SNRs. Pulsar J1617-5055 has very high \dot{E} and large L_x values (see Table 4.1), and pulsar J1105-6107 is located in between the Sagittarius and

the Scutum arms so that it is normal to observe the X-ray emission of these 2 pulsars. All the pulsars without detected X-ray radiation are located in the central directions and in the directions of Vela OB-associations (see Figure 4.7). Moreover, the pulsars with $d \leq 4.1$ kpc which have not been detected in X-rays (J0940-5428, J1809-1917, J1718-3825, J1531-5610, J1509-5850, J1913+1011) have all been found in recent pulsar surveys (Manchester & Lyne et al. (2001), Morris & Hobbs et al. (2002), Kramer & Bell et al. (2003)). In the near future, it is possible that all of these pulsars will be detected in X-rays.

4.4 Discussion and Conclusions

For single pulsars, the X-ray radiation due to the relativistic particles, which considerably exceeds the cooling radiation, is important and worth examining. Power and spectrum of this radiation depend on the number and the energy spectra of the relativistic electrons in the magnetospheres of pulsars. They also depend on the number density of charged particles and the magnetic field in the magnetosphere. The X-ray radiation of PWNe also depends on these quantities. X-ray radiation has also been observed from old single millisecond pulsars which is absolutely not cooling radiation but a result of Coulomb interaction between the accelerated particles and the charged particles in the magnetosphere. Since the parameters of millisecond pulsars practically do not vary in time and as they are not active as the young pulsars are, we do not consider them in this work.

From the investigations of single pulsars which radiate X-rays as a result of ejection of relativistic particles, we have concluded as follows:

- ▶ Luminosity in 2-10 keV band (often the total luminosity including the luminosity of the PWN) strongly depends on electric field intensity E_{el} (or τ), rate of rotational energy loss \dot{E} , magnetic field B, period, and in smaller degree on some other parameters of neutron stars.
- ▶ The dependence of L_x on \dot{E} is practically the same for pulsars with very different values of B and with $B=10^{12}$ - 10^{13} G. This is not true for the L_x - τ dependence.
- ▶ Pulsars with different initial values of B and with τ about 10^3 yr begin to evolve from different points of the L_x - \dot{E} dependence and then continue to evolve with similar trajectories until L_x drops to $\sim 10^{30}$ erg/s, but the same pulsars begin and end their evolution in different parts of the L_x - τ dependence and the evolutionary tracks are not parallel to the L_x - τ dependence for all the pulsars under consideration.
- ▶ The pulsars, which also radiate gamma-rays, with the same values of \dot{E} as the other pulsars without gamma-ray radiation have several times smaller X-ray luminosities.
- ▶ The pulsars which have PWNe practically always have X-ray luminosities greater than 10^{33} erg/s.
- ▶ Practically, values of τ and \dot{E} determine the X-ray luminosity. The increase in τ and the decrease in \dot{E} simultaneously lead to a rapid decrease in L_x . Value of L_x decreases from $\sim 10^{37}$ erg/s for $\dot{E} \sim 3 \times 10^{38}$ erg/s and $\tau \sim 10^3$ yr

to $\sim 10^{30}$ erg/s for $\dot{E} \sim 3 \times 10^{34}$ erg/s and $\tau \sim 3 \times 10^5$ yr.

► If we take into account these and also the strength and spectra of the X-ray radiation of millisecond pulsars (Possenti et al. (2002), Becker & Aschenbach (2002)), we can have some preliminary conclusions about the acceleration of particles and their radiation. As the characteristic time of millisecond pulsars is about 4-5 orders of magnitude smaller compared to the young pulsars, their E_{el} values must be 200-250 times smaller than the E_{el} values of young pulsars. On the other hand, the value of E_{el} does not have a strong influence on the X-ray radiation of pulsars. The X-ray spectra of young pulsars are, on average, steeper compared to the spectra of millisecond pulsars. If we also consider the strong dependence of the X-ray radiation of all the pulsars on the value of \dot{E} , we can conclude as follows:

- Acceleration of particles mainly takes place in the field of magnetodipole radiation wave. E_{el} has a role of only triggering this process.
- The high values of X-ray luminosity of young pulsars under the same \dot{E} values and the steeper spectra of such pulsars are related to the large amount of charged particles in their magnetospheres as compared to millisecond pulsars.

It is necessary to reexamine the X-ray flux values of J0205+6449, J0358+5413, and J0538+2817 in 2-10 keV band to understand the dependences of the X-ray luminosity on \dot{E} , E_{el} , B and P values and the possible dependence on the energy spectra of the ejected particles.

Also, in order to understand the dependence of the X-ray radiation on different parameters of pulsars better, it is necessary to observe pulsars J0940-5428, J1809-1917, J1718-3825, J1531-5610, J1509-5850, J1913+1011 preferably in the hard X-ray band.

*Reason has always existed,
but not always in a reasonable form*

Karl Marx

CHAPTER 5

GENERAL CONCLUSIONS

*For an idea that does not first seem insane,
there is no hope*

Albert Einstein

At the theoretical level we are standing it is difficult to construct correct and convincing theories to solve the mystery surrounding the magnetars. The problems can be overcome only by observational facts. Therefore, magnetars are continuously and intensively observed in γ , X, optic and radio bands, but still neither the models founded on accretion nor the ones in the magnetar category provide a successful understanding of these objects.

The existing theories, for example, the first generation accretion models (Chatterjee et al. (2000), Alpar (1999,2001), Marsden et al. (2001), van Paradijs et al. (1995)) neglect many observational data while trying to explain the properties of magnetars. The very early models do not even take into account the presence of SGRs; neither do they consider all of the data of AXPs.

As known, observations do not indicate the existence of the fall-back disks in general (Tagieva et al. (2003), Francischelli & Wijers (2002), see however Alpar (2003)). In particular, infrared radiation detected from AXPs 4U0142+61

(Hulleman et al. (2000), Hulleman (2002)), 1E2259+586 (Hulleman et al. (2001)) and 1E1048.1-5937 (Wang & Chakrabarty (2002), Israel et al. (2002)) does not seem to be the kind of infrared radiation of an accretion (see however Ertan & Cheng (2004) for opposing views). Moreover, the spectra of AXPs and SGRs are claimed to be in favor of the magnetar model (Perna et al. (2001)).

Due to these considerations, after getting rid of the great difficulties with rotational momentum loss by accepting the propeller mechanism working simultaneously with accretion, the last fall-back disk models attempt to take into consideration all of the observational properties of these objects. They tried to use all of the existing ideas like the ones in the magnetar models. However, instead of using the inner parameters such as the magnetic field, they related the observational properties to the surrounding matter that interacts with the NS (Rotschild et al. (2002), Menou et al. (2001), Rotschild et al. (2001)). Due to the fact that fall-back disk models are extended, they are now faced with some of the handicaps of the magnetar approach.

We believe that to understand the nature of magnetars it is necessary to extend the boundary of astrophysics and therefore we, like the majority of the authors, support the magnetar model despite its several great difficulties. To mention the greatest ones we can say that the activity of AXPs and SGRs does not seem to depend on age, which does not cause serious problems for accretion theories, but is a great difficulty for the magnetar model. The main problem of AXPs and SGRs is their sources of radiation. As known, the high value of magnetic fields (B) and their reconnection indicate large amount of X-ray radiation which can

be represented by a power and black-body radiation. In the frame of magnetar model the large value of \dot{P} and period noise imply a huge B and a lot of magnetic reconnection events occurring in SGRs and AXPs. Therefore according to this model and observational data, it is natural that these objects have larger X-ray luminosities than the amount which can be supplied by the rate of rotational energy loss. As seen from Table 3.1 persistent X-ray luminosities of SGRs are close to luminosities of AXPs but they are a little higher in average because SGR0526-60 is luminous. Consequently, we may expect L_x and kT_{bb} to depend on the degree of activity, i.e. \dot{P} or τ . Surprisingly, even though AXPs and SGRs have different characteristic ages (τ) and \dot{P} s their black-body temperatures and X-ray luminosities are quite similar (see Figures 3.1 and 3.2).

It seems that the ages of SGRs are higher than AXPs, of course also higher than the ages of SNRs. This is a great difficulty for the magnetar model, if in this model all the braking is connected with magneto-dipole radiation and if a magnetic field of $B \sim (5-10) 10^{14}$ G exists at birth. Therefore we preferred to use the magnetar model with a bulk dipole field $B \sim 3 \times 10^{14}$ G. At this point latest observations appeared to be working for our benefit. Some radio pulsars (PSRs), especially J1119-6127, J1814-1744, 1726-3539 and 1734-3333 were reported with magnetic field strengths $B \approx 4 \times 10^{13}$ G (Camilo et al. (2000), Morris et al. (2002)). Therefore, we may not need to assume a magnetic field of the order of $(5-10) \times 10^{14}$ G for magnetars. There might be a possibility of explaining AXPs and SGRs with the field close to the highest observed PSR fields, i.e. about $\sim 3 \times 10^{14}$ G. In fact, we do not really know whether such huge $(5-10) \times$

10^{14} G magnetic fields exist observationally. Moreover, we have never found any evidence of such a huge dipole magnetic field decays for single young NSs (Urpin & Muslimov (1994)).

We know that \dot{P} s may be as large as $(5-7) \times 10^{-11}$ s/s in magnetars. So, to explain such large \dot{P} values with less magnetic fields, propeller mechanism should interact with the plasma, which is from time to time released as a consequence of star-quakes, volcano processes and reconnection events or the component of the magnetic field perpendicular to the rotation axis (B_{\perp}) must increase ~ 3 times. If this is the case, then the source of the huge \dot{P} is mostly due to the propeller mechanism and the increased value of B_{\perp} . In this approach the value of τ must not have correlation with the real age and τ can be about an order smaller than the real age. The characteristic age, τ , may strongly decrease from time to time when magnetars enter into periods of strong activity (AXP or SGR stage). Then, it is a possible scenario that magnetars oscillate between SGR, AXP and dim stages and spend most of their time in the inactive dim stage. In this approach, the difficulties with the absence of SNRs around SGRs are somewhat diminished and SGRs and AXPs have the same ages.

Braking index (n) gives clues about the energy loss mechanism which is slowing down the pulsar. In the standard theories for pure magnetic dipole radiation we have $n = 3$. Since the strength of magnetic dipole radiation is inferred from rotational energy loss it is also related to period derivative. If n is smaller than 3 then there are additional physical processes that give extra torque to the PSR. Glitches may be among these processes. Almost all the reported glitch activity

were in young PSRs. If we look at the numerical values found for few young PSRs we will see that n is smaller than its canonical value 3. We should also notice their association with SNRs. We think that the link between the type of a SNR and the braking index can be helpful in deeper investigations.

For this reason we inquired ≈ 50 PSRs with largest \dot{E} . We analysed the evolution of their X-ray luminosity in 2 - 10 keV energy band. We found that PWNe almost always exist around young PSRs whose X-ray luminosity exceeds 10^{33} erg/s. The characteristic parameters are subject to changes during the evolution of PSRs. Naturally, these changes reflect themselves in the radiation of the neutron star. As τ increases and \dot{E} decreases the X-ray luminosity decreases sharply (≈ 7 orders). We concluded that τ and \dot{E} are the most effective factors. As for the other evolutionary elements, the magnetic field decreases gradually whereas the decrease in periods is steeper.

It is possible to express the variation of L_X both with respect to τ and \dot{E} in terms of magnetic field and the period derivative. Obviously, the ratio of these expressions should not change significantly if we are able to estimate the luminosity of a PSR from either one of them. Controversially we showed that $L_x^\tau/L_x^{\dot{E}}$ depends too much on the period. As an adjustment we pointed that the power of the period in the ratio must be less than the values suggested by early studies. Instead, the contribution of magnetic field must be stressed increasing its power.

Independent of these studies we argued that the origin of PSRs whose ages change from 5×10^5 years to 10^7 years within the period range 0.1 - 0.3 seconds

might be understood if they somehow spent a portion of their life in a binary. Depending on the kinematical arguments we proved that the binary should be a HMXB. During their evolution these binaries should survive the first supernova explosion but be disrupted by a second supernova explosion. We point the presence of lower magnetic fields with small periods as an evidence on behalf of this suggestion. We can test this proposal by observing X-ray radiation from PSRs that are on the evolution path of the ones originated from HMXBs. During the HMXB phase X-rays might be curtailed so that with the disruption neutron star can be released and its pulsations in X-ray can be detected.

You can not shake hands with a clenched fist

Indira Gandhi

REFERENCES

- [1] Allakhverdiev, A.O., Alpar, M.A., Gok, F., Guseinov, O. H., 1997, Turkish Jour. of Phys., 21, 688
- [2] Allakhverdiev, A.O., Guseinov, O.H., Tagieva, S.O., 1997, AstL., 23, 628
- [3] Alpar, M.A., 1999, astro-ph/9912228
- [4] Alpar, M.A., 2001, ApJ., 554, 1245
- [5] Alpar, M.A., Ankay, A., Yazgan, E., 2001, ApJ., 557, L61
- [6] Amnuel' P.R., Guseinov, O.K., 1968, Izv. Akad. Nauk. Azer. SSR, ser. Fiz.-Tekh Mat. Nauk., 3, 70
- [7] Amnuel, P.R., Guseinov, O.H., 1972, AN., 294, 139
- [8] Amnuel, P.R., Guseinov, O.H., Kasumov, F.K., 1973, SvA, 16, 932
- [9] Amnuel' P.R., Guseinov, O.H., 1973, Variable Stars, 19, 19
- [10] Amnuel' P.R., Guseinov, O.H., Rakhamimov, Sh.Yu., 1974, Ap&SS., 331, 29
- [11] Ankay, A., Guseinov, O.H., Alpar, M.A., Tagieva, S.O., 2001, astro-ph/0110092
- [12] Aschenbach, B., 1998, Nature, 396, 141
- [13] Aschenbach, B., Iyudin, A.F., Schonfelder, V., 1999, A&A., 350, 997
- [14] ATNF Pulsar Catalog, 2005, <http://www.atnf.csiro.au/research/pulsar/psrcat>
- [15] Baade, W., Zwicky, F., 1934, Phys. Rev., 45, 138
- [16] Bailes, M., Manchester, R.N., Kesteven, M.J. et al., 1990, MNRAS., 247, 322
- [17] Baykal, A., Swank, J., 1996, ApJ., 460, 470
- [18] Baym, G., Pines, D., 1971, Ann. Phys., 66, 816
- [19] Becker, W., Trümper, J., 1997, A&A., 326, 682

- [20] Becker, W., Aschenbach, B., 2002, Proceedings of the 270th WE-Heraeus Seminar on Neutron Stars, Pulsars and Supernova Remnants, In: W. Becker, H. Lesch and J. Trümper (Eds.), MPE Report, Vol, 278, 64
- [21] Bertsch, D.L., Brazier, K.T.S., Fichtel, C. E. et al., 1992, Nature, 357, 306
- [22] Bisnovatyi-Kogan, G.S., Komberg, B.V., 1974, SvA., 217, 18
- [23] Bisnovatyi-Kogan, G.S., Komberg, B.V., 1976, SvAL., 130, 2
- [24] Blaauw, A., 1961, B.A.N., 15, 265
- [25] Braun, R., Goss, W.M., Lyne, A.G., 1989, ApJ., 340, 355
- [26] Brazier, K.T.S., Johnston, S., 1999, MNRAS., 305, 671
- [27] Camilo, F., Kaspi, V.M., Manchester, R.N. et al., 2000, ApJ., 541, 367
- [28] Camilo, F., Bell, J.F., Manchester, R.N. et al., ApJ., 2001, 557, L51
- [29] Chakrabarty, D., Pivovarov, M.J., Hernquist, L.E. et al., 2001, ApJ., 548, 800
- [30] Chatterjee, P., Hernquist, L., Narayan, R., 2000, ApJ., 534, 373
- [31] Chevalier, R.A., 1989, ApJ., 346, 847
- [32] Colgate, S.A., White, R.H., 1966, ApJ., 143, 626
- [33] Corbel, S., Wallyn, P., Dame, T. M. et al., 1997, ApJ., 478, 624
- [34] Corbet, R.H.D., Smale, A.P., Ozaki, M. et al., 1995, ApJ, 443, 786
- [35] Corbet, R.H.D., Mihara, T., 1997, ApJ., 475, L127
- [36] Crampton, D., Georgelin, Y.M., Gergelin, Y.P., 1978, A&A., 66, 1
- [37] Dall’Osso, S., Israel, G.L., Stella, L. et al., 2003, ApJ., 599, 485
- [38] Danner, R., Kulkarni, S.R., Trumper, J., 1998, BAAS., 30, 875
- [39] Davis, L., Goldstein, M., 1970, ApJ., 159, L81
- [40] Dechristopher, B.M., Winkler, P.F., 1994, BAAS., 26, 951
- [41] De Luca, A., Mereghetti, S., Caraveo, P.A. et al., 2002, astro-ph/0211101
- [42] Duncan, R.C., Thompson, C., 1992, ApJ., 392, L9
- [43] Duncan, R.C., Thompson, C., 1996, High Velocity Neutron Stars, edited by R.E. Rothschild and R.E. Lingenfelter, New York: American Institute of Physics Press., AIP Conference Proceedings, Vol. 366, p.111

- [44] Eikenberry, S.S., 2002, astro-ph 0203054
- [45] Eksi, K.Y., Alpar, M.A., 2005, ApJ., 620, 390
- [46] Erkut, M.H., Alpar, M.A., 2004, ApJ., 617, 461
- [47] Ertan, Ü., Alpar, M.A., 2003, ApJ., 593, L93
- [48] Ertan, Ü., Cheng, K.S., 2004, ApJ., 605, 840
- [49] Evans, W., Belian, R., Conner, J., 1970, ApJ., 57, L159
- [50] Fahlman, G.G., Gregory, P.C., 1981, Nature, 293, 202
- [51] Feroci, M., Hurley, K., Duncan, R.C., Thompson, C., 2001, ApJ., 549, 1021
- [52] Fomalont, E., Goss, W.M., Manchester, R.N., Lyne, A.G., 1997, MNRAS., 286, 81
- [53] Frail, D.A., Goss, W.M., Whiteoak, J.B.Z., 1994, ApJ., 437, 781
- [54] Frail D.A., Kulkarni S.R., Bloom, J.S., 1999, Nature, 398, 127
- [55] Francischelli, G.J., Wijers, R., 2002, astro-ph/0205212
- [56] Furst, E., Reich, W., Seiradakis, J.H., 1993, A&A., 276, 470
- [57] Gaensler, B.M., Gotthelf, E.V., Vasisht, G., 1999, ApJ., 526, L37
- [58] Gaensler, B.M., Slane, P.O., Gotthelf, E.V., Vasisht, G., 2001, ApJ., 559, 963
- [59] Gavriil, F.P., Kaspi, V.M., Woods, P.M., 2002, Nature, 419, 142
- [60] Gavriil, F.P., Kaspi, V.M., 2002, ApJ, 567, 1067
- [61] Gavriil, F.P., Kaspi, V.M., Woods, P.M., 2003, astro-ph/0301092
- [62] Gavriil, F.P., Kaspi, V.M., 2004, ApJ, 609, L67
- [63] Ghosh, P., Lamb, F.K., 1979, ApJ., 232, 259 (1979a)
- [64] Ghosh, P., Lamb, F.K., 1979, ApJ., 234, 296 (1979b)
- [65] Ghosh, P., Angelini, L., White, N.E., 1997, ApJ., 478, 713
- [66] Giacconi, R., Gursky, H., Paolini, F.R., Rossi, B.B., 1962, Phys. Rev. Lett., 9, 439
- [67] Giacconi, R., Murray, S., Gursky, H. et al., 1972, ApJ., 178, 281
- [68] Ginzburg, V.L., 1964, Dokl. Akad. Nauk. SSSR., 156, 43

- [69] Gold, T., 1968, *Nature*, 218, 731
- [70] Gonzalez, M., Safi-Harb, S., 2003, *ApJ.*, 591, L143
- [71] Gotthelf, E.V., Petre, R., Hwang, U., 1997, *ApJ.*, 487, L175
- [72] Gotthelf, E.V., Vasisht, G., Dotani, T., 1999, *ApJ.*, 522, L49
- [73] Gotthelf, E.V., Vasisht, G., Gaensler, B.M., Torii, K., 2000, *Pulsar Astronomy-2000 and Beyond*, ASP Conference Series, Vol. 202, p.707
- [74] Gögüs, E., Kouveliotou, C., Woods, P.M. et al., 2002, *ApJ*, 577, 929
- [75] Green, D.A., 1989, *MNRAS.*, 238, 737
- [76] Gregory, P.C., Fahlman, G.G., 1980, *Nature*, 287, 805
- [77] Gunn, J.E., Ostriker, J.P., 1970, *ApJ.*, 160, 979
- [78] Guseinov, O.H., Saygac, A.T., Allakhverdiev, A.O. et al., 2000, *AsTL.*, 26, 725
- [79] Guseinov, O.H., Ankay, A., Sezer, A., Tagieva, S.O., 2003, *A&AT.*, 22, 273
- [80] Guseinov, O.H., Yazgan, E., Ankay, A., Tagieva, S.O., 2003, 12, 1 (2003a)
- [81] Guseinov, O.H., Ankay, A., Tagieva, S.O., 2003, *SerAJ.*, 167, 97 (2003b)
- [82] Guseinov, O.H., Taşkin, Ö., Yazgan, E., Tagieva, S., 2003, *IJMPD.*, 12, 1333 (2003c)
- [83] Guseinov, O.H., Yerli, S.K., Ozkan, S. et al., 2004, *A&AT.*, 23, 357 (astro-ph/0206050)
- [84] Guseinov, O.H., Ankay, A., Tagieva, S.O., 2004, *IJMPD.*, 13, 1805 (2004a)
- [85] Guseinov, O.H., Ankay, A., Tagieva, S.O., 2004, *SerAJ.*, 168, 55 (2004b)
- [86] Guseinov, O.H., Ankay, A., Tagieva, S.O., 2004, *SerAJ.*, 169, 65 (2004c)
- [87] Guseinov, O.H., Allakhverdiev, A.O., Tagieva, S., Taşkin, Ö, 2004, *A&AT.*, 23, 385 (2004d)
- [88] Guseinov, O.H., Ankay, A., Tagieva, S.O., Taşkin, M. Ö., 2004, *IJMPD.*, 13, 197 (2004e)
- [89] Guseinov, O.H., Ankay, A., Tagieva, S.O., 2005, *IJMPD.*, 14, 865
- [90] Hailey, C.J., Craig, W.W., 1995, *ApJ.*, 455, L151

- [91] Hambaryan, V., Hasinger, G., Schwobe, A.D., Schulz, N.S., 2002, *A&A.*, 381, 98
- [92] Harriees, J., 1967, *Nature*, 38, 215
- [93] Harrison, P.A., Lyne, A.G., Anderson, B., 1993, *MNRAS.*, 261, 113
- [94] Hayakawa, S., Matsuoka, M., 1964, *Progr. Theor. Phys. Suppl.*, 30, 204
- [95] Helfand, D.J., Becker, R.H., Hawkins, G., White, R.L., 1994, *ApJ.*, 434, 627
- [96] Helfand, D.J., Collins, B.F., Gotthelf, E.V., 2003, *ApJ.*, 582, 783
- [97] Hellier, C., 1994, *MNRAS.*, 271, L21
- [98] Heyl, J.S., Hernquist, L., 1997, *ApJ.*, 489, L67 (1997a)
- [99] Heyl, J.S., Hernquist, L., 1997, *ApJ.*, 491, L95 (1997b)
- [100] Heyl, J.S., Hernquist, L., 1998, *MNRAS.*, 300, 599
- [101] Hoyle, F., Narlikar, J.V., Wheeler, J.A., 1964, *Nature*, 203, 914
- [102] Hughes, V.A., Harten, R.H., van den Bergh, S., 1981, *ApJ.*, 246, 127
- [103] Hughes, V.A., Harten, R.H., Costain, C.H. et al., 1984, *ApJ.*, 283, 147
- [104] Hulleman, F., van Kerkwijk, M.H., Kulkarni, S.R., 2000, *Nature*, 408, 689
- [105] Hulleman, F., Tennant, A.F., van Kerkwijk M.H. et al., 2001, *ApJ.*, 563, L49
- [106] Hulleman, F., 2002, *Neutron Stars in Supernova Remnants*, ASP Conference Series, edited by Slane, O.P. and Gaensler, B.M., Vol. 271, p.282 (astro-ph/0111561)
- [107] Hulse, R.A., Taylor, J.H., 1975, *ApJ.*, 195, L51
- [108] Hurley, K., Li, P., Kouveliotou, C. et al., 1999, *ApJ.*, 510, L111
- [109] Hurley, K. 2000, *The Fifth Compton Symposium*, edited by M. L. McConnell and J. M. Ryan, AIP Conference Proceedings, Vol. 510, p.515 (astro-ph/9912061)
- [110] Ibrahim, A.I., Safi-Harb, S., Swank, J.H. et al., 2002, *ApJ.*, 574, L51
- [111] Israel, G.L., Covino, S., Stella, L. et al., 1999, *ApJ.*, 518, L107 (1999a)
- [112] Israel, G. L., Oosterbroek, T., Angelini, L. et al., 1999, *A&A.*, 346, 929 (1999b)

- [113] Israel, G.L., Cavino, S., Stella, L. et al., 2002, *ApJ.*, 580, L143
- [114] Israel, G.L., 2004, *The Spectrum of Neutron Stars*, NATO ASI, edited by A. Baykal, S.K. Yerli, Ç. İnam, Marmaris (Turkey), Vol.
- [115] Juett, A.M., Marshall, H.L., Chakrabarty, D., Schulz, N.S., 2002, *ApJ.*, 568, L31
- [116] Kaminker, A.D., Yakovlev, D.G., Gnedin O.Y., 2001, *A&A.*, 383, 1076
- [117] Kaplan, D.L., Fox, D.W., Kulkarni, S.R. et al., 2002, *ApJ.*, 564, 935
- [118] Kaspi, V.M., Manchester, R.N., Johnston, S. et al., 1996, *AJ.*, 111, 2028
- [119] Kaspi, V.M., Lackey, J.R., Chakrabarty, D., 2000, *ApJ.*, 537, L31
- [120] Kaspi, V.M., Roberts, M.E., Vasisht, G. et al., 2001, *ApJ.*, 560, 371
- [121] Kaspi, V.M., Gavriil, F.P., Chakrabarty, D. et al., 2001, *ApJ.*, 558, 253 (2001a)
- [122] Kaspi, V.M., Helfand, D.J., 2002, *Neutron Stars in Supernova Remnants*, ASP Conference Series, edited by Patrick O. Slane and Bryan M. Gaensler, Vol. 271, p.3 (astro-ph/0201183)
- [123] Kaspi, V.M., Gavriil, F.P., 2002, *IAU Circ.*, No. 7924
- [124] Kern, B., Martin, C., 2002, *Nature*, 417, 527
- [125] Kothes, R., Uyaniker, B., Pineault, S., 2001, *ApJ.*, 560, 236
- [126] Kouveliotou, C., van Paradijs, J., Fishman, G.J. et al., 1996, *IAU Circ.*, No. 6503 (1996b)
- [127] Kouveliotou, C., Fishman, G.J., Meegan, C.A. et al., 1996, *IAU Circ.*, No. 6501 (1996a)
- [128] Kouveliotou, C., Dieters, S., Strohmayer, T. et al., 1998, *Nature*, 393, 235
- [129] Kouveliotou, C., Strohmayer, T., Hurley. K. et al., 1999, *ApJ.*, 510, L115
- [130] Kouveliotou, C., Tennant A., Woods, P.M. et al., 2001, *ApJ.*, 558, L47
- [131] Kramer, M., Bell, J.F., Manchester, R.N. et al., 2003, *MNRAS.*, 342, 1299
- [132] Kuiper, L., Hermsen, W., Mendez, M., 2004, *ApJ.*, 613, 1173
- [133] Kulkarni, S.R., Kaplan, D.L., Marshall, H.L. et al., 2003, *ApJ.*, 585, 948 (astro-ph/0209520)
- [134] Landau, L.D., 1932, *Phys. Z. Sowjetunion*, 1, 285

- [135] Li, X.-D., 1999, *ApJ.*, 520, 271
- [136] Lin, D.N.C., Woosley, S.E., Bodenheimer, P.H., 1991, *Nature*, 317, 827
- [137] Lipunov, V.M., Postnov, K.A., 1985, *A&A.*, 144, L13
- [138] Lipunov, V.M., 1992, *Astrophysics of Neutron Stars*, Springer-Verlag
- [139] Lorimer, D.R., Lyne, A.G., Camilo, F., 1998, *A&A.*, 331, 1002
- [140] Lovelace, R.V.E., Romanova, M.M., Bisnovatyi-Kogan, G.S., 1995, *MNRAS.*, 275, 244
- [141] Lyne, A.G., Anderson, B., Salter, M.J., 1982, *MNRAS.*, 201, 503
- [142] Lyne, A.G., Graham-Smith, F., 1998, *Pulsar Astronomy*, Cambridge University Press
- [143] Manchester, R.N., Lyne, A.G., Camilo, F. et al., 2001, *MNRAS.*, 328, 17
- [144] Manchester, R.N., Bell, J. F., Camilo, F. et al., 2002, *Neutron Stars in Supernova Remnants*, ASP Conference Series, edited by Patrick O. Slane and Bryan M. Gaensler, Vol. 271, p.31
- [145] Marsden, D., Rothschild, R.E., Lingenfelter, R.E., Puetter, R.C., 1996, *ApJ.*, 470, 513
- [146] Marsden, D., Lingenfelter, R.E., Rothschild, R.E., 2001, *ApJ.*, 550, 397
- [147] Marsden, D., White, N.E., 2001, *ApJ.*, 551, L155
- [148] Menou, K., Perna, R., Hernquist, L., 2001, *ApJ.*, 559, 1032
- [149] Mereghetti, S., Stella, L., 1995, *ApJ.*, 442, L17
- [150] Mereghetti, S., Cremonesi, D., Feroci, M., Tavani, M., 2000, *A&A.*, 361, 240
- [151] Mereghetti, S., 2001, *The Neutron Star - Blackhole Connection*, NATO ASI, edited by C. Kouveliotou, J. Ventura, E. van den Heuvel, Elounda (Crete - Greece), Vol. 567, p. 351 (2001b,astro-ph/9911252)
- [152] Mereghetti, S., 2001, Invited Talk presented at the Workshop Frontier Objects in Astrophysics and Particle Physics, Vulcano (Italy) (2001a,astro-ph/0102017)
- [153] Mereghetti, S., Chiarlone, L., Israel, G.L., Stella, L., 2002, *astro-ph/0205122*
- [154] Mereghetti, S., Tiengo, A., Stella, L. et al., 2004, *ApJ*, 608, 427

- [155] Michel, F.C., Goldwire, H.C., 1970, *ApJ.*, 5, L21
- [156] Migdal, A.B., 1959, *Zh. Eksp. Teor. Fiz.*, 37, 249
- [157] Morini, M., Robba, N.R., Smith, A., van der Kliss, M., 1988, *ApJ.*, 333, 777
- [158] Morris, D.J., Hobbs, G., Lyne, A.G. et al., 2002, *MNRAS.*, 335, 275
- [159] Murakami, T., Tanaka, Y., Kulkarni, S.R., et al., 1994, *Nature*, 368, 127
- [160] Murakami, T., Kubo, S., Shibazaki, N. et al., 1999, *ApJ.*, 510, L119
- [161] Murray, S.S., Ransom, S., 2001, Two Years of Science with Chandra, Abstracts from the Symposium held in Washington, DC, 5-7 September
- [162] Nagase, F., 1998, *Nature*, 282, 587
- [163] Novikov, I.D., Zel'dovich, Y.B., 1966, *Nuovo Cim. Suppl. (I)*, 4, 810
- [164] Oppenheimer, J.R., Volkoff, G.M., 1939, *Phys. Rev.*, 55, 374
- [165] Özel, F., 2001, *ApJ.*, 563, 276
- [166] Özel, F., Psaltis, D., Kaspi, V.M., 2001, *ApJ.*, 563, 255
- [167] Pacini, F., 1967, *Nature*, 216, 567
- [168] Paczynski, B., 1990, *ApJ.*, 365, L9
- [169] Parmar, A.N., Oosterbroek, T, Favata, T. et al., 1998, *A&A.*, 330, 175
- [170] Paul, B., Kawasaki, M., Dotani, T., Nagase, F., 2000, *ApJ.*, 537, 319
- [171] Pavlov, G.G., Kargaltsev, O.Y., Sanwal, D., Garmire, G.P., 2001, *ApJ.*, 554, L189
- [172] Pavlov, G.G., Zavlin, V.E., Sanwal, D., 2002, Proc. of the 270th Heraeus Seminar on Neutron Stars, Pulsars and Supernova Remnants, In: W. Becker, H. Lesch and J. Truemper (eds.), MPE Reports, Vol. 278, p. 283 (astro-ph/0206024)
- [173] Perna, R., Heil, J.S., Hernquist, L. et al., 2001, *ApJ.*, 557, 18
- [174] Pikel'ner, S.B., 1956, *Astron. Zh.*, 33, 785
- [175] Pivovarov, M.J., Kaspi, V. M., Camilo, F. et al., 2001, *ApJ.*, 554, 161
- [176] Possenti, A., Cerutti, R., Colpi, M., Mereghetti, S., 2002, *A&A.*, 387, 993
- [177] Rho, J., Petre, R., 1997, *ApJ.*, 484, 828

- [178] Roger, R.S., Milne, D.K., Kesteven, M.J., 1988, *ApJ.*, 332, 940
- [179] Rothschild, R.E., Marsden, D., Lingenfelter, R.E., 2001, *astro-ph/0105419*
- [180] Rothschild, R.E., Lingenfelter, R.E., Marsden, D., 2002, *Neutron Stars in Supernova Remnants*, ASP Conference Series, edited by O.P. Slane, B.M. Gaensler, Vol. 271, p.257 (*astro-ph/0112121*)
- [181] Ruderman, M., 1969, *Nature*, 223, 597
- [182] Ruderman, M., Sutherland, P.G., 1975, *ApJ.*, 196, 51
- [183] Salpeter, E.E., 1964, *ApJ.*, 140, 796
- [184] Sanbonmatsu, K.Y, Helfand, D.J., 1992, *ApJ.*, 104, 2189
- [185] Sanwal, D., Pavlov, G.G., Zavlin, V.E., Teter, M.A., 2002, *ApJ.*, 574, L61
- [186] Seward, F.D., Harnden, F.R.Jr., Helfand, D.J., 1984, *ApJ.*, 287, L19
- [187] Seward, F.D., Charles, P.A., Smale, A.P., 1986, *ApJ.*, 305, 814
- [188] Seward, F.D., Wang, Z.R., 1988, *ApJ.*, 332, 199
- [189] Shklovskii, I.S., 1953, *Astron. Zh.*, 30, 15
- [190] Shklovskii, I.S., 1967, *Astron. Zh.*, 44, 930
- [191] Sonobe, T., Murakami, T., Kulkarni, S.R. et al., 1994, *ApJ.*, 436, L23
- [192] Sturrock, P., 1971, *ApJ.*, 164, 529
- [193] Sun, X., Anderson, S., Aschenbach, B. et al., 1996, *Proc. Röntgenstrahlung from the Universe*, In: Zimmermann, H. U., Trümper, J. and Yorke, H., MPE Report, Vol. 263, p.195
- [194] Tagieva, S.O., Yazgan, E., Ankay, A., 2003, *IJMPD.*, 12, 825 (*astro-ph/0201068*)
- [195] Tagieva, S.O., Ankay, A., 2003, *A&AT.*, 22, 59
- [196] Tatematsu, K., Fukui, Y., Nakano, M. et al., 1987, *A&A.*, 184, 279
- [197] Thompson, C., Duncan, R.C., 1995, *MNRAS.*, 275, 255
- [198] Thompson, C., Duncan, R.C., 1996, *ApJ.*, 473, 322
- [199] Thompson, C., Blaes, O., 1998, *Phys. Rev. D.*, 57, 3219
- [200] Thompson, C., Duncan, R.C., Woods, P.M. et al., 2000, *ApJ.*, 543, 340

- [201] Thorsett, S.E., Briskin, W.F., Goss, W. M., 2002, ApJ., 573, L111
- [202] Torii, K., Kinugasa, K., Katayama, K. et al., 1998, ApJ., 503, 843
- [203] Trimble, V., 1968, A.J., 73, 535
- [204] Tsuruta, S., Cameron, A.G.W., 1966, Nature, 211, 356
- [205] Urpin, V.A., Muslimov, A.G., 1994, ARep., 38, 225
- [206] Usov, V.V., 1994, ApJ., 427, 984
- [207] van Paradijs, J., Taam, R.E., van den Heuvel, E.P.J., 1995, A&A., 299, L41
- [208] Vasisht, G., Gotthelf, E.V., 1997, ApJ., 486, L129
- [209] Vasisht, G., Kulkarni, S.K., Anderson, S.B. et al., 1997, ApJ., 476, L43
- [210] Veltman, M.J.G., 2003, Facts and Mysteries in Elementary Particle Physics, World Scientific
- [211] Wang, Z., Chakrabarty, D., 2002, ApJ., 579, L33
- [212] White, N.E., Angelini, L., Ebisawa, K. et al., 1996, ApJ., 463, L83
- [213] Woltjer, L., 1964, ApJ., 140, 1309
- [214] Woods, P. M., Kouveliotou, C., van Paradijs, J. et al., 1999, ApJ., 518, L103 (1999a)
- [215] Woods, P. M., Kouveliotou, C., van Paradijs, J., et al., 1999, ApJ., 524, L55 (1999b)
- [216] Woods, P.M., 2002, astro-ph/0204369
- [217] Yakovlev, D.G., Haensel, P., 2003, A&A., 407, 259 (astro-ph/0209026)
- [218] Yusifov, I.M., Alpar, M.A., Gok, F., Guseinov, O.H., 1995, The Lives of the Neutron Stars, edited by Alpar, M.A., Kiziloglu, U., van Paradijs, J., Kluwer, Dordrecht, Vol. 450, p.201
- [219] Zel'dovich, Ya.B., Guseynov, O.K., 1964, ApJ., 144, 840
- [220] Zwicky, F., 1957, Morphological Astronomy, Springer-Verlag, Berlin, p. 258

VITA

Mustafa Özgür Taşkın was born in İstanbul on February 16, 1975. He received his B.S and M.S degrees in Physics from the Middle East Technical University in 1998 and 2001 respectively. He worked in Physics Department of the Middle East Technical University from 1998 to 2005 as a research assistant. His area of interest covers different kinds of pulsars, X-ray binaries, supernova remnants and in general high energy astrophysics.